# Investigation of the Wind-borne Debris Regions in ASCE 7-22

## Final Report

June 15, 2025

Florida Department of Business and Professional Regulation
Florida Building Commission

and

Engineering School of Sustainable Infrastructure and Environment (ESSIE)
University of Florida (UF)

## Table of Contents

## Executive Summary

The ASCE 7-22 standard introduced an update to the definition of Windborne Debris Region (WBDR) for regions where design wind speeds are between 130 and 139 mph. In the previous version of this standard (ASCE 7-16), the WBDR designation was limited to within one mile of *the coast* for 130 – 139 mph regions. The ASCE 7-22 definition removed specific reference to the coast and designated the WBDR to be within one mile of *any* body of water where an Exposure D condition exists upwind of the water line. An Exposure D condition is created over open water with at least 5,000 ft of fetch in the upwind direction, which includes large inland water bodies. This updated definition was initially adopted in the 8th Ed. Florida Building Code (FBC); however, the current version of the 8th Ed. FBC has reverted to the WBDR definition in the 7th Ed. FBC/ASCE 7-16 which designates WBDR as coastal locations only for the 130 to 139 mph regions. Both ASCE 7-16 and 22, and previous versions, also designate as WBDR any region at or above the 140-mph contour regardless of water proximity or terrain exposure.

The ASCE 7-22 expansion of WBDR definition increases the number of locations where glazing protection would be required for new construction–notably within one mile around the perimeter of inland lakes with water fetch greater than 5,000 ft and where ultimate (design) wind speeds are between 130 and 139 mph.

A comprehensive review of post-hurricane damage assessments reveals several storms that resulted in wind-borne debris (WBD) damage from wind speeds between 125 and 140 mph in regions adjacent to coastal Exposure D conditions. After Hurricane Charley (2004), WBD damage was noted in several locations more than three miles from the coast. Extensive WBD damage was documented during Hurricanes Ike and Harvey (2008 and 2017, respectively). Damage from WBD was also noted after Hurricane Michael (2018) more than three miles from an inland bay. These observations demonstrate the need to evaluate the one-mile distance with respect to WBD damage risk, and that the risk exists without direct coastline exposure. We have not identified reports of damage during design wind speed events in inland areas with Exposure D conditions from lakes with design wind speeds between 130 and 1139 mph, likely due to the limited number of design level wind events in these regions. Post-storm damage assessments are intended to provide a representative sampling rather comprehensive documentation and are typically prioritized to coastal regions due to relatively higher damage levels, so a dearth of observations does not preclude that such damage occurs.

A review of wind-borne debris research reveals that there have not been specific studies to guide the designation of wind-borne debris regions relative to upwind terrain conditions or how the risk for wind-borne debris damage varies with distance from terrain transitions. While some limited research has demonstrated how transition between terrain conditions impacts wind loads, this research has not yet been extended to its influence on debris generation, transport, and damage.

Researchers at the University of Florida (UF) and Applied Research Associates, Inc. (ARA) carried out a study to evaluate the WBD risk to the envelope of a subject structure. The goal was to determine the WBD risk for locations that meet the ASCE 7-22 WBDR designation, relative to a frame of reference WBDR designation that has been consistent through many sequential versions of ASCE 7. This reference structure was chosen to be located at the 140-mph wind speed contour

in Exposure B (not in proximity to a large body of water). That is, the WBD risk to a 'subject structure' located within one mile of a large body of water and within the 130 – 139 wind speed contour was evaluated in ratio with the WBD risk of the 'reference structure' located at the 140-mph contour and in Exposure B. This is referred to as the 'relative hit' value in the detailed presentation herein, referring to the number of debris hits on the wall of the subject structure.

In the simulation performed for this study, the location of the subject structure with respect to the large body of water was varied from waterfront to 5,000 feet from the waterfront to determine the sensitivity of the relative hit value to water proximity. The goal is to identify the equivalence distance at which the relative hit value is 1.0, indicating that the subject structure has an equivalent WBD risk to the reference structure. This provides a rational means of evaluating the WBD risk associated with structures that fit within the new ASCE 7-22 WBDR designation relative to the WBD risk to structures minimally (140-mph border) meeting the long-time accepted and enforced WBDR designation.

The WBD risk evaluation methodology is stochastic in nature to capture the influence of the many uncertainties regarding knowns and assumptions. Therefore, the equivalence distance defined above is evaluated and presented within a probabilistic framework. It is also the case that this probabilistic outcome will vary depending upon the specific neighborhood being investigated, and so investigating the equivalence distance for one neighborhood is necessary but not sufficient to draw conclusions regarding a risk-consistent WBDR designation standard.

With the above motivation, thirty neighborhoods within the wind speed zones of interest (130-139 mph) and within one mile of a large body of water (23 inland and 7 coastal) were selected from a map of Florida for this study. These locations exhibit a wide variety of directionally dependent terrain conditions, which is an important parameter when determining WBD risk. For each neighborhood, directional surface roughness values ($Z_0$) were determined based on terrain conditions extracted from land cover data. Results show that the inland neighborhoods near large water bodies have surface roughness conditions similar to the coastal neighborhoods. As such, it is valid to consider inland regions on lakes as potentially having WBD risk similar to coastal locations. That is, the ASCE 7-22 extension of the WBDR in 130 – 139 mph regions from coastal only to proximate to any large body of water is justified in concept. What remains is then to evaluate the distance from the body of water that the WBD risk drops below that of the reference structure at the 140-mph contour in Exposure B. That is, determine the equivalent distance from the water body where WBD risk is consistent with the 140-mph suburban terrain contour. This distance is not necessarily aligned with the current ASCE 7-22 assigned distance of one mile.

For each of the selected neighborhoods the directional minimum average surface roughness values were used with stochastic WBD simulation tools developed and by ARA and validated with post-event field data. The WBD risk modeling results indicate that neighborhoods within 3,000 feet of a large body of water subjected to wind speeds between 130 and 139 mph experience WBD risk comparable to or greater than those at the 140-mph contour at Exposure B (relative hit value greater than 1.0). Beyond the 3,000-foot proximity to water, the relative hit value drops below 1.0. Changing the current WBDR designation from a one-mile proximity to water to a 3,000-foot proximity to water is rational and consistent with WBD risk at the 140-mph contour in Exposure

B. This change will reduce the area of land near the coast and around inland lakes subject to WBDR designation as per ASCE 7-22 by 43-56%.

The cost of impact resistant windows increases the total new construction cost of homes in Florida by 1.7 to 2.7 percent. For homes subject to 130 mph winds in Exposure C, the benefit of these opening protections, quantified as a reduction in losses realized over a ten-year period, is between 61 and 110 percent. These benefit-cost ratios are higher than for homes in current WBDRs (140 mph, Exposure B). In addition to the loss reduction provided by opening protection, it also reduces the intangible losses associated with home damage that are not fully captured by reduction in insured losses.

The overall findings of this report have important implications for the Florida Building Code. A proposed code modification to add inland WBDRs while reducing the boundary to 3,000 feet would result in a more risk-consistent approach to regulating building protections in Florida. In inland regions where the design wind speed is between 130 and 139 mph, this recommendation would increase the number of homes requiring opening protection according to the 8$^{th}$ Ed. FBC; however, it would decrease the number of homes requiring opening protections along the coast.

# 1 Introduction and Background

## 1.1 Background

Damage to the windward facing envelope of buildings from the impact of wind-borne debris (WBD) can result in damaging water entry and increased internal pressures that can lead to failure of the primary structural system. Buildings in designated wind-born debris regions (WBDR) require higher levels of protection from debris impact. Prior to 2022, American Society of Civil Engineers (ASCE) 7, designated WBDRs as those where design wind speeds are above 140 mph or those between 130 and 140 mph and within one mile of the coast (coastal mean high-water line) (ASCE 7-16). The definition of WBDRs for design wind speeds between 130 and 140 mph was updated in ASCE 7-22 to remove the word "coastal" and add that an Exposure D condition must exist at the water line. An Exposure D condition is a site exposed to water surfaces in the upwind direction with a fetch of at least 5,000 ft. The result of this definition change is the designation of inland WBDRs where lakes and inland waterways provide at least 5,000 ft of fetch in the upwind direction where design wind speeds are between 130 and 140 mph; design wind speeds above 140 mph in hurricane prone regions are designated WBDR regardless of adjacent exposure conditions.

## 1.2 Project objectives and scope

The objective of this study is to provide the Florida Building Commission with a science-based analysis on the appropriateness of water adjacent inland regions being designated as WBDRs that require increased protection for buildings. In particular, the study will seek to evaluate the differences between coastal and inland WBDRs across a number of contributing factors (e.g. exposure, land coverage, and development trends). The objective will be achieved through an investigation into the origin of the language change (the removal of the requirement for the region to be coastal) in ASCE 7-22, a review of all relevant literature related to the designation of WBDRs, a comprehensive evaluation of available damage assessments conducted in the coastal and proposed inland WBDRs, and an analysis of the risk of WBD building damage in the proposed regions through modeling and analysis. In addition, this study will conduct a cost analysis to estimate the cost of construction to meet the design requirements for WBDRs.

The scope of work for this project consists of five tasks and accompanying deliverables:

- Task 1: Background and Literature Review
- Task 2: Data Acquisition and Analysis
- Task 3: Modeling
- Task 4: Cost Benefit Analysis
- Task 5: Reporting and Recommendations

# 2 Standard and Code Definitions

## 2.1 ASCE 7 and Florida Building Code

The ASCE 7 Standard provides the minimum design loads for buildings and other structures, and since 1995 it has included provisions related to the design for wind-borne debris. The Florida Building Code has largely adopted ASCE 7 since its first edition (FBC 2001). The historical

WBDR definitions in the Florida Building Code and corresponding ASCE 7 are summarized in Table 1.

Table 1. Summary of WBDR Definitions in Florida Building Code editions (ARA Wind-loss Mitigation Study, 2024).

| **Building Code(s)** | **ASCE Map** | **WBDR Definitions** |
|---|---|---|
| FBC 2001, 2004, 2007 | 7-98, 7-02, 7-05 | ≥120 mph<br>≥110 mph w/in 1 mi. of coast |
| FBC 2010, 2014, 2017, 2020 | 7-10, 7-16 | ≥140 mph<br>≥130 mph w/in 1 mi. of coast |
| FBC 2023 | 7-22 | ≥140 mph<br>≥130 mph w/in 1 mi. mean water line where Exp. D exists |

The 7th Ed. (2020) of the Florida Building Code for residential buildings (FBC(R), 2020) references the ASCE 7-16 WBDR definition, which are areas in hurricane-prone regions that are one of the following:

1. Within 1 mi (1.6 km) of the coastal mean high water line where the basic wind speed is equal to or greater than 130 mi/h (58 m/s), or
2. In areas where the basic wind speed is equal to or greater than 140 mi/h (63 m/s).

The original version of the FBC(R) 8th Ed. (2023) references the WBDR definition in ASCE 7-22, which are areas within hurricane-prone regions located in accordance with one of the following:

1. Within 1 mile (1.61 km) of the mean high water line where an Exposure D condition exists upwind at the waterline and the ultimate design wind speed, $V_{ult}$, is 130 mph (58 m/s) or greater.
2. In areas where the ultimate design wind speed, $V_{ult}$, is 140 mph (63.6 m/s) or greater; or Hawaii.

An Exposure D condition occurs where Surface Roughness D (flat terrain and water) prevails in the upwind direction for a distance of at least 5,000 ft.

FBC(R) requires that buildings located in WBDRs provide protection for exterior glazed openings (meeting specific ASTM requirements). The result of the updated definition of WBDR in ASCE 7-22/FBC(R) 2023 is that inland regions in central Florida and the panhandle adjacent to large lakes or inland bays with design wind speeds between 130 and 140 mph will now also require buildings to have opening protections. There are stakeholders within Florida that are interested in reverting the 9th Ed. FBC(R) to the WBDR definition in the 7th Ed. based on ASCE 7-16.

Figure 1 shows the results of a preliminary analysis conducted by project research partner, Applied Research Associates, Inc. (ARA), superimposed over the ASCE 7-22 wind speed map for Florida. The highlighted inland regions in the 130-140 mph wind speed band are within one mile of the water line of lakes and inland waterways with at least 5,000 ft of fetch in the upwind direction.

Figure 2 shows a detailed view of these regions in central Florida and Figure 3 shows a detailed view of these regions in the Florida panhandle.

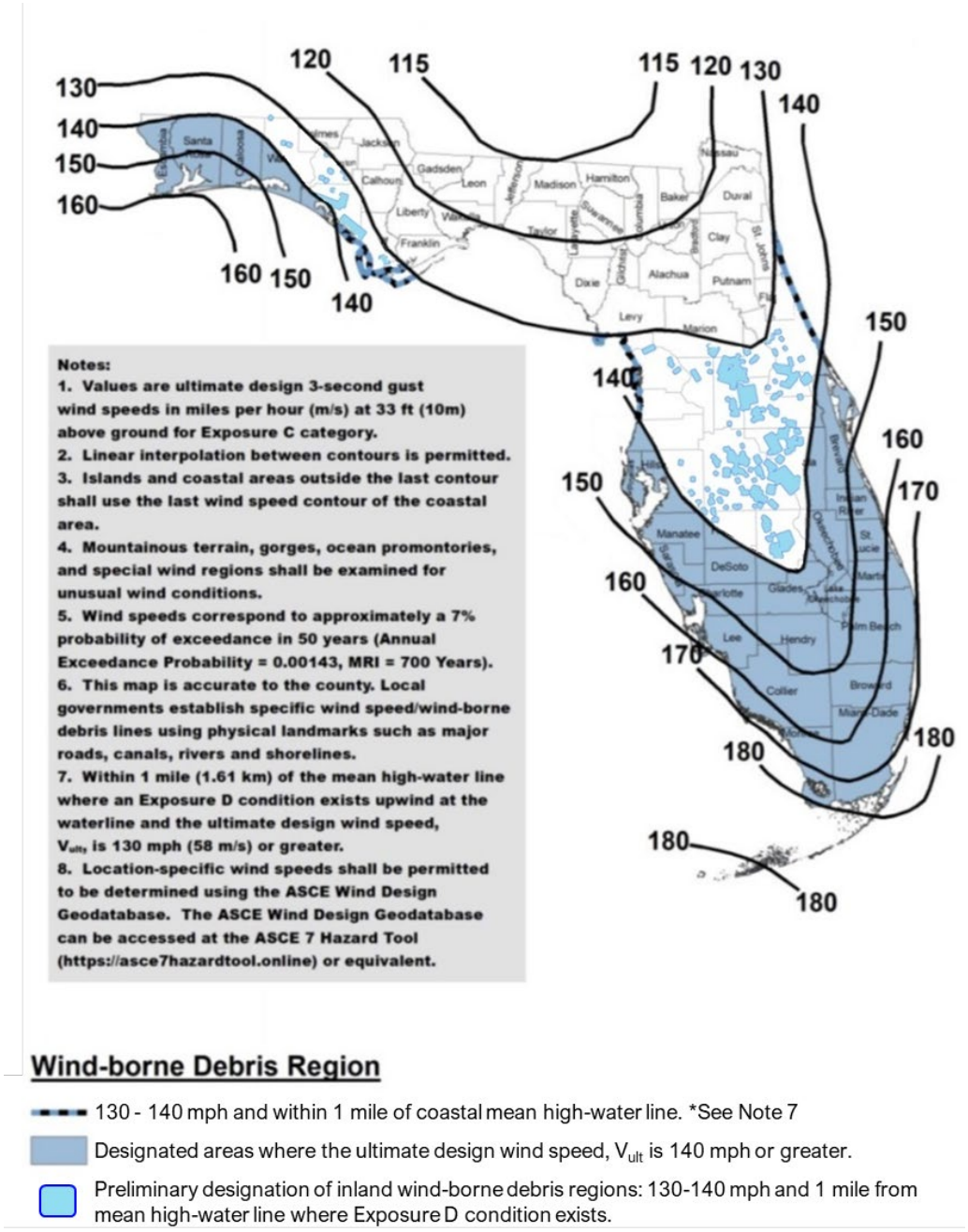


Figure 1. Designation of inland wind-born debris regions on ASCE 7-22 Wind Speed Map.

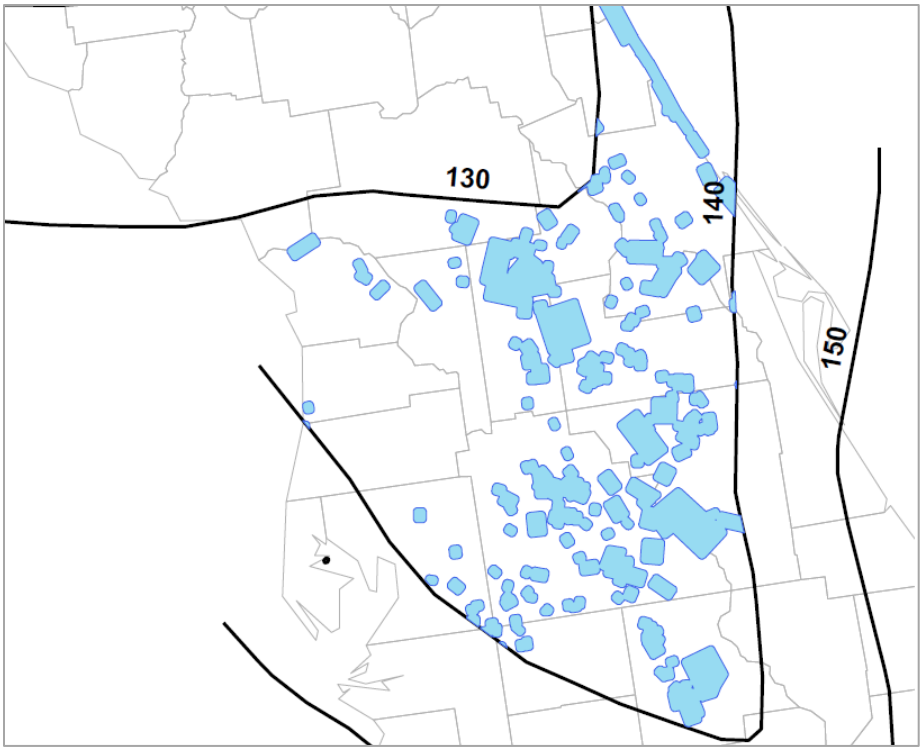


Figure 2. Detail of preliminary designation of inland WBDR in central Florida (courtesy of ARA).

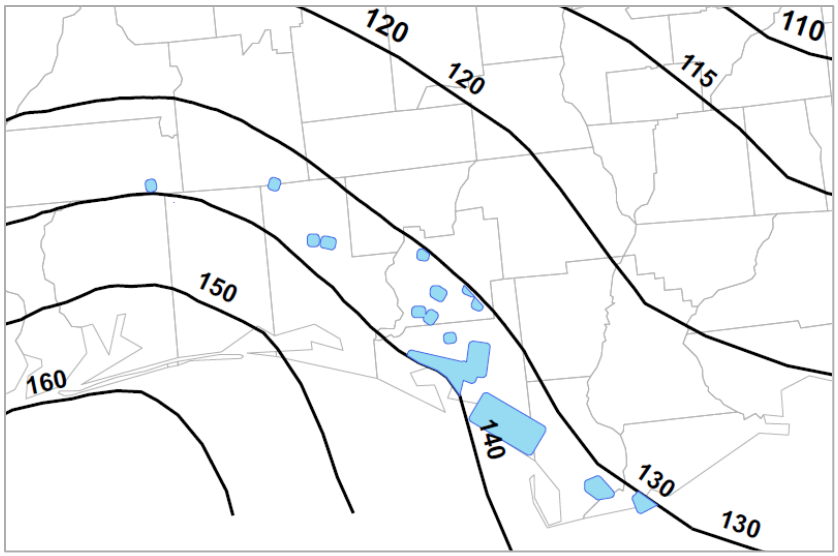


Figure 3. Detail of preliminary designation of inland WBDR in Florida panhandle (courtesy of ARA).

## 2.2 History of WBDR in ASCE 7

To understand the reasoning behind the WBDR definition in ASCE 7-22, it is important to review the history of WBD provisions in ASCE 7. This summary is drawn from conversations with members of the Wind Loads Subcommittee of ASCE 7 who have first-hand experience researching, developing, and updating the provisions[1].

Researchers began documenting damage from WBD during windstorms (primarily tornadoes) as early as the 1970s, which resulted in several unsuccessful proposals to include WBD criteria in ASCE 7. As a result of the observation of extensive glazing damage during Hurricanes Alicia (1983), Hugo (1989), and Andrew (1992), the ASCE Task Committee on Wind Loads again sought to include WBD design criteria to ASCE 7. The initial rationale for this update was to protect the building envelope from breaches to avoid damage to nonstructural elements. At the time, the glazing industry was only in early phases of developing impact resistant products and since has matured significantly.

In 1995 the first requirement for design for WBD was incorporated into ASCE 7, triggered only by a 110 mph (49 m/s) wind speed, based on a load factor of 1.6. In ASCE 7-98, the WBD windspeed trigger was increased to 120 mph, except for regions within one mile of the coast with wind speeds greater than 110 mph. This reduction in the WBDRs was driven primarily by resistance from building officials and authorities having jurisdictions to adopt the previous designation, and not on new research or observations. The Committee's criteria for using the one-mile distance was based largely on anecdotal evidence from damage assessments; no specific research had been conducted to inform the selection of this specific distance.

Starting with ASCE 7-10, the windspeed trigger for WBDRs was increased to 140 mph with a load factor of 1.0, and 130 mph within one mile of the coast. During subsequent standard cycles, the ASCE 7 Wind Loads Subcommittee began considering removing "coastal" for the 130 mph regions. There was a recognition that an Exposure D condition is likely to occur regardless of whether the large body of water (at least 5,000 ft of fetch) is coastal or inland (i.e. "the wind can't tell the difference"). The fact that the word "coastal" was ever included was thought to be in error and an artifact of the damage assessments after Hurricanes Andrew and Hugo that drove the initial adoption of WBD criteria. These events largely produced reported damage in coastal regions and the priority for damage assessments was driven by damage severity.

Another issue with the coastal designation was confusion in how to define the coastline. The term "mean high water level" does not have a clear definition; as a result, the definition of the coast was left up to the local authority having jurisdiction to determine. An official inquiry by a building official for clarification on this definition prompted the Committee to further consider the removal of the word "coastal". To avoid confusion, ASCE 7-22 opted to make the designation based on an Exposure D condition, without reference to the coast.

---

[1] The history of WBDR designations in ASCE presented in this report is synthesized from personal communication with Mr. Don Scott (past chair of the ASCE 7 Wind Loads Subcommittee) and Mr. Tom Smith (Consultant and member, ASCE 7 Wind Loads Subcommittee with extensive post-disaster investigation experience).

# 3 Literature Review

This section provides an overview of research studies on the generation, transport, and impacts of wind-borne debris, including experimental and numerical studies. Much of the research summarized is general in nature; there are limited numbers of studies focused specifically on the designation of WBDRs, how transitions between terrain exposures impacts debris risk, how the risk of wind-borne debris damage varies between inland and coastal regions, and how the risk decreases with increasing distance from the shoreline.

## 3.1 Overview

Wind-borne debris is a critical factor in structural damage during extreme wind events such as hurricanes and tornadoes. Generated and propelled by strong winds, wind-borne debris imposes impact loads on building envelopes, leading to structural failures and further debris generation. High-velocity debris can breach walls, openings, and roofs. In addition to providing a means of water infiltration, these breaches can increase internal pressure and significantly increase the net load on structures, often culminating in catastrophic failures (Lin, 2005; Wills et al., 2002). The unpredictable nature of wind-borne debris, including its variability in size, shape, and velocity, complicates efforts to mitigate its effects. Understanding wind-borne debris behavior and its impacts on structures is therefore essential for minimizing damage and economic losses.

The economic implications of wind-borne debris during wind events are profound, with losses often amounting to billions of dollars. Dr. Joseph Minor's investigations, starting in 1972, identified wind-borne debris as a primary cause of building envelope failure and subsequent economic loss. His analyses of wind events, including Hurricanes Alicia (1983), Hugo (1989), and Andrew (1992), demonstrated the role of wind-borne debris in widespread structural damage and underscored the need for more resilient building designs (Minor, 2005; Minor et al., 1972).

In urban areas, wind-borne debris risks are heightened due to the density of buildings and infrastructure with debris generating capability. Minor et al. (1978) explored the sources of urban debris and the severe damage these items can inflict. The study emphasized the necessity of robust risk assessment methodologies and mitigation strategies tailored to urban environments. These include impact-resistant materials such as laminated glass, reinforced wall systems, and secure roofing designs to reduce debris generation. Advances in urban planning, such as wind-tunnel studies and strategic placement of structures, can help mitigate debris exposure.

Minor's later work (2005) further highlighted the vulnerabilities of building materials to debris impact during windstorms. For instance, roof gravel or wood fragments can breach tempered glass and other commonly used durable materials. These findings prompted significant updates to building codes in hurricane-prone areas, requiring materials and designs capable of withstanding debris impacts. Modern testing protocols now evaluate impact resistance. Innovations such as laminated glass systems and advanced glass anchoring techniques reflect a shift toward ensuring functionality after impact.

The research emphasizes that improving the resilience of building materials, enhancing urban planning, and updating building codes are crucial steps in reducing the risks associated with wind-borne debris. By addressing these challenges through engineering and policy measures, the destructive effects of wind-borne debris can be significantly mitigated.

### 3.2 Numerical simulations of wind-borne debris

Numerical simulations play a critical role in understanding and predicting the behavior of wind-borne debris during extreme wind events. These studies often categorize wind-borne debris into compact, sheet, and rod types based on shape. Various analytical and numerical methods have been employed to model wind-borne debris motion. These approaches utilize differential equations and multi-species fluid dynamics models to simulate trajectories (Holmes, 2004; Lin, 2005; Dowell et al., 2005; Moghim & Caracoglia, 2012). Experiments have validated these simulations, and empirical equations have been developed to approximate wind-borne debris behavior (Lin & Vanmarcke, 2010; Bourriez et al., 2020).

Twisdale et al. (1996) introduced a six-degree random orientation (RO 6-D) model to simulate three-dimensional debris flight trajectories, incorporating drag, lift, and side forces. Comparing model results with post-damage hurricane survey data demonstrated the model's efficacy. Holmes (2004), Holmes et al. (2006), and Lin et al. (2007) focused on two-dimensional simulations of debris, using quasi-steady force coefficients derived from wind tunnel experiments and validating results with observed trajectories. Baker (2007) proposed an alternative non-dimensional scheme to Tachikawa's (1983) model and investigated numerical solutions for debris motion equations. Richards et al. (2008) extended this work by simulating the three-dimensional motion of plate- and rod-type debris, aligning with Tachikawa's (1988) wind-tunnel findings.

Probabilistic trajectory models have emerged as essential tools for predicting wind-borne debris behavior under turbulent wind conditions. These models integrate randomness in wind fields and debris properties to simulate outcomes like impact location and velocity. Monte Carlo simulations assess multiple scenarios by sampling debris characteristics and wind conditions. Aerodynamic effects are incorporated to enhance accuracy for complex debris types like plates (Wang et al., 2023). Validated through wind tunnel experiments, these models provide valuable insights for use in risk assessments and the development of protective measures.

Abdelhady et al., (2022) present a framework to determine the necessary extent of surrounding buildings to include in simulations for accurately modeling hurricane-induced damage. Exogenous wind-borne debris, originating from neighboring subdivisions, is a significant factor in damage. The authors use a simulation-based iterative approach to define the radius of neighboring areas needed to account for wind-borne debris. Some of the factors influencing the radius of neighboring areas are the maximum wind speeds, the density of the neighborhoods, and the building strength. The study highlights the importance of exogenous debris in damage models and offers a scalable, computationally efficient framework for integrating these effects.

Computational Fluid Dynamics (CFD) simulations have advanced the understanding of wind-borne debris dynamics by modeling complex aerodynamic behaviors during flight. These simulations compute critical forces such as drag, lift, and rotational moments acting on debris, particularly plate-like objects, which exhibit phenomena like vortex shedding and lift hysteresis (Kakimpa et al., 2010). Three-dimensional CFD models enhance accuracy by capturing intricate flow structures, such as ring vortices, that are less detailed in 2D simulations. High-fidelity turbulence models, such as Realizable k−ε and Large Eddy Simulation (LES), further refine predictions by resolving unsteady flow effects like separation and reattachment. Studies validate CFD outputs against experimental data, providing a reliable tool for understanding debris motion and informing mitigation. Insights from CFD simulations have guided the design of hurricane-resistant structures and protective barriers by predicting how debris interacts with wind fields.

### 3.3 Experimental studies

Experimental approaches often use wind tunnels and laboratory equipment to simulate wind-borne debris motion and its impacts. These experiments are useful in improving and validating numerical models used in debris damage risk assessment. Lin (2005) conducted wind tunnel and aircraft-generated wind experiments, developing empirical equations to estimate wind-borne debris trajectories and impact speeds. Kordi and Kopp (2011) examined initial wind-borne debris conditions and identified flight behaviors such as "3-D spinning" and "no flight," influenced by local wind dynamics. Experimental studies, such as those by Crawford (2012), validated numerical models for wind-borne debris trajectories in tornadic wind fields.

Tachikawa (1983, 1988) pioneered experiments on plate and prism debris in boundary-layer wind tunnels, establishing non-dimensional equations of debris motion and introducing the "Tachikawa Number," a parameter describing debris flight behavior (Holmes et al., 2006). Lin et al. (2006, 2007) expanded these findings by conducting extensive wind-tunnel experiments, deriving non-dimensional empirical relationships for flight distance and speed as functions of the Tachikawa Number. Visscher and Kopp (2007) examined roof sheathing panel trajectories in wind tunnel experiments, noting higher variability and sensitivity to flight conditions compared to earlier studies by Tachikawa (1983) and Lin et al. (2006, 2007).

It is noteworthy that none of the wind tunnel tests on debris transport involved study of the impact of upwind exposure and exposure transitions.

### 3.4 Impact of terrain transitions on wind loads

The interaction between wind and the built environment is a complex phenomenon that significantly influences the design and safety of low-rise buildings. Understanding how surrounding conditions, terrain transitions, topography, and wind loads affect wind-borne debris behavior is crucial for developing accurate WBD risk models. Variability in wind turbulence caused by nearby structures, changes in terrain, and the generation and transport of debris can

influence building performance, especially in urban, suburban, and inland contexts. Compounding these challenges is the limited research on wind-borne debris impacts over inland exposure conditions, leaving significant gaps in understanding the mechanisms of damage.

Topography plays a key role in influencing wind behavior, often leading to the strongest winds flowing over relatively smooth areas such as large bodies of water (resulting in Exposure D condition defined in ASCE 7). This smooth terrain allows the mean flow to accelerate relative to upstream overland exposures, creating localized zones of amplified wind speeds and increased turbulence as the flow transitions from water to land. Such conditions are particularly concerning in inland regions with large lakes or inland bays, where this acceleration effect can amplify wind loads on structures near the body of water.

Previous research has investigated the effects of surrounding structures and terrain transitions on wind loads. For example, Ho et al. (1991) demonstrated how the alignment and proximity of buildings or the presence of suburban patches can significantly influence wind flow patterns and pressure distributions. These factors can result in amplified wind loads or localized pressure peaks, particularly at vulnerable areas like roof edges and corners. Kim et al. (2024) explored the impact of upwind terrain transitions, from open to suburban, on wind pressures and forces acting on low-rise buildings. Wind tunnel experiments were conducted to analyze how the distance and size of the terrain transition patch affect wind dynamics and pressure distribution. The presence of an upwind suburban patch consistently reduces mean wind speeds, leading to decreased mean pressures on building surfaces. Turbulence intensity increases due to the upwind transition, resulting in greater fluctuations in wind pressures. Negative pressure effects were particularly pronounced at edges and corners. Localized intensifications in wind pressures near upwind transitions can have critical design implications for structural integrity and safety. The study recommends accounting for these effects in building codes and design practices, even for short suburban patches. Such investigations have focused on wind pressure effects, with limited attention given to the interaction between wind-borne debris and exposure transitions, especially in inland regions where smooth water surfaces can intensify mean wind speeds.

Research on wind-borne debris has predominantly addressed coastal and urban environments, where debris sources and wind intensities are well-documented. In contrast, inland areas, where terrain transitions (e.g., from open water to suburban) play a critical role in debris dynamics, remain underexplored. This gap limits the ability to accurately model wind-borne debris generation, transport, and impact under inland exposure conditions. Moreover, the amplification of wind speeds over large bodies of water in these regions further complicates predictive modeling and risk assessment. Addressing the gaps in inland exposure studies is vital for enhancing building codes and design practices to ensure resilience against extreme wind events and associated debris impacts across diverse exposure zones.

## 3.5 Vulnerability and risk assessment

Statistical approaches are essential in analyzing the dynamics of wind-borne debris (WBD) during extreme wind events. WBD risk models incorporate stochastic methods to estimate the trajectory and impact probabilities of WBD. Probabilistic trajectory models account for uncertainties such as turbulence and debris orientation, which significantly influence the flight and impact energy of debris (Grayson, 2011; Karimpour & Kaye, 2012). Including these uncertainties is crucial for accurate assessments of flight distances and impact energies.

Twisdale et al. (1996) proposed a probabilistic model to estimate the mean WBD damage risk in residential areas. This model assumes that impact parameters, such as the number of impacts and momentum, are identically distributed across all debris types and houses in the area. The model also assumes that the total number of debris impacts follows a Poisson distribution. Lin and Vanmarcke (2008) refined this model by showing that the number of objects of each type of debris generated from a building can also follow a Poisson distribution, which helps to better estimate over-threshold impacts. This method links the stochastic processes of debris generation, flight, and impact, avoiding the common assumption of uniform risk across buildings.

Twisdale's model has been applied in vulnerability analysis for residential buildings, where it has been used to estimate the debris risk parameters for typical residential subdivisions. These analyses contributed to the ASTM recommendations for debris-impact risk analysis (ASTM E1886-05 2005) and informed the FEMA HAZUS-MH Hurricane Model (Vickery et al., 2006) for estimating hurricane damage and losses. Additionally, the Florida Public Hurricane Loss Projection (FPHLP) model (Gurley et al., 2005) used a simplified debris risk model based on exponential distribution for structural vulnerability analysis.

Wind-borne debris significantly increases the risk of building envelope failures during hurricanes. Component-specific studies have identified critical weak points, particularly in residential windows, where lightweight debris poses a significant threat (Lin & Vanmarcke, 2010). Protective systems have proven effective in mitigating damage.

## 3.6 Literature review summary

While significant progress has been made in understanding WBD through numerical simulations and experimental studies, substantial gaps remain, particularly regarding inland exposure conditions. Most existing research focuses on urban and suburban settings, with limited attention to transitional zones between water and land, or regions categorized as Exposure D. These areas present unique challenges posed by increased turbulence and wind amplification over water bodies.

# 4 Damage Reports

This review focuses on damage assessment reports of hurricanes affecting areas where design wind speeds range between 130 and 140 mph. Special attention is given to regions with unique geographic features, such as inland water bodies.

## 4.1 Methodology

The methodology for this review focused on selecting hurricanes that closely align with current design wind speeds for inland WBDRs. Storms were chosen based on four primary criteria: wind speeds within the 130–140 mph range, their impact on both coastal and inland areas, the presence of water bodies such as lakes or inland bays along their paths, and storm intensity.

Storms considered in this review, along with the primary observations, are provided in Figure 4 and Table 2, respectively.

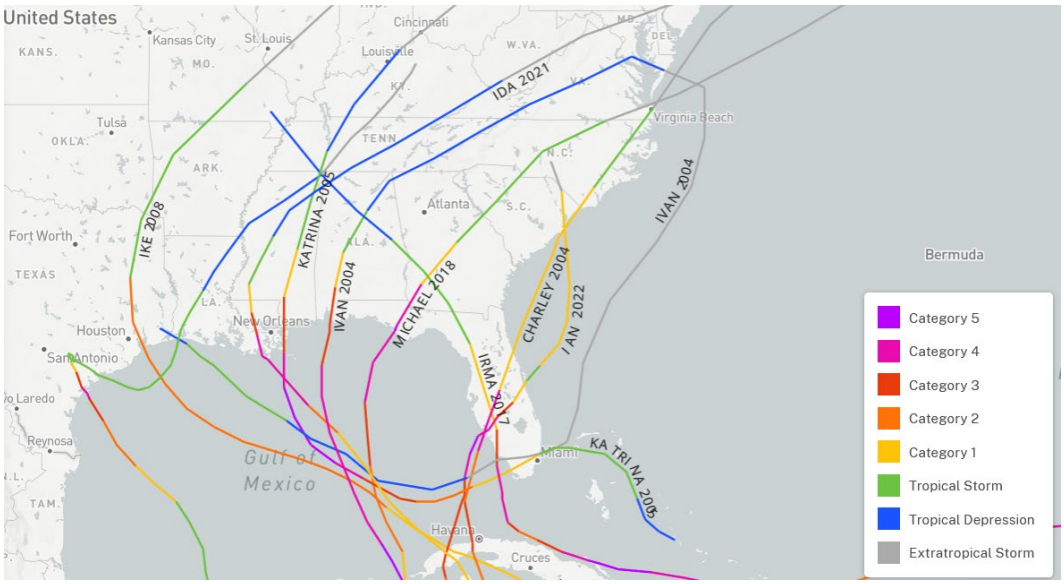


Figure 4. Recent hurricanes (2004 – 2022)

Two primary regions where the design wind speeds, as specified by ASCE 7, range between 130 and 140 mph are Central Florida and the Florida Panhandle. These regions also feature water bodies, such as lakes or inland bays, that might contribute to generating Exposure D condition. Hurricanes Charley (2004), Irma (2017), Michael (2018), and Ian (2022) were identified as significant events that impacted these areas. According to damage assessment reports, most hurricanes making landfall in these regions did not exceed the design wind speeds.

Following the selection of storms, publicly available damage assessment reports were extensively reviewed to identify evidence of wind-borne debris damage, particularly in inland areas. Notably, hurricanes Charley and Michael provided limited but significant evidence of wind-borne debris damage. These hurricanes are highlighted in green in Table 2, as their reports confirmed debris impacts, even in inland locations. Both affected areas are as WBDRs in ASCE 7-22.

Table 2. Recent hurricanes (2004 – 2022)

| Hurricane | Year | Primary Observations |
|---|---|---|
| **Charley** | 2004 | Affected Punta Gorda, FL. Estimated wind speeds exceeded design levels (at landfall). Classified as WBDR. Evidence of wind-borne debris damage, including some inland areas. |
| **Ivan** | 2004 | Affected Pensacola, FL. Estimated wind speeds were below design levels. Pensacola is classified as WBDR. |
| **Katrina** | 2005 | Affected Mississippi, Louisiana, and Alabama. Estimated wind speeds were below design levels. Imagery focused on structural failures due to storm surge; no wind-borne debris evidence. |
| **Ike** | 2008 | Affected Texas. Estimated wind speeds were below design levels. |
| **Harvey** | 2017 | Affected Texas. Estimated wind speeds were below design levels. |
| **Irma** | 2017 | Affected Florida. Estimated wind speeds were below design levels. Classified as WBDR. |
| **Michael** | 2018 | Affected Florida Panhandle. Estimated wind speeds exceeded design levels in some areas. Significant evidence of wind-borne debris damage, but no evidence in inland areas. |
| **Ian** | 2022 | Affected Punta Gorda, FL. Estimated wind speeds below design levels. Classified as WBDR. Imagery focused on structural damage with limited documentation of wind-borne debris. |

## 4.2 Limitations

The damage assessments review faced several limitations for the purposes of this study. Most damage assessment reports and imagery prioritized and focused on the most severely impacted areas at landfall, particularly along shorelines, providing minimal data on wind-borne debris impacts in inland areas near lakes or other water bodies. Research teams' investigations were constrained to accessible locations, often overlooking areas near inland water bodies. Additionally, there was a significant lack of very specific investigations into wind-borne debris effects in inland regions, leaving critical data gaps that limit comprehensive analysis. The absence of this data in these reports does not preclude the occurrence of debris damage in areas outside the assessment regions.

## 4.3 Summary of damage assessment findings

A summary of critical findings from each storm is presented in Table 3, followed by detailed analyses in subsequent sections. Table 3 summarizes wind speed observations and performance outcomes for selected hurricanes across various U.S. coastal locations. Each row includes the hurricane name and year, the type of location affected (e.g., coastal, inland, or near open water), the specific location, the maximum wind speed recorded or estimated during the event, and the applicable design wind speed from the ASCE 7 standard in effect at the time. The final column provides key observations from post-storm assessments, such as the presence of wind-borne debris damage, structural failures, or exceedance of design conditions. In the case of Hurricane Charley and Hurricane Ivan, the design wind speeds in 2004 were governed by ASCE 7-98 which was the applicable standard prior to the publication of ASCE 7-02 and the later ASCE 7-05. At that time,

design wind speeds were defined using fastest-mile wind speed, not the current 3-second gust format. Table 3 presents the design wind speeds for Hurricane Charley and Hurricane Ivan in the ASCE 7-98 format and in 3-second gust terms for comparison purposes. The design wind speeds for the remaining events in Table 3 are presented in the applicable ASCE 7 version.

The impacts of Hurricanes Ike and Harvey provide further insight into wind-borne debris risks and structural vulnerabilities. Hurricane Ike, despite having wind speeds below ASCE 7-05 design thresholds (90–110 mph compared to the design range of 130–150 mph), caused extensive damage due to wind-borne debris from failing asphalt shingles, vinyl siding, and fiber cement siding. Many failures resulted from improper material selection and poor installation practices. The FEMA Mitigation Assessment Team (MAT) observed widespread soffit and attic ventilation failures, which allowed water intrusion, exacerbating interior damage. Improper shutter installations also left many buildings vulnerable.

Hurricane Harvey made landfall with sustained winds of 130 mph, with observed speeds between 120 and 140 mph, near ASCE 7 design thresholds. Despite this, significant damage occurred, especially in older structures with weaker Main Wind Force Resisting Systems (MWFRSs). The IBHS investigation found that wind acceleration over Copano Bay contributed to extreme damage in Rockport Northwest and Holiday Beach. Windborne debris—including shingles, roofing materials, and siding—punctured walls, doors, and windows, leading to internal pressurization and water infiltration. Newer homes performed better than older ones, but failures were still observed despite wind speeds not exceeding design values.

These findings align with inland wind-borne debris observations from other hurricanes. After Hurricane Charley (125–130 mph winds), damage was recorded over three miles inland, raising questions about the adequacy of the one-mile WBDR designation. Similarly, Hurricane Michael (125–140 mph winds) caused debris impacts over three miles inland from St. Andrew Bay in Panama City, reinforcing concerns about debris risks near inland bays. The collective findings from these storms highlight the need for further research into wind-borne debris distribution and its implications for building codes and mitigation strategies.

Table 3. Summary of the damage assessments observed for the hurricanes impacting the Atlantic coast of the U.S (2004 – 2022).

| Hurricane | Year | Type of Location | Location | Wind Speed Recorded | Design Wind Speed in the Applicable ASCE 7 Version | Main Observations |
|---|---|---|---|---|---|---|
| **Charley** | 2004 | Charlotte Harbor | Mangrove Point, just southwest of Punta Gorda, Florida. | 145-150 mph | 130 mph (fastest-mile in ASCE 7-98) ≈ 150–160 mph 3-second gust (equivalent to current format) | The wind speed observed exceeded the design wind speeds. Extensive wind-borne debris damaged observed in Punta Gorda, however Punta Gorda is currently considered within the wind-borne debris due to the being located between 140 - 150 mph design wind speed. Some damage was observed in Orlando and Pine Island. Some wind-borne debris damage was observed in Acadia; however, this specific place located further than 1 mile from Exposure D condition. |
| **Ivan** | 2004 | Inland Bay | Pensacola, FL area | 95-120 mph | 130 mph (fastest mile in ASCE 7-98) ≈ 150-160 mph 3-second gust (equivalent to current format) | Hurricane Ivan did not exceed the design wind speeds. There is no evidence in the Mitigation Assessment Team Report from FEMA and in the wind investigation report from RICOWI of wind-borne debris damage. |
| **Katrina** | 2005 | Coastal | Mississippi: from Pascagoula westward to Ocean Springs. Mississippi Coast. Biloxi, D'Iberville, and Gulfport, Mississippi. | 90-120 mph.<br>120-130 mph.<br>120-130 mph | 140-150 mph<br>(ASCE 7-02) | Hurricane Katrina did not exceed the design wind speeds. There is no evidence of wind-borne debris damage in the wind investigation report from RICOWI. |
| **Ike** | 2008 | Galveston Bay | Houston, Friendswood, Webster, Anahuac, Stowell, Liberty and Winnie, Texas. Deer Park, Friendswood, Cooper Field, Houston and Pasadena. | 90 mph.<br>100-110 mph | Anahuac and Stowel: 140 - 150 mph<br>All others: 130-140 mph<br>(ASCE 7-05) | Hurricane Ike (2008) made landfall near Galveston, Texas, with wind speeds of 90–110 mph, below ASCE 7-05 design thresholds (130–150 mph). Despite this, significant damage occurred due to wind-borne debris from failing asphalt shingles, vinyl siding, and fiber cement siding. The FEMA MAT attributed much of the damage to non-hurricane-rated materials, poor installation, and weak code enforcement. The findings emphasized the need for stronger building standards and enforcement to improve resilience in hurricane-prone areas. |
| **Harvey** | 2017 | Aransas Bay, Copano Bay. Port Aransas South: Coastal | Rockport Northwest, TX.<br>Port Aransas South, TX.<br>Holiday Beach, TX.<br>Rockport Southeast, TX. | 120- 130 mph.<br>120- 130 mph.<br>120- 130 mph.<br>130- 140 mph. | 140 - 150 mph<br>(ASCE 7-16) | Hurricane Harvey (2017) made landfall in Texas with sustained winds of 130 mph, with observed speeds between 120 and 140 mph. The FEMA MAT documented failures in MWFRSs in older buildings, along with extensive damage to roof coverings and rooftop equipment. Windborne debris, including shingles, roofing materials, and siding, caused structural breaches, leading to internal pressurization and severe water damage. The IBHS identified Rockport Northwest and Holiday Beach as experiencing the most severe structural damage due to wind acceleration over Copano Bay. |

| Hurricane | Year | Type of Location | Location | Wind Speed Recorded | Design Wind Speed in the Applicable ASCE 7 Version | Main Observations |
|---|---|---|---|---|---|---|
| **Irma** | 2017 | Coastal (WBDR) | Naples, Marco Island, Goodland, Everglade City, Ponte Vedra Beach, St. Augustine, Miami, Marathon, Cudjoe Key, Key West. Collier, Lee, Miami-Dade, and Monroe Counties. | 60-120 mph | Naples: 160-170 mph. Marco Island: 165-175 mph. Goodland, Everglade City: 160-170 mph. Ponte Vedra Beach, St. Augustine: 120-130 mph. Miami: 175-185 mph. Marathon, Cudjoe Key, Key West: 170-180 mph. Collier and Lee Counties: 160 - 170 mph. Miami Dade: 175-185 mph. Monroe County: 170-185 mph. (ASCE 7-16) | Although there is plenty of evidence of wind-borne debris damage caused by hurricane Irma in multiple damage assessment reports (FBC, FEMA, RICOWI, etc.) all the surveys took place in the wind-borne debris region where the design wind speeds were not exceeded. Unfortunately, there are no inland areas that could provide evidence of wind-borne debris. |
| **Michael** | 2018 | Inland Bay | Florida Panhandle: Bay, Calhoun, Franklin, Gulf, Jackson, and Wakulla Counties. Panama City. | 161 mph. Panama City: 135-140 mph | Bay, Franklin, Gulf, Wakulla: 130-145 mph. Calhoun and Jackson: 100-120 mph. Panama City: 135 mph (ASCE 7-16) | Many communities along Michael's track experienced wind speeds exceeding the design wind speeds specified in ASCE 7-10 for Risk Category II buildings. Wind gusts surpassed design levels by over 10% in several counties. Data from the Florida Coastal Monitoring Program (FCMP) confirmed wind gusts exceeding 120 mph for extended periods near the affected areas. Notable wind-borne debris damage was observed and reported in areas like Mexico Beach and Panama City, where estimated wind speeds exceeded design levels, though these areas were not classified as wind-borne debris regions under ASCE-7 standards due to their distance from the coast. |
| **Ian** | 2022 | Charlotte Harbor | Ft. Myers, FL. Cape Coral, FL. Punta Gorda, FL. Port Charlotte, FL. | Ft. Myers and Cape Coral, 90-130 mph. Cayo Costa, 150 mph. Iona, 140.3 mph (peak wind gust). Punta Gorda, 135 mph. | Ft. Myers: 160-170 mph Cape Coral: 170-180 mph Punta Gorda: 160-170 mph (ASCE 7-22) | Estimated peak winds approached but remained slightly below the design levels specified under the building code. However, the event likely represented a design-level wind event for buildings constructed under pre-Hurricane Andrew code. Failures of auxiliary structures, roof coverings, and cladding elements created substantial wind-borne debris impacts, exacerbating the failure of openings like windows and doors. Limited imagery from multiple sources (IBHS, RICOWI and StEER reports). |

## 4.4 Detailed damage assessments by storm

### *4.4.1 Hurricane Charley (2004)*

Hurricane Charley struck Punta Gorda, Florida, in 2004. The storm crossed barrier islands, including Cayo Costa and Gasparilla, with recorded wind speeds reaching 150-145 mph. The design wind speed for the area where damage assessments were carried out by the Mitigation Assessment Team (MAT) from the Federal Emergency Management Agency (FEMA) was noted to be 110-130 mph, indicating that the observed wind speeds exceeded the design wind speeds for the sites of interest (FEMA, 2005).

The Port Charlotte and Punta Gorda areas, located within the wind-borne debris region, suffered extensive damage, while inland areas like Arcadia, outside this region, experienced less severe effects. Key findings from damage assessments (from the University of Florida and the Insurance Institute for Business & Home Safety: IBHS) highlight the vulnerability of unprotected glazing. In Punta Gorda and Port Charlotte, where wind speeds ranged from 125–130 mph, one-third of homes without shutters had broken windows, compared to minimal damage in areas with winds below 100 mph (Gurley and Masters, 2011). Homes with shutters or laminated glass experienced significantly less damage, demonstrating the importance of these protective measures. Debris from roof coverings caused significant damage even in lower-wind-speed areas.

Significant damage was frequently observed in areas with clay and concrete roof tiles and in neighborhoods where wood structural members were released as missiles. Many buildings with mortar-set tiles lost significant roof cover (Figure 5). Figure 6 shows the impact of a roof tile that punctured a Miami-Dade County-approved shutter and broke the window.

Figure 5. Extensive damage of pre-2001 FBC home. Broken windows caused by wind-borne debris during Hurricane Charley (2004).

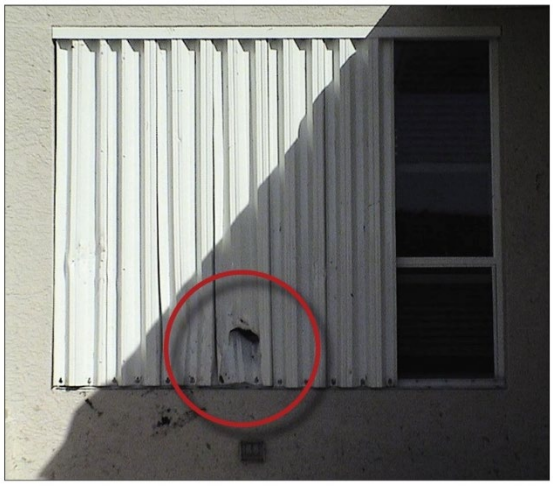

Figure 6. A roof tile punctured a Miami-Dade County approved shutter in Punta Gorda Florida during Hurricane Charley (2004).

The importance of the height at which debris was released was also evident as far inland as the Orlando area. When a piece of debris is released into the wind field at a significant height, there is greater potential for that debris to remain aloft and accelerate. An example of this was observed in the atrium of the hotel shown in Figure 7.

Figure 7. Damage to glass atrium in Orlando caused by wind-borne debris during Hurricane Charley (2004).

Wind-borne debris observed by the damage assessment team included roof coverings, structural and non-structural building elements, tree limbs, refuse containers, lawn furniture, and vehicles. Figure 8 through 10 show examples of wind-borne debris. Small debris, such as the roof shingle stuck in the side of the column in Figure 5, traveled a great distance (perhaps one mile) because this community only allowed tile roofs. As expected, larger items did not travel as far, although

the section of roofing from a wood-frame building on Captiva Island traveled approximately 200 yards after being separated from the original structure.

Figure 8. Asphalt shingle on a column in Punta Gorda during Hurricane Charley (2004)

Figure 9. Damage to a garage door in Punta Gorda during Hurricane Charley (2004)

Figure 10. Impact of structural wood in the gable end in Pine Island during Hurricane Charley (2004)

While the Florida Building Code does not apply directly to manufactured homes, a significant amount of aluminum and sheet metal debris from attached structures that failed and glazing damage was observed even in inland mobile home parks. A manufactured home park observed with homes spaced considerable distances apart appeared to have greater wind-borne debris damage (Figure 11).

Figure 11. Wind-borne debris damage on windows caused metal roof panel and siding in Port Charlotte during Hurricane Charley (2004).

Investigations at hospitals and other buildings with aggregate roof ballast revealed that the aggregate caused damage to windows on the debris-source building. Damage to windows in the intensive care unit of the hospital in Arcadia (Figure 12) is an example of this effect.

Figure 12. Damage in the windows in a hospital in Arcadia during Hurricane Charley (2004). EWS = 110-120 mph.

In addition to wind-borne debris, buildings were damaged by several types of falling objects, including trees, communications towers, rooftop equipment, and chimneys. The uprooting or fracture of large pine and hardwood trees was observed throughout the areas surveyed. On the barrier islands, tree damage resulted in severe access problems, blocking roads and driveways and

creating a severe fire danger. Inland, the tree damage was more isolated, but was frequently spectacular as trees came to rest on or sliced through buildings. Manufactured homes typically suffered the greatest damage from tree fall. Figure 13 shows a fallen communications tower at a fire station. Figure 14 to Figure 21 shows additional wind-borne debris damage caused by hurricane Charley in several locations (both site-built and manufactured).

Figure 13. Fire station with a missile (in the red circle) caused by Hurricane Charley (2004), in Punta Gorda.

Figure 14. Broken window from debris (in the red circle) caused by Hurricane Charley (2004), in Punta Gorda.

Figure 15. Broken windows in an office caused by Hurricane Charley (2004) in Punta Gorda.

Figure 16. Windows broken in a manufactured home by wind-borne debris during Hurricane Charley (2004) at the east of Port Charlotte.

Figure 17. Broken window by wind-borne debris during Hurricane Charley (2004), in Deep Creek.

Figure 18. Metal awning shutter penetrated by a missile in Zolfo Springs during hurricane Charley (2004).

Figure 19. Broken glass windows caused by wind-borne debris during hurricane Charley (2004) in Wauchula.

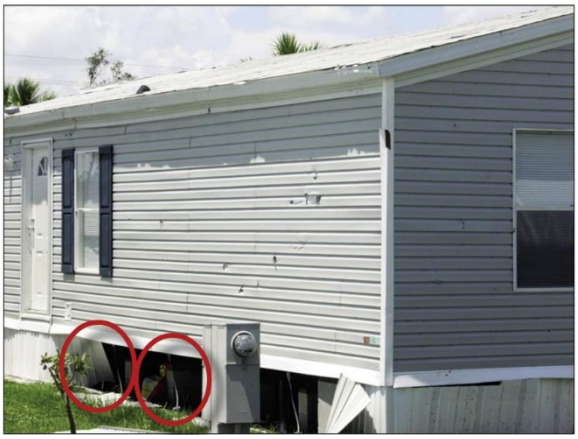

Figure 20. Vinyl siding affected in several location by wind-borne debris in Zolfo Springs during Hurricane Charley (2004).

Figure 21. Broken window caused by wind-borne debris in a high school in Punta Gorda during Hurricane Charley (2004).

### *4.4.2 Hurricane Ivan (2004)*

The analysis of wind speeds during Hurricane Ivan, performed by FEMA (2005), indicates that the maximum recorded 3-second peak gusts at 10 meters ranged from 109 mph in Gulf Shores and Pensacola Beach to 117 mph in Perdido Key. These values are significantly below the design wind speeds of 140–150 mph in current codes. However, they were close to or exceeded the design levels used in the Standard Building Code over the past two decades.

### *4.4.3 Hurricane Katrina (2005)*

Roofing Industry Committee on Weather Issues, Inc. (RICOWI), investigated damage caused by Hurricane Katrina in the landfall regions in Louisiana and Mississippi. Estimated wind speeds at damage locations came from simulated hurricane models prepared by Applied Research Associates. A dynamic hurricane wind field model was calibrated to actual wind speeds measured at 12 inland and offshore stations. The maximum estimated peak gust wind speeds in Katrina were in the 120–130 mph range. A significant portion of the regions that experienced the highest winds of Katrina were concurrently inundated with catastrophic storm surge that erased evidence of wind related damage.

### *4.4.4 Hurricane Ike (2008)*

Hurricane Ike made landfall on September 13, 2008, near Galveston, Texas. Although Hurricane Ike's wind speeds were below the design speeds prescribed by the American Society of Civil Engineers (ASCE) 7-05, significant damage to building envelopes, including wind-borne debris, highlighted vulnerabilities in construction practices, material choices, and code enforcement. The storm caused substantial losses of building materials such as roof coverings and siding, creating a significant debris hazard.

According to the Mitigation Assessment Team report 'Hurricane Ike in Texas and Louisiana' (FEMA, 2009), the MAT found that much of the damage was associated with building products not designed for hurricane-prone regions and improper installation practices. The most frequently observed issues were the loss of asphalt shingles, the predominant roofing material in affected areas, and damage to vinyl siding and fiber cement siding. Many failures stemmed from insufficient attachment methods or the use of materials not certified for high-wind zones. Figure 22 from the MAT report illustrates the extensive debris generated by these failures, which often became wind-borne hazards.

The MAT also observed that vinyl soffits and attic ventilation systems frequently failed, allowing water infiltration and damaging the interior and contents. Impact-resistant laminated glass window units were rarely used in the affected areas, with most homeowners relying on shutters to protect glazed openings from debris impacts. However, improper installation of some shutters, such as securing them only to window frames rather than structural components, reduced their effectiveness. In some cases, homeowners shuttered only seaward-facing windows or windows close to ground level, leaving other elevations vulnerable to Ike's winds. Figure 23 demonstrates the consequences of this selective shuttering practice.

Figure 22. Siding and roofing materials blew off these West Galveston houses during hurricane Ike (2008) becoming potential projectiles.

Figure 23. Window vulnerable to wind-borne damage due to improper installation of shutters.

### *4.4.5 Hurricane Harvey (2017)*

Hurricane Harvey made landfall in Texas in August 2017. As a Category 4 storm with sustained winds of 130 mph, it caused immense destruction. The wind pressures produced by the storm closely matched or exceeded design thresholds. Despite flooding causing the majority of Hurricane Harvey's overall damage, near-design-level wind speeds in areas close to the storm's landfall caused significant structural and envelope damage. The FEMA MAT observed damage to Main Wind Force Resisting Systems (MWFRSs) in older residential and non-residential buildings as described in their report 'Hurricane Harvey in Texas' (FEMA, 2019). The most common wind damage was to roof coverings and rooftop equipment. Many roofs were punctured or torn by wind-borne debris.

Figure 24 shows post-2009 construction located on the Intracoastal Waterway. The structure suffered major damage when its large, open, covered front porch experienced wind uplift. Figure

25 illustrates glazing damage from wind-borne debris. Such debris caused significant component and cladding (C&C) failures, including damage to metal roofing, the loss of window eyebrow roofs, and extensive water infiltration. Figure 26 shows a garage door damaged by debris impact.

Figure 24. Damage caused by wind-borne debris (green arrows) and wind uplift damage (red arrows) in a house in Rockport during Hurricane Harvey (2017). EWS = 130 mph, exposure C.

Figure 25. Damage in a window caused by the impact of wind-borne in a Key Allegro house during Hurricane Harvey (2017).

Figure 26. Damage caused by debris impact resulting in two bent rollers in Fulton during Hurricane Harvey (2017). EWS = 130 mph, exposure B.

The MAT documented widespread debris impacts throughout the affected areas, as illustrated in Figure 27 through Figure 32. These observations emphasized the importance of impact-resistant materials, robust MWFRS connections, and proper installation to mitigate wind and debris damage.

Figure 27. Damage in a post-2009 home caused by the impact of wind-borne debris (red arrows) in a Key Allegro house during Hurricane Harvey (2017). EWS = 140 mph, exposure C.

Figure 28. Damage on fiber cement siding (red arrow) caused by the impact of wind-borne debris in a Key Allegro house during Hurricane Harvey (2017). EWS = 120 mph, exposure C.

Figure 29. Damage on hardboard siding (red arrow) caused by the impact of plywood debris in a Port Aransas house during Hurricane Harvey (2017). EWS = 120 mph, exposure C.

Figure 30. Damage on stucco walls (red arrows) caused by small debris impact in Key Allegro. EWS = 120 mph, exposure C.

Figure 31. Damage on hardboard siding (red arrow) caused by multiple impact of debris in a Holiday Beach house during Hurricane Harvey (2017). EWS = 120 mph, exposure C.

Figure 32. Damage on a fiber cement wall (red arrow) caused by the impact of wind-borne debris in a Key Allegro house during Hurricane Harvey (2017). EWS = 140 mph, exposure C.

Lessons from Hurricane Harvey provide invaluable guidance for enhancing structural resilience and minimizing damage in future storms. By implementing stricter building codes, ensuring proper construction practices, and using debris-resistant materials, communities can significantly reduce the risks associated with extreme weather events.

The IBHS 'Hurricane Harvey wind damage investigation' (IBHS, 2018) reports Hurricane Harvey as the second-most costly hurricane in U.S. history (after adjusting for inflation), behind Hurricane Katrina (2005). IBHS suggests that the topography of the area resulted in the strongest winds flowing over the relatively smooth Copano Bay into two neighborhoods (Rockport Northwest and Holiday Beach). This allowed the mean flow to speed up relative to overland exposures upstream and these two neighborhoods had the most severe total damage of the areas investigated. The locations of both these neighborhoods are shown in Figure 33. Although Portland, Aransas Pass, Mustang Island and Port Aransas were within one half mile of the shore, the overland fetch reduced the mean wind speeds, thus causing less damage.

All the neighborhoods investigated by the IBHS team were located within the ASCE 7-10 design wind speed zone of 140–150 mph, and none of the areas investigated experienced peak 3-second gust wind speeds higher than 140 mph. Damage occurred to newer and older homes, summarized in the IBHS observations in Figure 34.

The IBHS team noted generally better performance of both residential and commercial buildings in areas of newer construction compared to older construction. Examples are shown in Figure 35 and Figure 36.

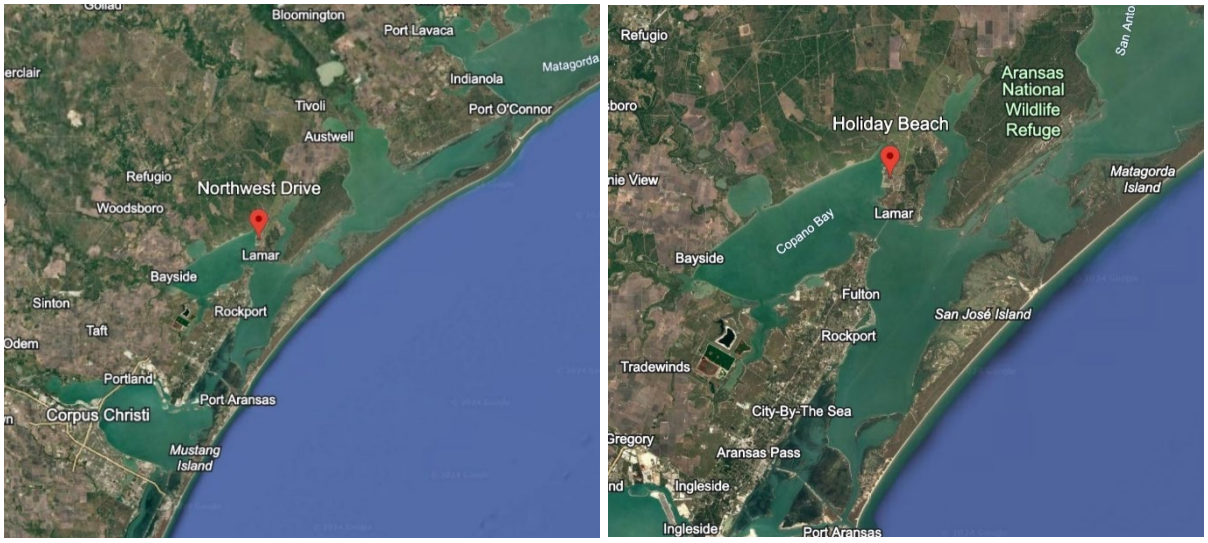

Figure 33. Location of Rockport Northwest (left) and Holiday Beach neighborhoods (right).

| Location | Construction Era | Estimated Wind Speed | General Damage State |
|---|---|---|---|
| *Portland* | 1960s–1970s | 80–90 mph | Minor: finishes, attached structures, roof cover |
| *Ingleside* | 1960s–1990s | 80–90 mph | Minor: finishes, garage, rooftop items, roof cover |
| *Mustang Island* | 1990s–2010s | 90–100 mph | Minor: finishes, garage, door, attached structures |
| *Aransas Pass* | 1990s–2000s | 110–120 mph | Minor: finishes, garage, rooftop items, roof cover |
| *Port Aransas North* | 1960s–2010s | 110–120 mph | Minor (newer homes), Major (older homes): finishes, wall structure, garage, windows, doors, attached structures, roof cover, roof structure |
| *Rockport Southeast* | 2000s | 120–130 mph | Minor: finishes, roof cover |
| *Holiday Beach* | 1960s–1990s | 120–130 mph | Major: finishes, wall structure, garage, windows, doors, attached structures, roof cover, roof structure |
| *Port Aransas South* | 2000s–2010s | 120–130 mph | Minor: finishes, wall structure, garage, windows, doors, attached structures, roof cover, roof structure |
| *Rockport Northwest* | 1960s–2010s | 130–140 mph | Major: finishes, wall structure, garage, windows, doors, attached structures, roof cover, roof structure |

Figure 34. Damage survey locations and characteristics. Source IBHS, Hurricane Harvey Wind Damage Investigation.

Figure 35. Port Aransas North: Two homes located 250 ft apart that experienced similar wind speeds during hurricane Harvey (2017). 1987 construction (left), 2006 construction (right).

Figure 36. Port Aransas North: Two commercial buildings located 1 mile apart that experienced similar wind speeds during hurricane Harvey (2017). 1984 construction (left), 2007 construction (right).

### *4.4.6 Hurricane Michael (2018)*

Many communities along the track of Hurricane Michael experienced wind speeds that exceeded design level wind speeds. Wind speeds in excess of ASCE 7-10 design levels occurred in Bay, Calhoun, Gadsden, Gulf, Jackson, and Liberty Counties (see Figure 37). In some locations, the wind speeds produced by Hurricane Michael exceeded ASCE 7 Risk Category II wind speeds by more than 10 percent. The highest wind gust recorded on land was 129 mph at a mobile weather station at Tyndall Air Force Base. This mobile weather station was installed by the University of Florida/Weatherflow in the hours preceding landfall. Shortly after recording the gust of 129 mph, the mobile weather station failed. A wind gust of 102 mph was recorded at the airport in Marianna, FL, near the state line with Georgia; the weather station at the airport remained in operation throughout the event. The mitigation assessment team report from FEMA found some wind-borne debris in residential buildings in Mexico Beach and Panama City (Figure 38). In those cases, the estimated wind speed exceeded the design wind speed. However, the observations correspond to areas not considered as wind-borne debris areas according to ASCE-7 because the observations were beyond 1-mile of the coast (Figure 39 to Figure 44).

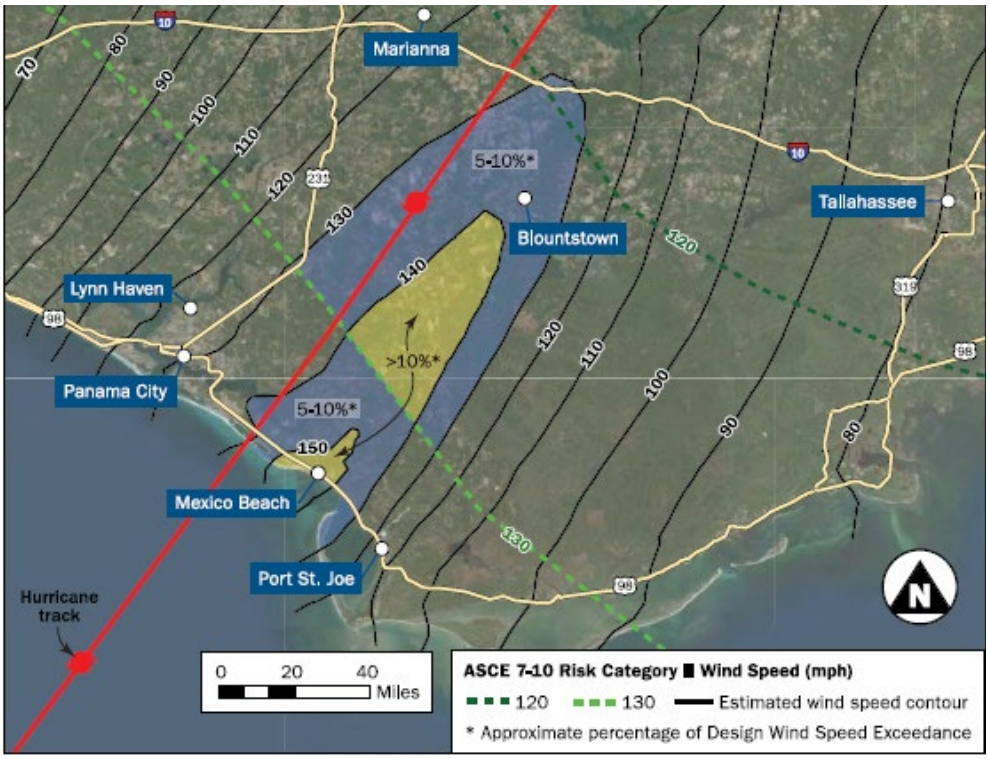


Figure 37. Wind swath plot showing the approximate exceedance of the design wind speed.

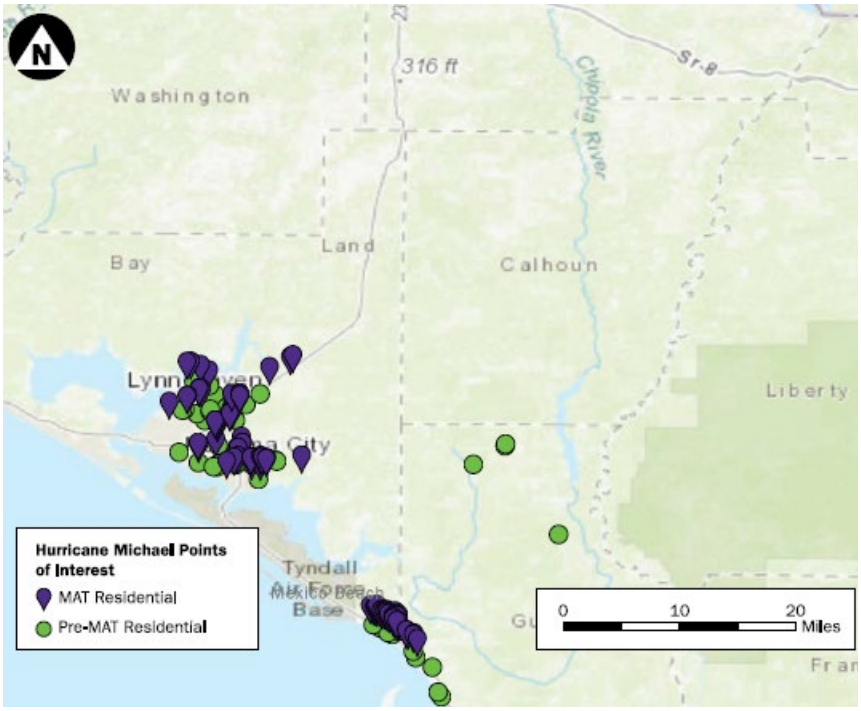


Figure 38. Residential and non-residential sites visited by FEMA hurricane Michael mitigation assessment team.

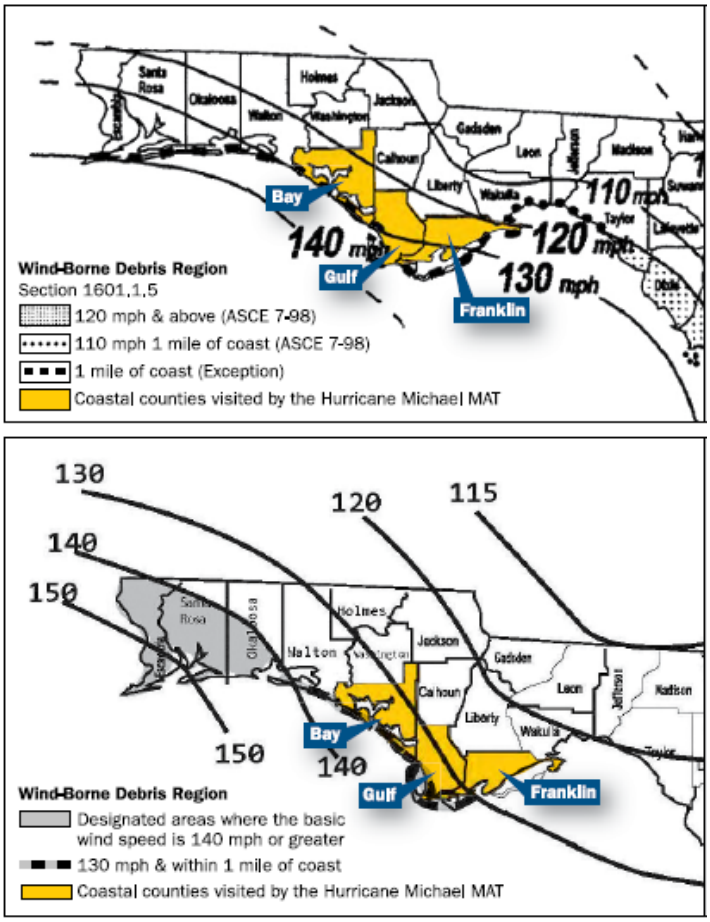


Figure 39. Design wind speeds according to ASCE 7-98 (top) and ASCE 7-10 (bottom) and the location of the counties visited by the Hurricane Michael Mitigation assessment team.

Figure 40. Impact resistant window after Hurricane Michael (2018) in a house built in 2010, located in Mexico Beach. Estimated wind speeds (150 mph) exceeded the design wind speeds (130 mph).


Figure 41. Glazed opening damage after Hurricane Michael (2018) in a house built in 2005, located in Panama City. Estimated wind speeds (128 mph) approached the design wind speed (133 mph).

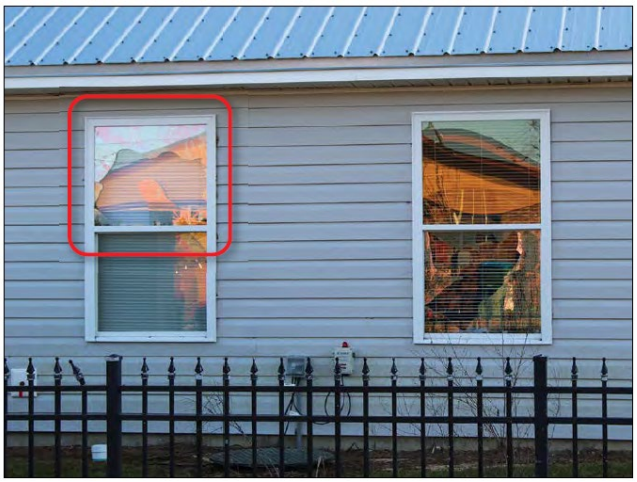

Figure 42. Glazed opening damage after Hurricane Michael (2018) in a house built after 2017, located in Panama City. Estimated wind speeds (134 mph) approached the design wind speeds (135 mph).

Figure 43. Glazed opening damage caused by an asphalt shingle after Hurricane Michael (2018) in a house built in 2012, located in Panama City. Estimated wind speeds (150 mph) exceeded the design wind speeds (126 mph).

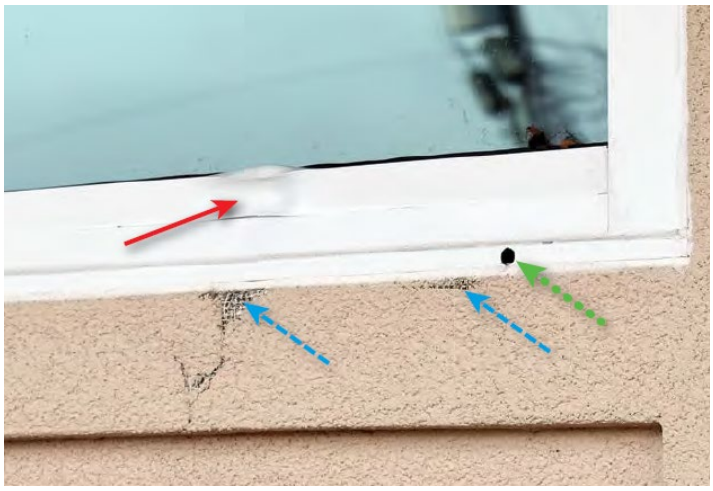

Figure 44. Window struck by wind-borne debris in Panama City during hurricane Michael (2018).

The StEER Hurricane Michael Preliminary Virtual Assessment Team Report (StEER, 2018) analyzed the impacts of Hurricane Michael. The report highlighted extensive wind and storm surge damage, with wind speeds exceeding design levels and storm surge causing catastrophic destruction, particularly in Mexico Beach (Figure 45). Older structures, especially those built before the 2002 Florida Building Code, experienced significant failures, including roof and wall collapses, while newer buildings fared better but still suffered damage to cladding, windows, and roof systems.

Figure 45. Widespread devastation to wood-framed single and multi-family residences in Mexico Beach with few survivors in areas with highest inundations (Source: New York Times)

Wind-borne debris posed a major threat, causing damage in areas not classified as wind-borne debris regions under ASCE-7 standards. Figure 46 to Figure 50 show some examples of the observed wind-borne debris damage caused by Michael in Panama City and Mexico Beach, often at distances exceeding three miles from St. Andrew Bay. The report emphasized the effectiveness of updated building codes while identifying gaps in addressing extreme wind and surge events. It recommended revising codes to include higher wind speeds and storm surge considerations, improving resilient designs with elevated construction and better anchoring, and enhancing risk assessments for inland exposure and wind-borne debris impacts. Strengthening critical infrastructure and promoting public awareness of resilient practices were also highlighted as priorities to enhance disaster preparedness and recovery.

Figure 46. Damage to roof and garage door in Panama City during Hurricane Michael (2018). House was built between 2000-2009 and located 3.39 miles from St. Andrew Bay. Estimated wind speeds (129-150 mph) might have exceeded the design wind speeds (135 mph).

Figure 47. Damage to a window cause by wind-borne debris in Panama City during Hurricane Michael (2018). House was built between 2000-2009 and located 3.27 miles from St. Andrew Bay. Estimated wind speeds (129-150 mph) might have exceeded the design wind speeds (135 mph).

Figure 48. Damage to windows in a house located in Panama City during Hurricane Michael (2018). House was built between 1990-1999 and located 3.25 miles from St. Andrew Bay. Estimated wind speeds (129-150 mph) might have exceeded the design wind speeds (135 mph).

Figure 49. Damage to a window in Panama City during Hurricane Michael (2018). House was built between 2010-2019 and located 3.39 miles from St. Andrew Bay. Estimated wind speeds (129-150 mph) might have exceeded the design wind speeds (135 mph).

Figure 50. Damage to a few windows in the shoreline of Mexico Beach during Hurricane Michael (2018). House was built between 2000-2009. Estimated wind speeds (150 mph) exceeded the design wind speeds (136 mph).

### *4.4.7 Hurricane Ian (2022)*

In the case of Hurricane Ian (2022), IBHS reported that estimated peak winds approached but fell just below modern design levels for the area impacted; however, the event likely was a design level event for older code regimes. The areas of Punta Gorda and Port Charlotte that were impacted by Hurricane Ian were the same areas hit by Hurricane Charley in 2004. The research report from IBHS states that the design wind speeds for the damage assessment areas where between 160 – 170 mph, and the maximum wind speeds where 150 mph, 140.3 mph and 135 mph in Cayo Costa, Iona and Punta Gorda, respectively. The same results were observed by RICOWI, Inc in their wind investigation report. According to RICOWI, in Cape Coral and Ft. Mayers, wind speeds between 90 – 130 mph were observed, while the design wind speeds for both places were 170 – 180 mph and 160 – 170 mph.

Wind induced structural damage was rare in site-built structures, even north of the track where peak wind estimates were highest, but there were isolated examples of structural roof failures and

partial wall collapses in older residential buildings built prior to the adoption of the Florida Building Code in 2002 (StEER report, 2022). Given the limitations of the imagery used in this study, it is difficult to determine if wind-borne debris impacts on tiles had an influence on damage location (Giammanco et al., 2023a). The failure of auxiliary structures, all roof cover types, and other cladding elements led to substantial wind-borne debris impacts on structures, exacerbating failures of openings such as windows and doors (Giammanco et al., 2023b).

# 5 Florida Lake Region Housing Analysis

This section analyzes the characterization of housing located within regions with designated design wind speeds of 130–140 mph and situated within one mile of bodies of water that contribute to an upwind Exposure D condition. This characterization provides critical insights into the distribution, geometry, and other attributes of typical neighborhoods in Florida, serving as essential input for the simulation-based approach to be conducted in this study by ARA (Task 3). Figures 1-3 (in Section 2) illustrate the locations of the primary bodies of water within the defined region of interest in Florida.

## 5.1 Methodology

The methodology begins with an investigation of major lakes, inland bays, and any body of water with a fetch greater than 5,000 feet in regions within the 130–140 mph design wind speeds. For this characterization, the identified water bodies were categorized into two regions: Central Florida and the Florida Panhandle.

Dr. David Roueche from Auburn University developed a GIS-based software application that provides detailed information on individual parcels across Florida, including geometry, year of construction, and other relevant attributes[2]. Using this app, a representative neighborhood was selected for each identified body of water. Within these neighborhoods, a typical residential building was chosen as an example for analysis. Table 4 and Table 5 present the characteristics of these selected residential buildings for Central Florida and the Florida Panhandle, respectively. These tables include information such as the county, associated lake or inland bay and its fetch, the construction year of the selected house, the house plan dimensions, spacing between houses (both on the same street and across the street), the number of stories, and the potential for future housing developments. Additionally, in Table 4 and Table 5 several of the lakes that are adjacent to state parks are highlighted, indicating that there is no potential for new housing developments.

Appendix A presents figures that represent the neighborhoods selected in Central Florida and the Florida Panhandle as part of the characterization methodology.

[2] Rouche, D. (2024). https://auburnuniversity.maps.arcgis.com/apps/mapviewer/index.html?webmap=6658c8891ba949bd9034d3a412640b88

## 5.2 Analysis results

For Central Florida, the majority of housing developments around lakes were constructed between 1980 and 1990, coinciding with a period of rapid population growth. Future development in these regions remains a possibility. A typical house in Central Florida is a single-story structure with a 45 x 60 ft plan. The typical spacing between houses is approximately 80 feet along the same street and 165 feet across the street.

In the Florida Panhandle, fewer lakes and inland bays meet the criteria for inclusion in the region of interest. While the majority of housing developments were built between 1980 and 1990, as in Central Florida, a significant portion of developments in this area predate this decade, resulting in a noticeable presence of older neighborhoods. The potential for future developments in this region is minimal, except for rebuilding to replace tear-downs. Typical houses in the Florida Panhandle also feature a single-story structure with a 45 x 60 ft plan. The typical spacing in these neighborhoods is approximately 90 feet along the same street and 165 feet across the street.

These characteristics inform the numerical simulations of wind-borne debris risk performed by ARA, described and presented in the next section. Recall that the goal of this effort is to determine the risk of damage from WBD to residential housing in the 130 – 139 mph design wind speed region, and within one mile of a body of water large enough to result in exposure D classification. This risk will be viewed in ratio with the WBD risk to homes in exposure B at the 140 mph contour.

Table 4. Characteristics of single-family neighborhoods in Central Florida in the 130-140 mph design wind speed region adjacent to large inland bodies of water.

| County | Lake/ inland bay | Fetch (ft) | Neighborhood | Building Year | House Plan | Distance between houses | | No. of stories | Potentially new dev. |
|---|---|---|---|---|---|---|---|---|---|
| | | | | | | Same street | Across street | | |
| **Lake County** | Lake Apopka | 39311 | Winter Garden | **2000-2009** | 50x60 ft | 90 ft | 150 ft | 2 | Yes |
| | John's Lake | 8530 | Killarney | **2000-2009** | 50x70 ft | 75 ft | 180 ft | 1 | Yes |
| | Clermont Chain of Lakes | | | | | | | | |
| | Lake Louisa | 14488 | Clermont | 1990-1999, **2000-2009** | 50x60 ft | 80 ft | 170 ft | 1 | Yes |
| | Lake Minnehaha | 17057 | Clermont | **1980-1989**, 1990-1999, 2000-2009 | 50x65 ft | 90 ft | 180 ft | 1 | Yes |
| | Lake Minneola | 11482 | Minneola | **2000-2009** | 45x60 ft | 85 ft | 170 ft | 1 | Yes |
| | Lake Harris Chain of Lakes | | | | | | | | |
| | Big Lake Harris | 27814 | Leesburg | **1950-1959**, 1960-1969, 1970-1979, 1980-1989, | 30x55 ft | 80 ft | 190 ft | 1 | Yes |
| | Little Lake Harris | 28491 | Howey-in-the-Hills | 1950-1959**,** **1960-1969**, 1970-1979, 1980-1989, | 45x75 ft | 95 ft | 170 ft | 1 | Yes |
| | Lake Eustis | 25387 | Leesburg | 1950-1959, 1960-1969, 1970-1979, **1980-1989**, 2000-2009 | 54x55 ft | 80 ft | 210 ft | 1 | Yes |
| | Lake Dora | 28592 | Tavares | 1950-1959, 1960-1969, 1970-1979, **1980-1989**, 2000-2009, 2010-2019, 2020-2029 | 40x50 ft | 75 ft | 150 ft | 1 | Yes |
| | Lake Griffin | Lake Griffin State Park | | | | | | | |
| | St. Johns River | River Preserve State Park | | | | | | | |
| **Sumter County** | Lake Panasoffkee | 42637 | Lake Panasoffkee | 1950-1959, 1960-1969, **1970-1979**, 1980-1989, 1990-1999, 2000-2009, 2010-2019, 2020-2029 | 55x45 ft | 75 ft | 160 ft | 1 | Yes |
| **Marion County** | Lake Weir | 18648 | Ocklawaha | **1950-1959,** 1960-1969, 1970-1979, 1980-1989, 2010-2019, 2020-2029 | 50x40 ft | 70 ft | 150 ft | 1 | Yes |
| **Volusia** | Lake George | 62247 | Georgetown | 1950-1959, 1960-1969, **1970-1979**, 1980-1989, 1990-1999, 2000-2009, | 45x40 ft | 90 ft | 140 ft | 1 | Yes |

| | | | | | | | | | |
|---|---|---|---|---|---|---|---|---|---|
| | | | | 2010-2019, 2020-2029 | | | | | |
| **Polk County** | Arbuckle | Blue Jordan Swamp | | | | | | | |
| | Lake Alfred | 7309 | Lake Alfred | 1950-1959, 1960-1969, **1970-1979**, 1980-1989, 1990-1999, 2000-2009, 2010-2019, | 60x40 ft | 85 ft | 155 ft | 1 | Yes |
| | Lake Ariana | 56492 | Auburndale | **1950-1959**, 1960-1969, 1970-1979, 1980-1989, 1990-1999, 2000-2009, 2010-2019, 2020-2029 | 55x45 ft | 80 ft | 140 ft | 1 | No |
| **Seminole County** | Lake Monroe | | Sanford | **1950-1959**, 1960-1969, 1970-1979, 1980-1989, 1990-1999, 2000-2009, 2010-2019, 2020-2029 | 50x40 ft | 60 ft | 160 ft | 2 | Yes |
| | Lake Jessup/Lake Harney | 14658 | Winter Springs | 1960-1969, **1970-1979**, 1980-1989, **1990-1999**, 2000-2009, 2010-2019 | 55x45 ft | 70 ft | 160 ft | 2 | Yes |
| **Orange County** | Lake Conway | 5944 | Belle Isle | **1950-1959**, 1960-1969, 1970-1979, 1980-1989, 1990-1999, 2000-2009, 2010-2019, 2020-2029 | 75x50ft | 80 ft | 175 ft | 1 | No - seems unlikely |
| | <u>Butler Chain of Lakes</u> | | | | | | | | |
| | Lake Butler | 7769 | Windermere | 1950-1959, 1960-1969, 1970-1979, **1980-1989**, 1990-1999, 2000-2009, 2010-2019, 2020-2029 | 80x60 ft | 100 ft | 200 ft | 2 | Yes |
| | Lake Down | 7893 | Windermere | 1970-1979, **1980-1989,** 1990-1999, 2000-2009, 2010-2019, 2020-2029 | 95x85 ft | 150 ft | 250 ft | 1 | Yes |
| | Lake Tibet | 10790 | Bay Hill | 1970-1979, 1980-1989, | 85x70 ft | 100 ft | 200 ft | 2 | No |

| | | | | | | | | | |
|---|---|---|---|---|---|---|---|---|---|
| | | | | 2010-2019, 2020-2029 | | | | | |
| | Lake Louisa | 14488 | Clermont | 1950-1959, 1970-1979, 1980-1989, 1990-1999, **2000-2009**, 2010-2019, 2020-2029 | 55x45 ft | 90 ft | 200 ft | 1 | Yes |
| **Osceola County** | Lake Kissimmee | 61062 | Uninhabited- Wildlife Reserve | | | | | | |
| | Lake Tohopekaliga | 43270 | Kissimmee | 1950-1959**,** 1970-1979, **1980-1989**, 2010-2019 | 70x60 ft | 115 ft | 200 ft | 1 | Yes |

Table 5. Characteristics of single-family neighborhoods in the Florida Panhandle in the 130-140 mph design wind speed region adjacent to large inland bodies of water.

| **County** | **Lake/ inland bay** | **Fetch (ft)** | **Building Year** | **House Plan** | **Distance between houses** | | **Land Size** | **No. of stories** | **Potentially new dev** |
|---|---|---|---|---|---|---|---|---|---|
| | | | | | **Same street** | **Across street** | | | |
| **Bay County** | Deer Point Lake | 12000-15000 | **1980-1989**, 1990-1999, 2000-2009 | 50x65 ft | 85-100 ft | 170-190 ft | 95x120 ft | 1 | Yes |
| | St. Andrews Bay | 30000-35000 | **1950-1959**, 1960-1969, 1970-1979 | 35x50 ft | 75 ft | 150 ft | 65x120 ft | 1 | No |
| | East Bay | 25000-30000 | **1980-1989** | 50x60 ft | 90-100 ft | 160-180 ft | 75x120 ft | 1 | Yes |
| **Gulf County** | Lake Wimico | 12000-14000 | Surroundings not populated | | | | | | No |
| | St Joseph Bay | 25000-30000 | 1960-1969, 1970-1979, **1980-1989** | 45x50 ft, 25x60 ft | 100 ft | 160 ft | 110x120 ft | 1 | Yes |
| **Walton County** | Lake Powell | 7500-8000 | WBDR | | | | | | |
| **Washington County** | Gap Lake | 5000-5500 | Lake not large enough | | | | | | |

# 6 Windborne Debris Modeling

The primary objective of this modeling effort is to assess the spatial extent of wind-borne debris (WBD) risk in residential neighborhoods located near large open water bodies, where Exposure D conditions prevail, and having design peak gust wind speeds ranging from 130 mph to 139 mph. The study evaluates 30 representative locations across central Florida and the Florida panhandle area, including both coastal and inland lake sites. Directional surface roughness lengths ($Z_o$) were first computed for each location. Subsequently, the Hurricane Missile (HurMis) modeling tool was used to simulate debris generation, transport, and impact frequencies across a modeled single-family residential neighborhood.

The simulations incorporate directionally dependent $Z_o$ values, hurricane wind trace with turbulence characteristics, and detailed component-level failure modeling for typical residential construction. For each site, simulations were conducted across multiple relative wind directions and at offset distances ranging from 0 to 5,000 feet from the water body, to capture the influence of surface roughness gradients on WBD risk. Debris impact results were normalized against a benchmark Exposure B scenario at 140 mph, producing "relative hit" metrics that quantify WBD risk on a consistent basis across locations. The modeling framework and detailed analysis results are presented in the following sections.

## 6.1 Methodology

The HurMis modeling tool was developed by ARA in the late 1990s and early 2000s to simulate wind-borne debris trajectories and impacts in residential neighborhoods during hurricane events. The tool employs a simulation methodology, based on a 3D physics-based framework, which was validated by performing simulations of entire subdivisions. In these simulations, debris missiles originating from failed components of upstream structures are individually tracked by integrating their equations of motion and assessing their trajectories and impacts on building envelopes and glazed openings.

Figure 51 illustrates the key components of the HurMis modeling framework. The model begins with a site-specific mean hurricane wind speed time history, onto which turbulent wind fluctuations are superimposed based on the site's surface roughness characteristics. The generation of hurricane wind fields and associated turbulence is described in detail by Twisdale et al. (1996). Unrestrained debris, such as failed tree limbs (when present), may become wind-borne if conditions permit, and are transported by numerically integrating their equations of motion at each time step. Each structure in the modeled subdivision acts both as a potential missile source and as a target. A three-dimensional load-and-resistance model is used to assess the failure of structural components including roof cover, roof sheathing, roof framing, and fenestrations under simulated hurricane conditions. If any roof components fail, the resulting debris is treated as new missiles, whose trajectories are governed by aerodynamic forces (drag, lift, and side force), as described in Twisdale et al. (1979). In the event of fenestration failure, internal pressures within the damaged structure are recalculated.

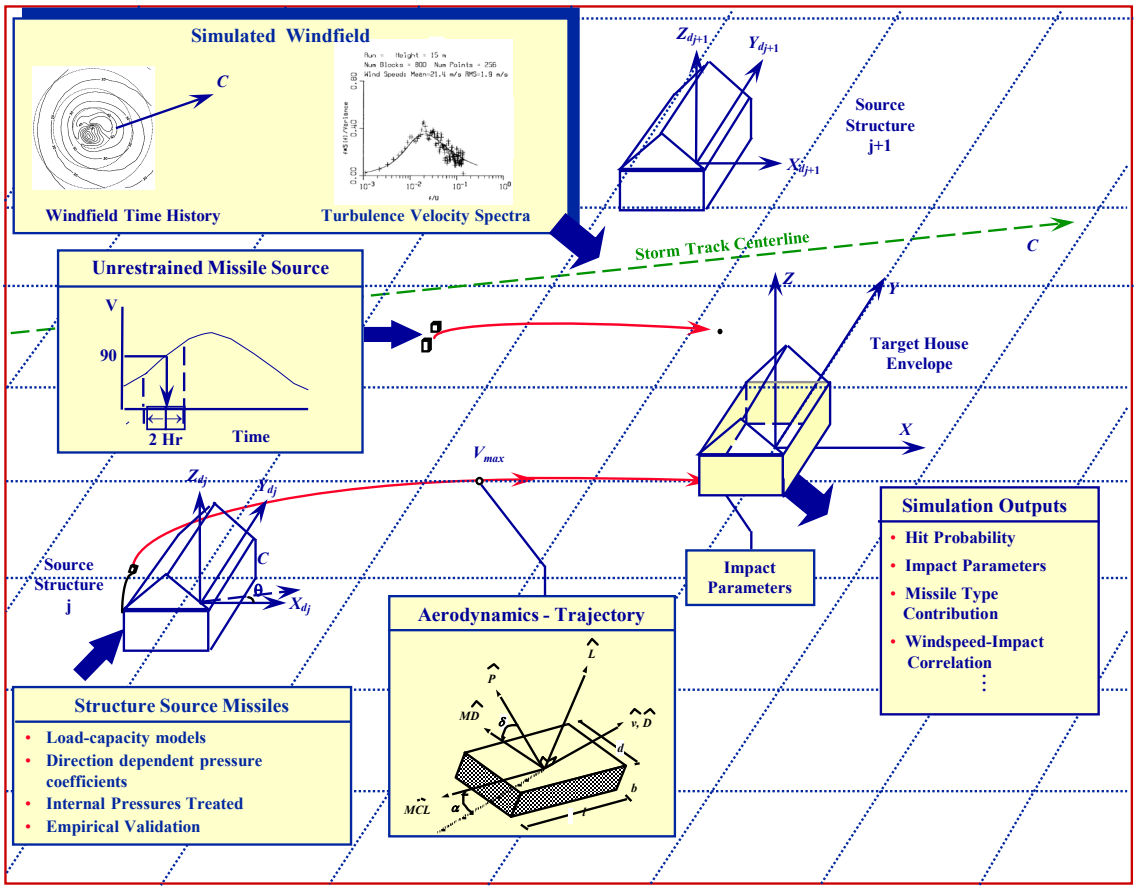


Figure 51. Wind generated missile source-target simulation modeling.

The HurMis model has been validated against post-storm damage surveys from multiple subdivisions impacted by Hurricanes Andrew, Erin, and Opal (Twisdale et al., 2002; Vickery et al., 2006). Validation included comparisons between modeled missile trajectories and observed damage patterns. Figure 52 presents a representative simulation output, showing missile impacts on a modeled subdivision. Blue markers indicate missile impact locations, while green boxes represent single-family residences, which serve as both missile sources and impact targets within the simulation domain. The HurMis model has been used for the development of ARA's HurLoss model as well as for Florida Depart of Community Affairs (DCA) projects.

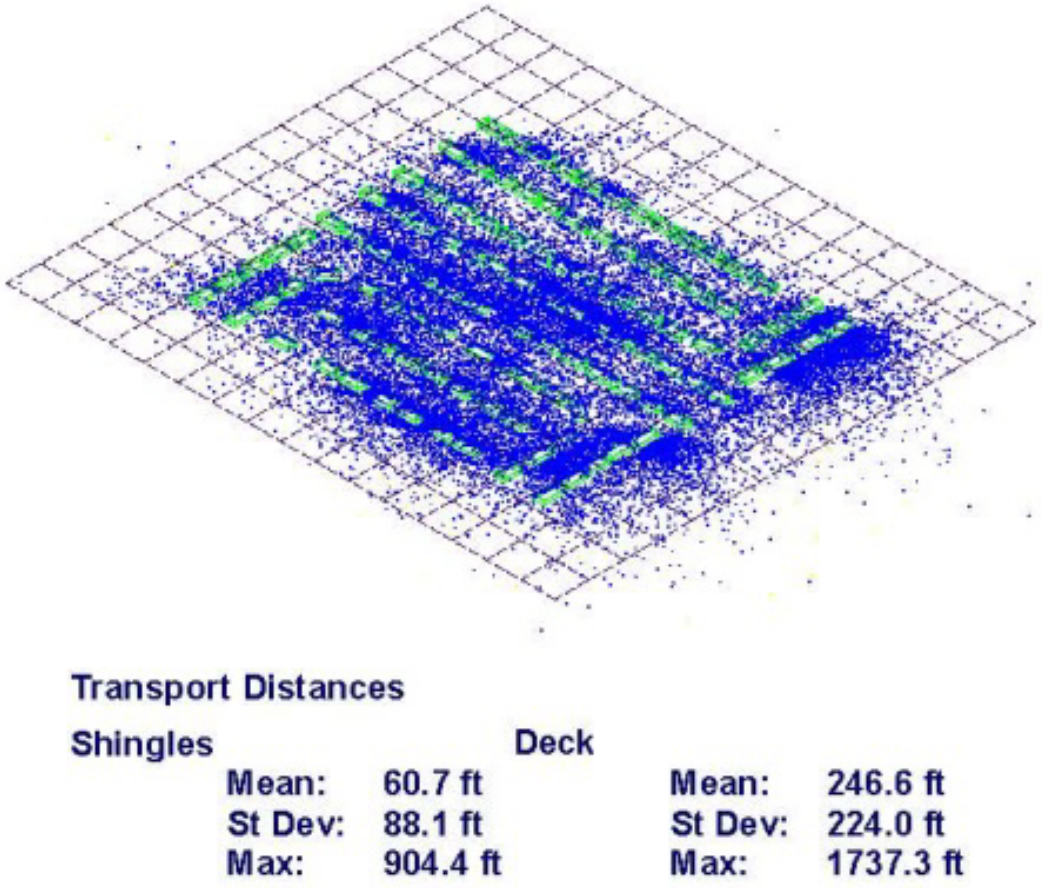


Figure 52. Realization of missile impact points (blue) within a subdivision of houses (green).

## 6.2 Application of Methodology to Inland & Coastal Regions

The following subsections discuss; (1) details of the residential neighborhood model used for this study, (2) directional estimation of surface roughness changes with distance from large water bodies, (3) simulation cases considered in this study, and (4) assumptions made to complete and limitations of this analysis.

### *6.2.1 Details of Neighborhood Modeled*

For this study, a residential neighborhood was modeled in HurMis to perform wind-borne debris simulations. The modeled neighborhood spans 1,000 feet by 1,000 feet and comprises 84 identical houses. These houses are uniformly distributed, with 12 houses per row and 7 rows in total, as illustrated in Figure 53.

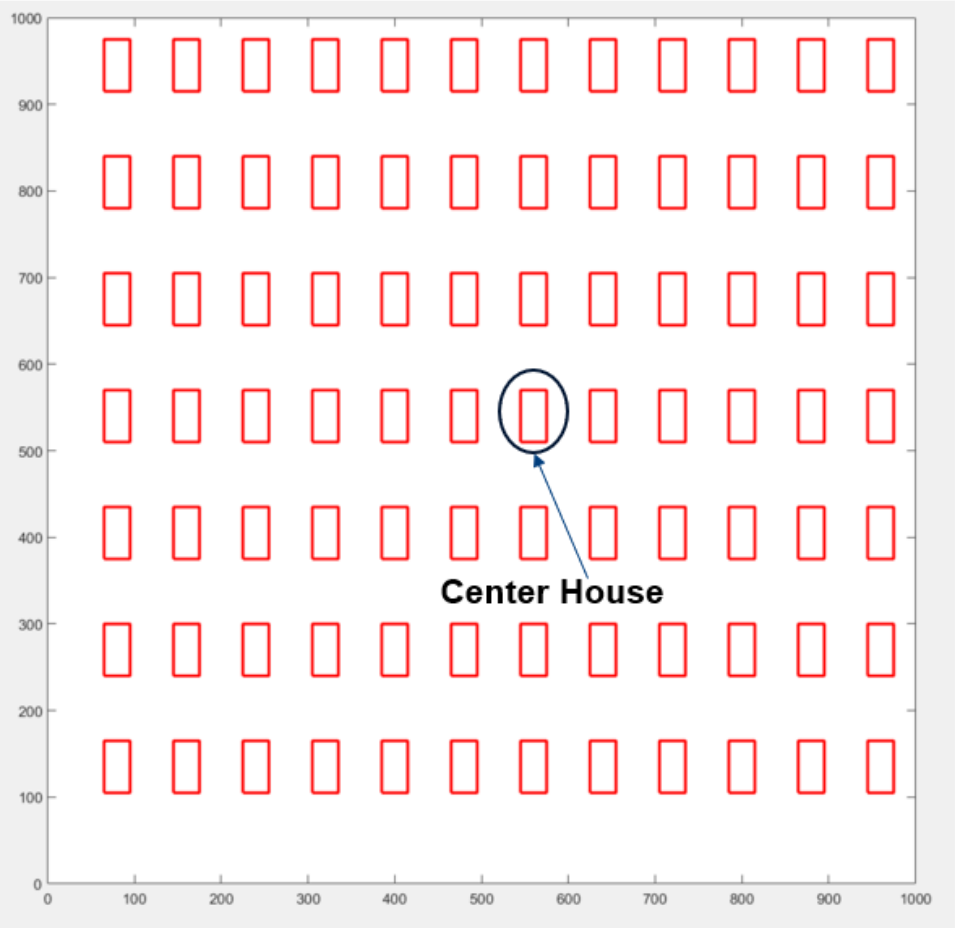


Figure 53. Plan view of the modeled neighborhood.

Each house is a one-story, wood-frame building with a gable roof, measuring 60 feet by 30 feet in plan with a mean roof height of 12 ft. The roof system consists of an average-quality Non-FBC asphalt shingle covering installed over plywood roof deck panels, which are attached to the roof framing using 8d nails with 6in/12in spacings. Each house has 27 windows, two non-engineered entry doors, and one non-engineered garage door. None of these openings are protected against wind-borne debris impacts. The long axis of each structure is oriented 90 degrees relative to the East. No tree debris is modeled within the neighborhood. The simulation considers only house-generated debris, specifically roof cover elements, roof deck panels, and roof framing components. The model includes 84 roof deck panels and 1,800 roof cover elements. Pressure coefficients for the roof cover elements and roof deck panels, corresponding to 36 different wind directions, were obtained from wind tunnel experiments conducted during the development of HurMis. For the purposes of this analysis, only debris impacts on wall surfaces are recorded across all houses.

### *6.2.2 Surface Roughness Changes with Distance from Exposure D Conditions*

To quantify the influence of terrain on WBD risk surface roughness length values ($Z_o$) were developed based on National Land Cover Dataset (NLCD). Twenty-three of the neighborhoods described in Tables 4 and 5 (see section 5.2) were used as inland neighborhoods to study across Central Florida and the Florida Panhandle in this analysis. An additional 7 locations were added

to consider coastal locations to compare the WBD risks for inland Exposure D conditions and coastal Exposure D conditions.

The coastal locations were chosen based on residentially developed areas between the 130-140 mph contours of the ASCE 7-22 Wind Speed Map. Table 6 presents all the locations considered for the simulation study. Figure 54 shows a Google Map View of the locations analyzed with the inland locations shown as green pins and the coastal locations shown as blue pins.

Table 6. Modeled neighborhood locations.

| Lake/Open Water Location | Location Type | Latitude (Degrees) | Longitude (Degrees) |
|---|---|---|---|
| Apalachicola | Coastal | 29.72 | -84.99 |
| Big Lake Harris | Inland | 28.80 | -81.88 |
| Coconut Palms | Coastal | 29.04 | -80.89 |
| Daytona | Coastal | 29.17 | -81.00 |
| Daytona Beach 2 | Coastal | 29.18 | -80.98 |
| Deer Point Lake | Inland | 30.24 | -85.67 |
| East Bay | Inland | 30.12 | -85.57 |
| Hernando Beach | Coastal | 28.49 | -82.67 |
| Lake Alfred | Inland | 28.09 | -81.73 |
| Lake Ariana | Inland | 28.07 | -81.80 |
| Lake Butler | Inland | 28.50 | -81.54 |
| Lake Conway | Inland | 28.47 | -81.35 |
| Lake Dora | Inland | 28.80 | -81.71 |
| Lake Down | Inland | 28.51 | -81.52 |
| Lake Eustis | Inland | 28.85 | -81.76 |
| Lake George | Inland | 29.37 | -81.62 |
| Lake Jessup | Inland | 28.71 | -81.28 |
| Lake Louisa | Inland | 28.50 | -81.74 |
| Lake Minnehaha | Inland | 28.54 | -81.77 |
| Lake Minneola | Inland | 28.59 | -81.76 |
| Lake Monroe | Inland | 28.81 | -81.25 |
| Lake Panasoffkee | Inland | 28.79 | -82.12 |
| Lake Tibet | Inland | 28.45 | -81.52 |
| Lake Tohopekaliga | Inland | 28.25 | -81.38 |
| Lake Weir | Inland | 29.04 | -81.93 |
| Little Lake Harris | Inland | 28.72 | -81.77 |
| Mexico Beach | Coastal | 29.94 | -85.40 |
| Palm Coast | Coastal | 29.59 | -81.18 |
| St Joseph Bay | Inland | 29.80 | -85.30 |
| St. Andrews Bay | Inland | 30.14 | -85.65 |


Figure 54. Google map view of the neighborhood locations with ASCE 7-22 wind speed contours.

#### *6.2.2.1 Methodology of Determining $Z_o$ Values*

The determination of $Z_o$ for each location considered in this study requires the establishment of an origin point and the use of an appropriate upstream fetch distance. For this purpose, the Big Lake Harris neighborhood was selected as a representative location, as it is characterized by a single source of Exposure D conditions on its southern side.

Figure 55 shows a Google Map View of Big Lake Harris and a location for the representative neighborhood is shown with a green pin. This location was selected to minimize the influence of other Exposure D conditions, such as Lake Griffin, located over 1 mile to the north-northeast of the chosen location.

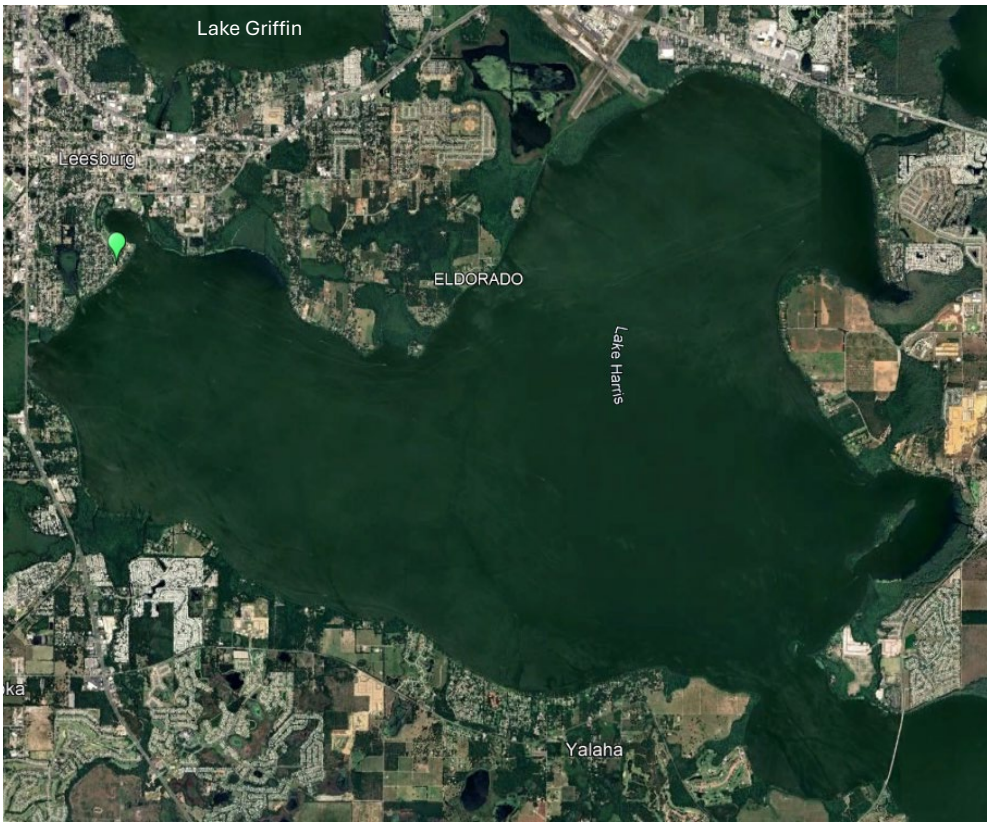


Figure 55. Google map view of Lake Harris.

When determining $Z_o$ for each location analyzed, directional mean $Z_o$ values were developed at 10-degree intervals ranging from 0° to 350°. For each of these directions a rectangular strip of 300 meters (i.e., width of the modeled neighborhood) by 1,500 meters (i.e., upwind fetch distance), with an additional 5-degree sector added on both sides as shown in Figure 56 over the Big Lake Harris neighborhood. For example, 0° direction denotes true North and includes influence of terrain from 355° to 5° directions. The rationale for selecting a fetch distance of 1,500 meters is discussed later in this section.

ARA develops surface roughness data from the Multi-Resolution Land Characteristic (MLRC) NLCD 2019 for use in its HurLoss software and FEMA's Hazus software. This process involves assigning surface roughness values, $Z_o$, to each land use/land cover (LULC) category in the NLCD, as listed in Table 7. $Z_o$ values associated with each LULC category were determined through review of actual terrain in several locations for each LULC category in a given region as described in the Hazus Hurricane Technical Manual (FEMA 2022). For two LULC categories ("Developed, Open Space"; and "Developed, Low Intensity"), the effect of 2016 NLCD tree canopy layer was used to adjust the assigned $Z_o$ values as described in FEMA (2022) to account for trees within these areas. The resulting product is a continuous raster of surface roughness which was subsequently used to determine the average directional surface roughness for each location analyzed in this study.

Figure 57 compares Google Earth Imagery to the NLCD raster data. The black regions in Figure 57(b) represent open water with an average $Z_o$ value of 0.003m while the white regions represent treed regions with an average $Z_o$ value of 0.9m.

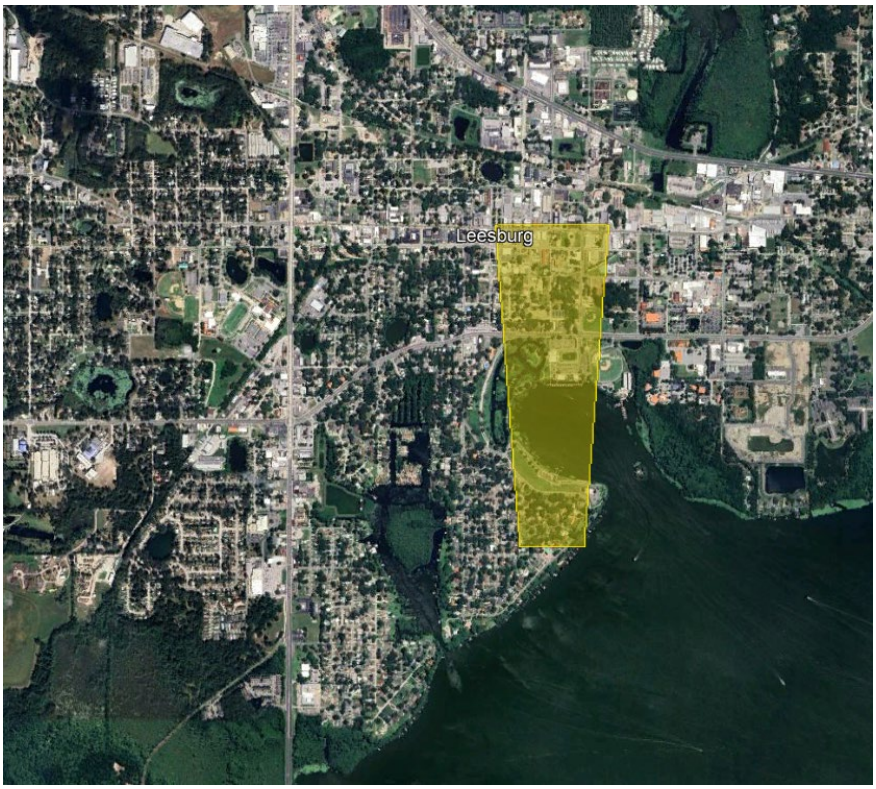


Figure 56. Strip for $Z_o$ averaging for Big Lake Harris for 0° direction.

Table 7. NLCD Land Use/Land Cover categories.

| NLCD Category | Description |
|---|---|
| 11 | Open Water |
| 12 | Perennial Ice/Snow |
| 21 | Developed, Open Space |
| 22 | Developed, Low Intensity |
| 23 | Developed, Medium Intensity |
| 24 | Developed, High Intensity |
| 31 | Barren Land |
| 41 | Deciduous Forest |
| 42 | Evergreen Forest |
| 43 | Mixed Forest |
| 52 | Shrub/Scrub |
| 71 | Grassland/Herbaceous |
| 81 | Pasture/Hay |
| 82 | Cultivated Crops |
| 90 | Woody Wetlands |
| 95 | Emergent Herbaceous Wetlands |

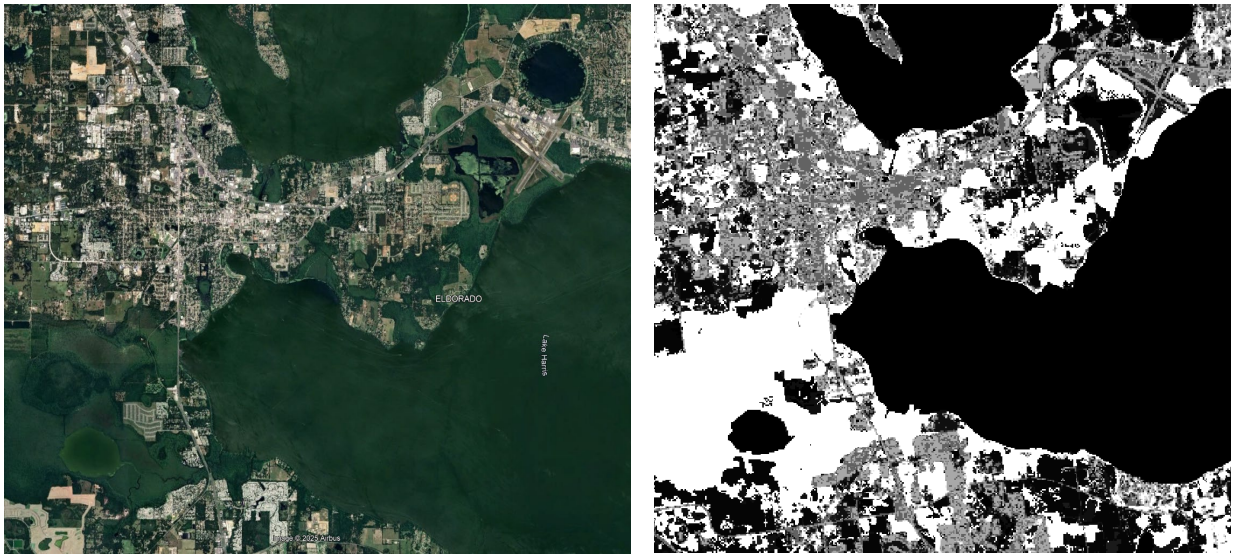


a) Google Earth Imagery of Big Lake Harris

b) NLCD Zo Raster of Big Lake Harris

Figure 57. Big Lake Harris map to raster comparison.

To determine the initial location (i.e., origin point of the location for the analysis), five distances from open water were analyzed starting at 50 meters from open water and 25-meter intervals after that towards inland. Figure 58 shows the points analyzed to determine an initial location for determining $Z_o$ values for Big Lake Harris location and Figure 59 displays the average $Z_o$ values for the origin points for each of the 36 directions. While houses located on the first row will

experience higher local wind speeds, they will not experience increased wind missiles due to the dearth of potential missiles upwind (when the wind comes off the water). As such, the 100-meter offset was chosen because it represents a location just behind the first row of houses in the Big Lake Harris neighborhood and behind the first few rows in the modeled neighborhood (Figure 53) capturing conditions typical for interior houses that are shielded from peak shoreline wind speeds but are more susceptible to wind-borne debris due to their downwind position. Other downwind locations, such as 125 meters and 150 meters, could be considered; however, as shown in Figure 59, these offsets yield higher $Z_0$ values than the 100-meter location for wind directions originating over the lake.


Figure 58. Locations of the origin point for Big Lake Harris sensitivity analysis.

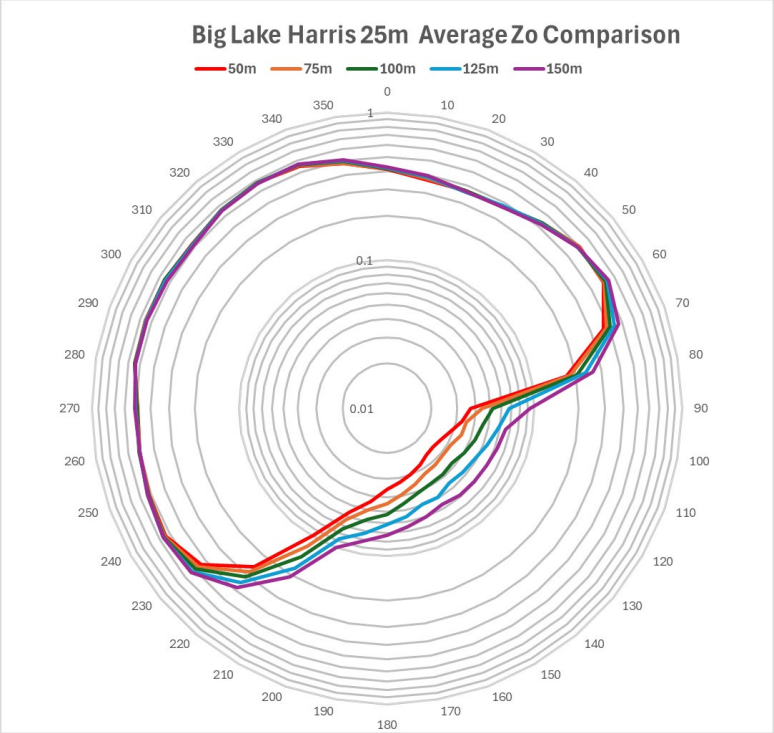


Figure 59. Average $Z_o$ (in meters) by 25-meter Increment from open water.

The upstream fetch distance used to calculate the directional $Z_o$ values was determined through a sensitivity analysis that considered three different fetch lengths: 500m, 1,000m, and 1,500m. Figure 60 illustrates circular areas corresponding to these three different fetch distances overlaid for all analyzed directions at the same origin point in the Big Lake Harris neighborhood. Figure 61 plots the resulting average $Z_o$ values by direction for each fetch distance showing the variability in average $Z_o$ by direction.

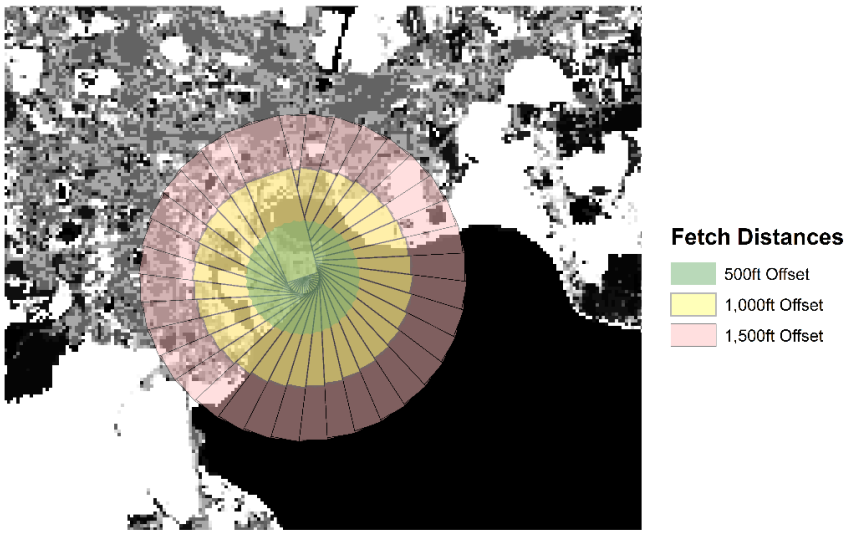


Figure 60. Extent of fetch distances analyzed on the $Z_o$ raster.

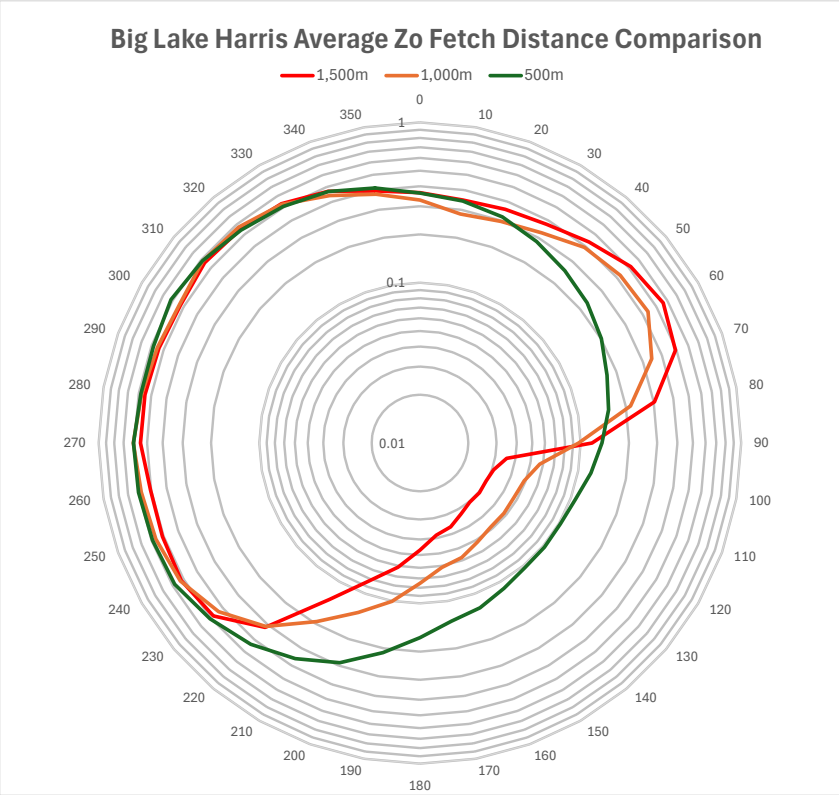


Figure 61. Comparison of average $Z_o$ by fetch distance.

In Figure 61, all three fetch distances result in similar directional $Z_o$ for directions clockwise from southwest to northeast where the upwind terrain is homogenous for each direction. On the other hand, we see decreases in average $Z_o$ for directions clockwise from east to southwest as the fetch distance is increased due to the inclusion of additional open water areas. As a result, we chose to use fetch distance of 1,500 meters in our directional surface roughness calculations to accurately account for the effects of upwind open water consistent with exposure determination guidance in ASCE 7 and with the literature, such as Yu et al., (2020).

Figure 62 shows the mean $Z_o$ values for the 1,500-meter distance by direction. As shown in the figure, the minimum $Z_o$ values are associated with wind directions originating from the southeast.

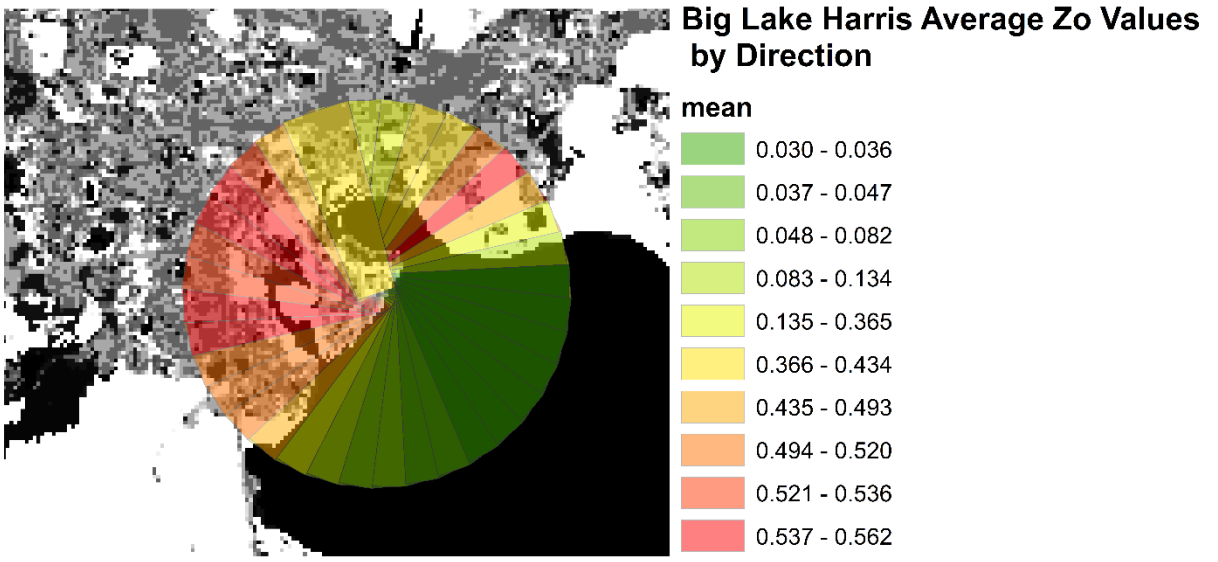


Figure 62. Average $Z_o$ (in meters) for 1,500-meter upstream fetch distance at 10-degree intervals.

*6.2.2.2 Development of $Z_o$ Values over Inland Terrain*

Using the initial origin point location and fetch distance determined in the previous section, the change in $Z_o$ moving inland was developed by moving in 1,000-foot intervals away from the origin location and calculating $Z_o$ values at each offset. The specific direction of the intervals for each location was based on the direction that produces minimum average $Z_o$ at the origin point, and the $Z_o$s for all five intervals were based on averaging along that direction using the method described in section 6.2.2.1. It is important to note that the calculated minimum $Z_o$ at each offset may not represent the minimum $Z_o$ for that location in all directions, as variations in terrain or the presence of additional large water bodies or open terrain could affect the $Z_o$ values in different directions. Generally, it is expected that surface roughness will increase while moving inland from the initial Exposure D condition. However, reversals in this trend occur when additional open water or open terrain area exists downwind of the original open water condition. While such reversals were observed in a few instances during this study, the first three intervals (i.e., origin, origin + 1,000 ft, origin + 2,000 ft) for all locations followed the expected trend. Figure 63 shows the selected rectangle for Big Lake Harris containing the minimum average $Z_o$ and the following offset points where the $Z_o$ averaging process was performed.

Figure 64 shows the cumulative distribution functions (CDF) of $Z_o$ for the 30 neighborhoods analyzed in this study. The $Z_o$ values are shown for the origin and the prescribed offset distances for each neighborhood. Inland and coastal neighborhood results are denoted with triangle and circle markers, respectively. The analysis of the CDF reveals a general trend of increasing terrain roughness moving inland along the direction of minimum bearing from the origin point near an open water source. 53% of the minimum average $Z_o$ at the origin are below the 0.03 expected surface roughness for open terrain. Approximately 60% of the $Z_o$ values at the origin fall within the range of 0.02 to 0.04, reflecting relatively smooth terrain commonly associated with water-proximate environments.

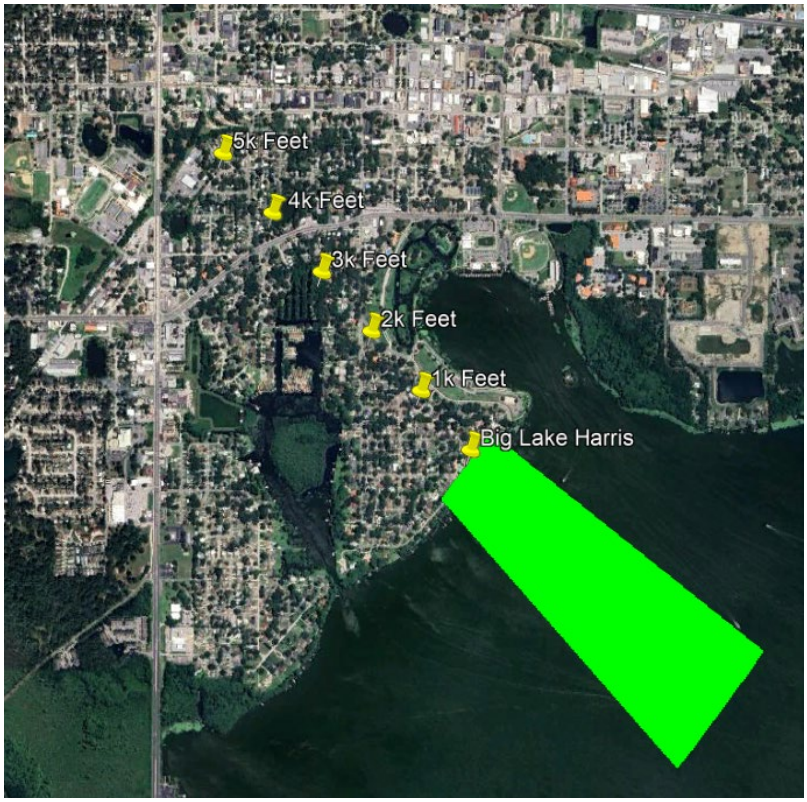


Figure 63. Offset points analyzed from the minimum average $Z_o$ at the origin for Big Lake Harris.

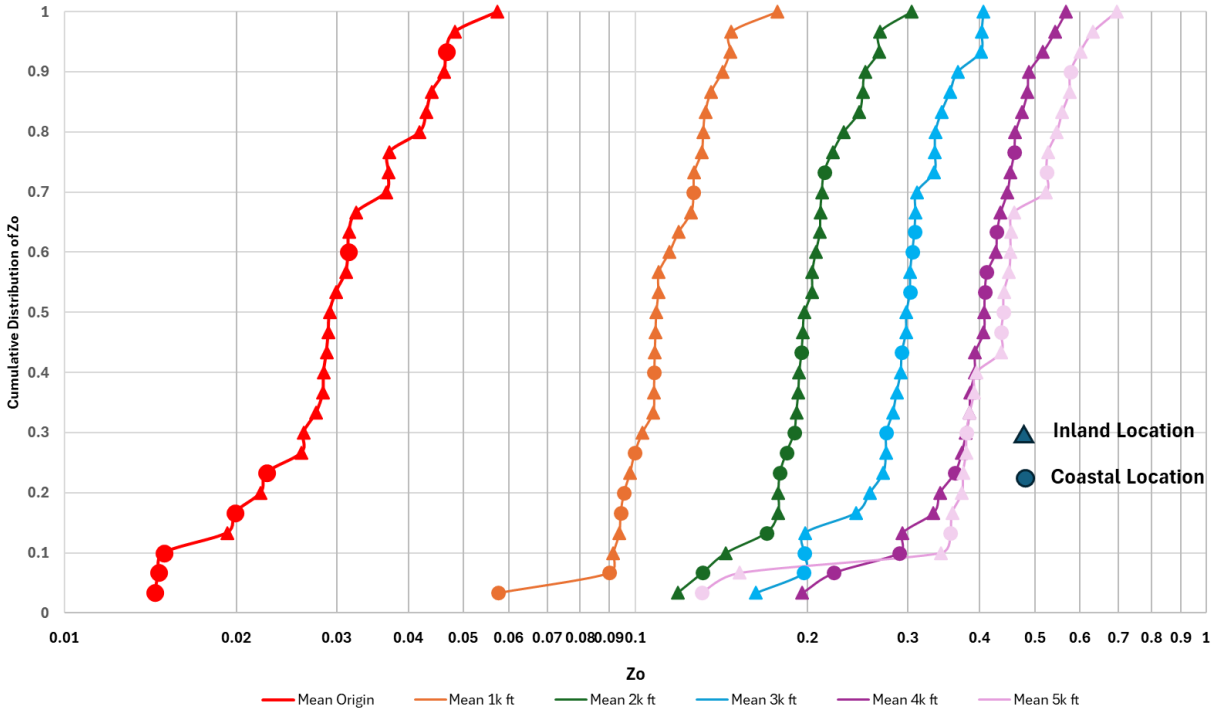


Figure 64. CDF of the minimum average directional $Z_o$ (in meters) for all locations.

The three origin locations with the lowest mean $Z_0$ values (red circles in Figure 64) are coastal sites where the first 100 m from the shoreline characterized by relatively flatter terrain with minimal obstructions.

At the 5,000 ft offset, some locations begin to show reversals in the expected $Z_0$ trend. This occurs due to the presence of multiple open terrain features and water bodies in the vicinity. For example, at the Daytona Beach 2 location shown in Figure 65, where an intracoastal waterway lies along the direction of minimum $Z_0$ from the origin point. At the 5,000 ft offset, the upstream fetch includes more water surface area than at the 2,000, 3,000, or 4,000 ft offsets, resulting in a lower $Z_0$ value at 5,000 ft than those offsets.

Figure 66 compares directional $Z_0$ values at the origin and each offset point of the Daytona Beach 2 location. The minimum $Z_0$ at the origin occurs in the 50-degree upstream direction, which also corresponds to the observed reversal—where the $Z_0$ at 5,000 ft is lower than that at 2,000, 3,000, and 4,000 ft.


Figure 65 Offset locations for the Daytona Beach 2 location.

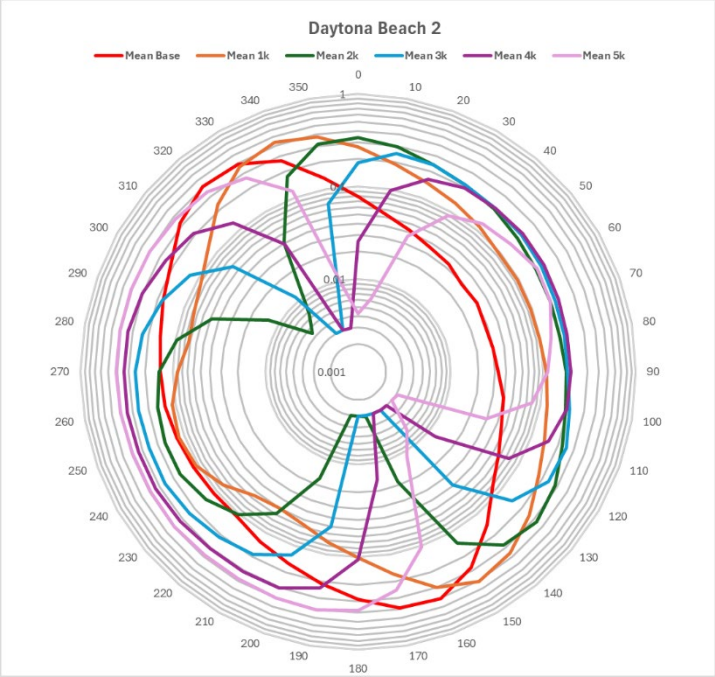


Figure 66. Comparison of average directional $Z_o$ (in meters) values at Daytona Beach 2.

### *6.2.3 Simulation Cases*

Wind-borne debris (WBD) simulations under straight-line wind conditions were conducted for 30 neighborhood locations, comprising the 23 inland lake sites and 7 coastal locations discussed above. Simulations were performed for reference wind speeds of 130 mph and 139 mph. The reference wind speed for the simulations is a peak gust wind speed at 33 ft in open terrain exposure. For each location, the minimum directional $Z_o$, as computed in section 6.2.2, were used to define the terrain for the origin point and five offset positions located at distances of 1,000 ft, 2,000 ft, 3,000 ft, 4,000 ft, and 5,000 ft from the origin.

At each of the 30 locations, simulations were carried out for three relative orientations of the modeled neighborhood with respect to the direction of minimum $Z_o$: 0°, 215°, and 270°. These orientations correspond to wind directions that are approximately parallel to the roof ridge, quartering to the ridge, and perpendicular to the ridge, respectively. For example, if the minimum directional $Z_o$ occurs at 10° clockwise from true North, the neighborhood model is oriented as follows:

- In the first case, the long axis of the houses is aligned parallel to the 10° direction.
- In the second case, the long axis is rotated 215° relative to the 10° direction.
- In the third case, the long axis is rotated 270° relative to the 10° direction.

For each combination of location, offset position and wind direction, 10 simulation runs were performed. From these simulations, the mean number of wall impacts was computed for each

house, and then averaged over all 84 houses to determine the mean wall impacts for the entire neighborhood. In addition, the mean wall impacts for a representative house located near the geometric center of the neighborhood were separately computed.

To assess relative WBD risk, simulations were conducted for the modeled neighborhood using Exposure B terrain ($Z_0$ = 0.35 m) subjected to a 140 mph reference wind speed, using the three wind directions described above. For each location and offset distance, the relative hits metric was calculated as the ratio of the mean wall impacts under the site-specific exposure conditions to those obtained under Exposure B conditions. A relative hits value of 1.0 indicates equivalent risk to a neighborhood situated in a standard WBDR (i.e., 140 mph, Exposure B), while values less than 1.0 indicate reduced relative risk.

Table 8. Debris impact simulation cases.

| **Straight Line Reference Wind Speed** | **Surface Roughness** | **Relative Wind Directions** | **Distances from Origin (ft)** |
|---|---|---|---|
| 130 mph | Varying: minimum average directional $Z_0$ | 0°, 215°, 270° | 0, 1000, 2000, 3000, 4000, 5000 |
| 139 mph | Varying: minimum average directional $Z_0$ | 0°, 215°, 270° | 0, 1000, 2000, 3000, 4000, 5000 |
| 140 mph | Exp. B ($Z_0$ = 0.35 m) | 0°, 215°, 270° | N/A |

### *6.2.4 Assumptions and Limitations*

Several assumptions and limitations are inherent in the modeling and simulation of WBD Risks debris. These include

- The directional surface roughness length ($Z_0$) was estimated as the mean value of surface roughness features within a 1,500 m × 300 m rectangular area upwind of each site.
- A single, representative house model with a fixed orientation was used to characterize the residential structures within the neighborhood.
- A uniform housing density and regular spacing between homes were assumed throughout the simulated neighborhood.
- Only debris originating from failed roof components such as shingles, roof sheathing, and framing within the modeled neighborhood were considered as source debris.
- Tree-related debris and other non-structural sources were excluded from the simulations.

## 6.3 Modeling Results

Figure 67 presents the simulation results for Big Lake Harris, one of the sites analyzed in this study. The mean number of wall impacts at a reference wind speed of 130 mph is normalized by the corresponding value for Exposure B conditions at a reference wind speed of 140 mph, and the resulting ratio is presented as the relative hit value on the ordinate. Figure 68 shows similar plots; however, in this case, the relative hits are computed by normalizing the mean wall impacts at each offset location by the corresponding value at the origin point. As expected, relative hit values generally decrease with increasing distance from the water body, reflecting the effect of increasing surface roughness on WBD impact. This decreasing trend is consistently observed across all modeled relative wind directions.

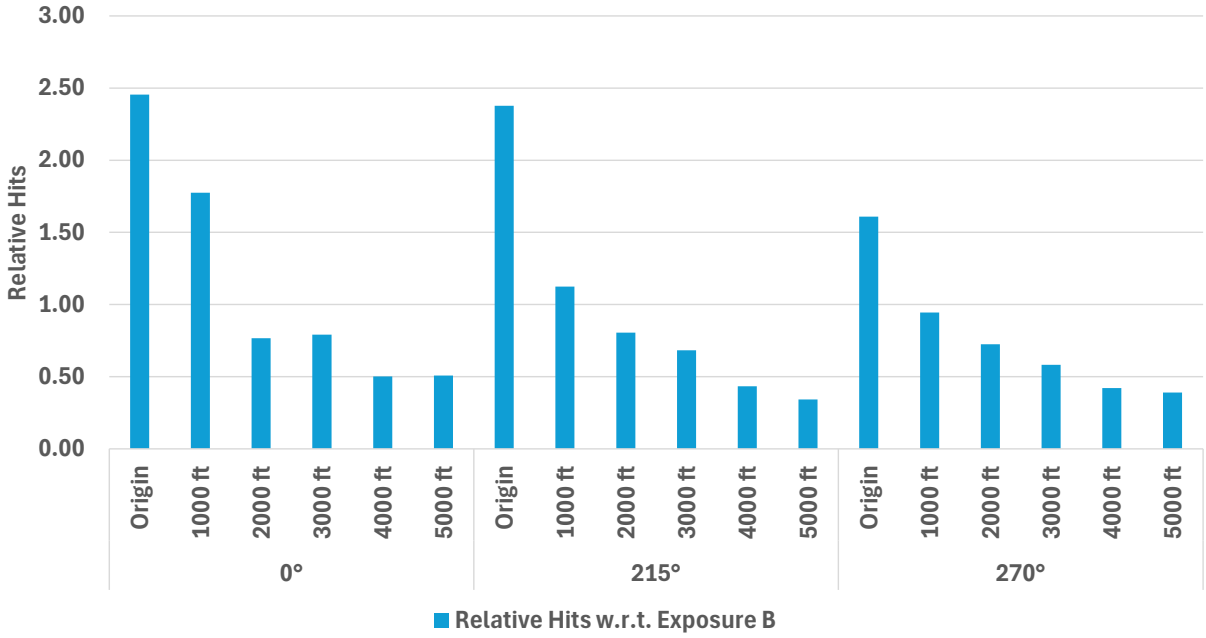


Figure 67. Relative mean WBD hits with respect to 140 mph Exposure B for three relative wind directions for the Big Lake Harris neighborhood.

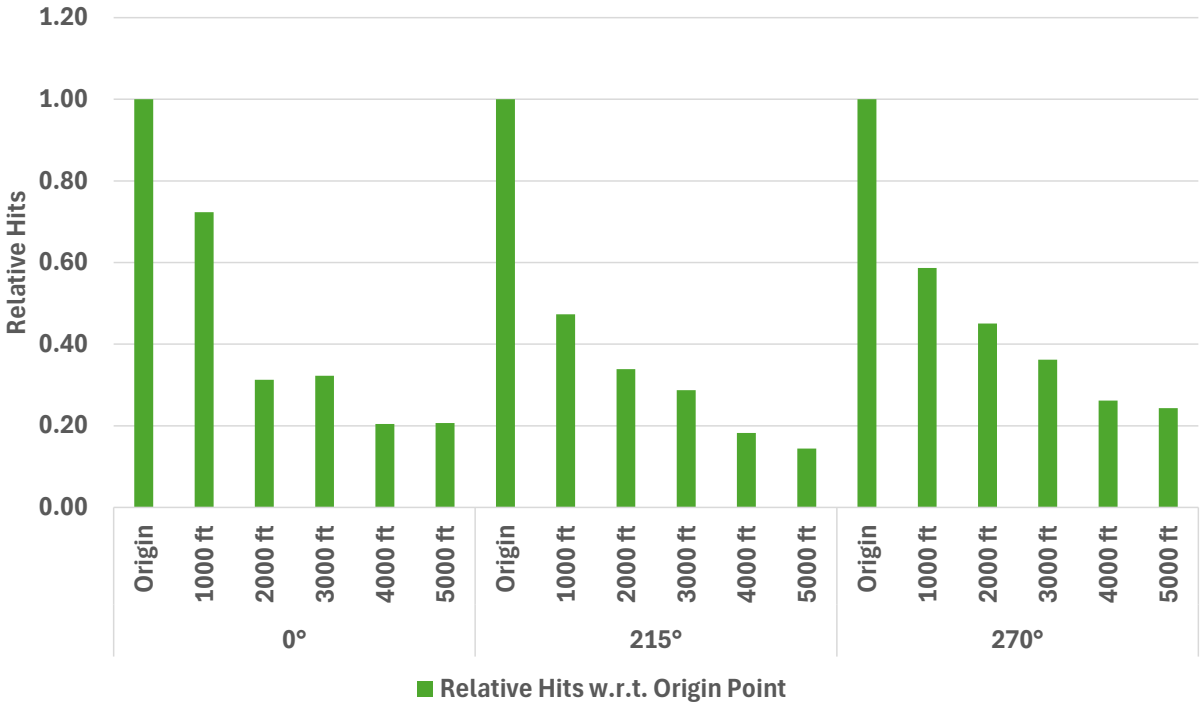


Figure 68. Mean number of hits relative to the origin point for three relative wind directions for the Big Lake Harris neighborhood.

### *6.3.1 Directional Relative Hits*

This section presents relative hit values computed using directional $Z_0$ values from all 36 wind directions for the origin points of four selected sites. Among them three are inland lake locations: Big Lake Harris, Lake Deer Point, and Lake Conway; and the other is a coastal location, Daytona 2. These locations were chosen to reflect a range of wind exposure conditions.

Among the inland sites, Lake Deer Point is moderately exposed to an upwind water body and exhibits one of the higher minimum $Z_0$ values. Lake Conway, which has lakes to the north and south, has the lowest minimum $Z_0$ among the inland locations. The Big Lake Harris location has a minimum $Z_0$ near the 50th percentile of the 23 inland sites analyzed. Directional relative hits were computed as the ratio of mean wall impacts under 130 mph reference wind speed using the directional minimum $Z_0$, to the corresponding impacts under 140 mph reference wind speed in Exposure B terrain ($Z_0$ = 0.35 m). This ratio provides a comparative index of debris risk under local exposure conditions relative to standard WBDR criteria.

**Big Lake Harris**

Figure 69(a) shows the relative hit values across 36 wind directions in a radar plot for the mean wall hits across the neighborhood, while Figure 69(b) presents the same for the center house hits. Figure 69(c) shows the modeled neighborhood location on a Google Maps view. Elevated relative hit values (>1.0) are observed in the southern and southeastern sectors, attributed to the low upwind $Z_0$ values resulting from the nearby lake. In contrast, wind directions from the north, northeast,

northwest, and west yield significantly lower relative hits due to greater upwind surface roughness. Averaged across all directions, the site shows relative hit values of 0.78 and 0.84 based on mean and center house hits, respectively. This inland lake case illustrates that when the 130-mph design reference wind speed originates from the north, northeast, or west, the WBD risk is substantially lower than that of a standard WBDR.

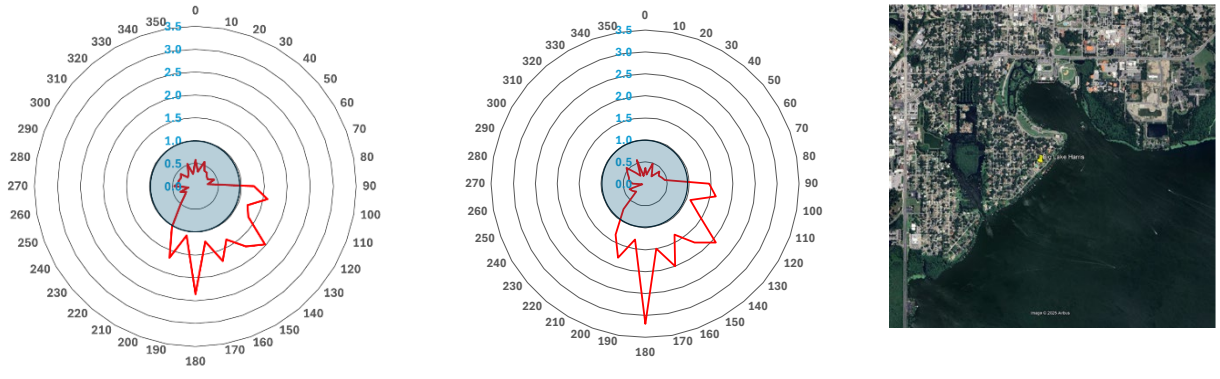

(a) Relative mean hits (b) Relative hits (center house) (c) Google Map view

Figure 69. Relative hits by direction for Big Lake Harris location.

**Daytona 2 (Coastal Site)**

Figure 70(a) and Figure 70(b) display the directional relative hit values for mean and center hits, respectively, while Figure 70(c) shows the neighborhood location. Unlike the inland locations, Daytona 2 location shows relative hit values exceeding 1.0 in most directions. This is due to consistently low directional $Z_0$ values caused by the presence of the Atlantic Ocean to the east and the Intracoastal Waterway to the west. The average relative hit values for Daytona 2 are 1.48 (mean hits) and 1.12 (center hits), indicating a significantly higher WBD risk relative to Exposure B.

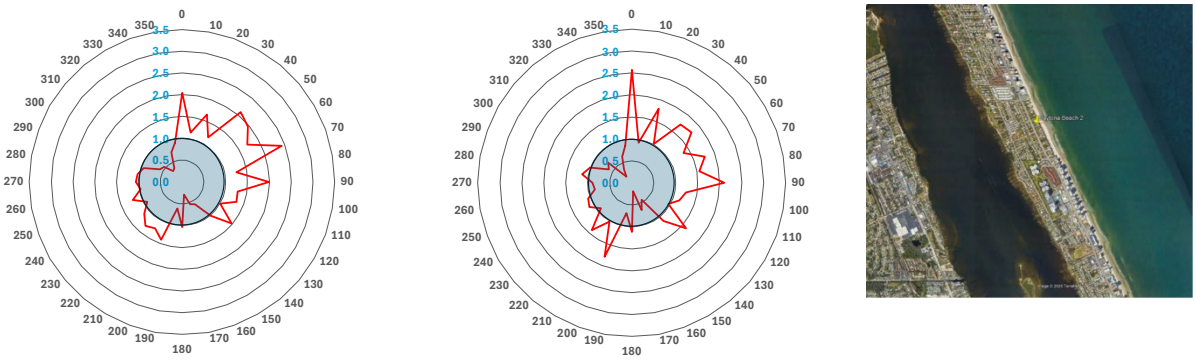

(a) Relative mean hits (b) Relative hits (center house) (c) Google Map view

Figure 70. Relative hits by direction for Daytona 2 location.

**Lake Deer Point**

Figure 71(a) and Figure 71(b) present the directional relative hits based on mean and center house impacts, while Figure 71(c) shows the neighborhood location. Here, relative hit values exceed 1.0 only in the northwesterly directions due to a long stretch of water body in that sector, which significantly lowers $Z_0$. For all other directions, the relative hit values remain well below 1.0. Averaging across all directions, the relative hit values are 0.59 and 0.60 for mean and center house hits, respectively, indicating substantially reduced debris risk compared to a WBDR standard.

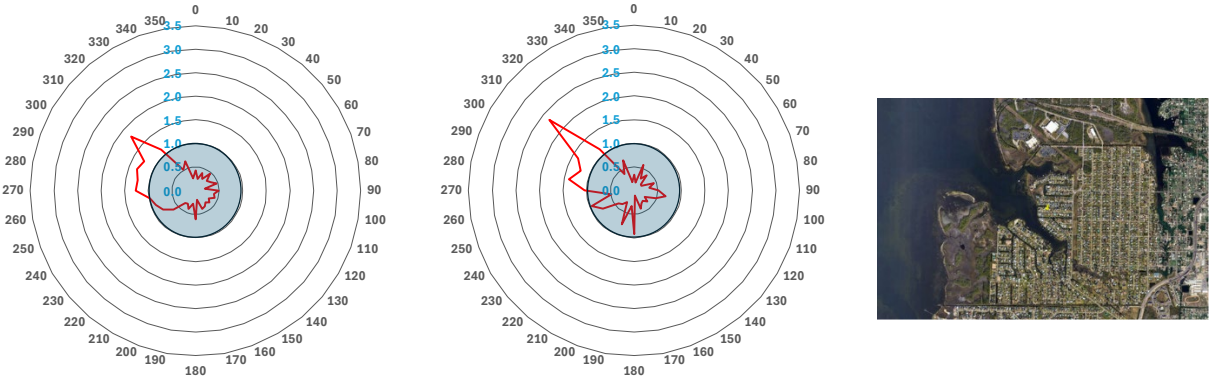

(a) Relative mean hits (b) Relative hits (center house) (c) Google Map view

Figure 71. Relative hits by direction for Lake Deer Point location.

**Lake Conway**

Figure 72(a) and Figure 72(b) present the directional relative hits for mean and center house hits, respectively, and Figure 72(c) shows the neighborhood's location. Higher relative hit values (>1.0) are observed in the north, northeast, and southwest directions, consistent with the presence of water bodies on both the north and south sides of the site. The average values across all 36 directions are 0.93 for both mean and center house hits, which shows that this location has a WBD risk slightly lower than the standard WBDR conditions.

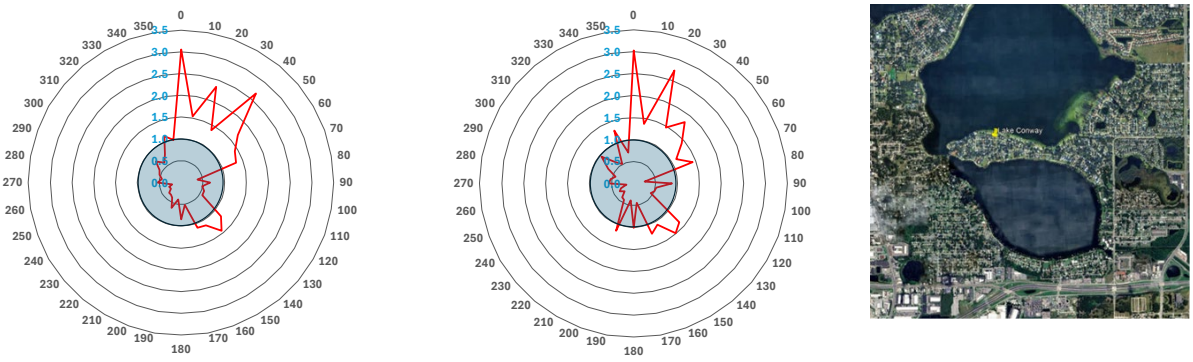

(a) Relative mean hits (b) Relative hits (center house) (c) Google Map view

Figure 72. Relative hits by direction for Lake Conway location.

### *6.3.2 Comparison of Risk to Currently Accepted WBDR*

Results for the 130-mph straight-line reference wind simulations across all 30 modeled locations are presented in Figure 73. In this figure, the mean number of hits for all three modeled wind directions are normalized by the corresponding values from 140 mph reference wind simulations under Exposure B conditions, and their cumulative distribution is plotted. A relative hit value of one indicates that the risk of WBD hits is the same as the neighborhood in an established WBDR. At an offset distance of 2,000 feet from the origin, approximately 50% of the 90 simulation cases fall below the WBDR threshold. This proportion increases to about 90% at 3,000 feet, indicating a significant reduction in debris risk with increasing distance from the water body.

Figure 74 presents similar results using the 139-mph reference wind speed. At 3,000 ft from the origin, approximately 50% of the simulation cases have risk below established WBDR at 140 mph Exposure B and at 4,000 ft this increases to approximately 80%.

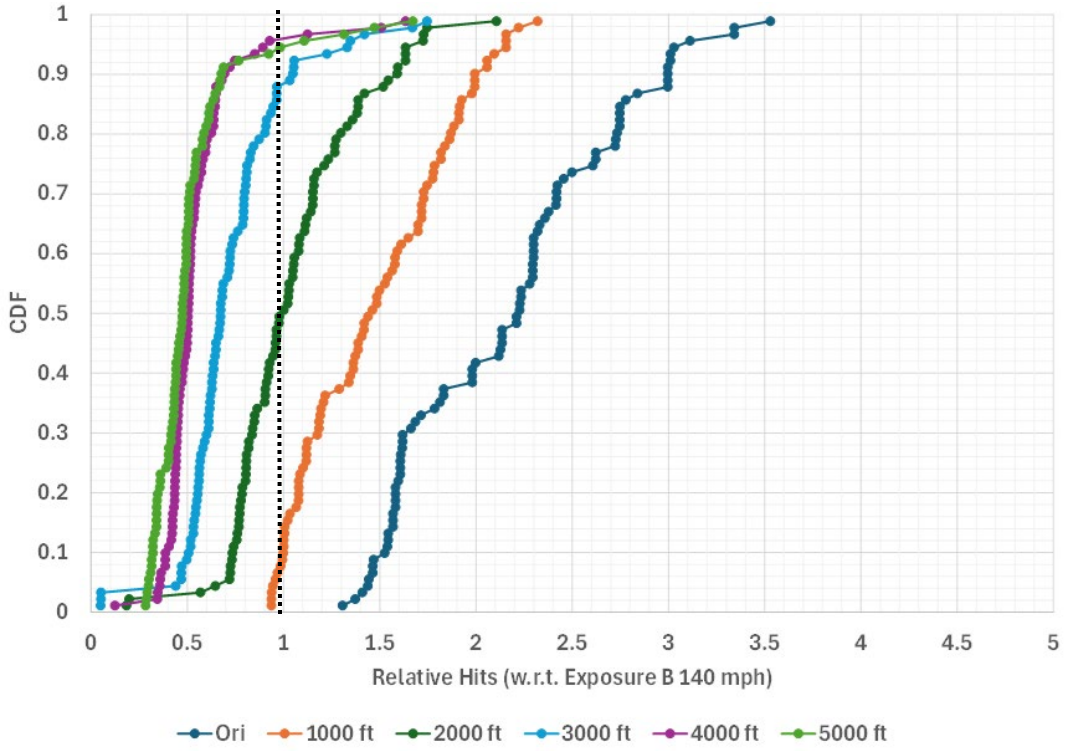


Figure 73. CDF of relative mean hits at origin and offset distances for 30 locations based on 130 mph reference wind speed.

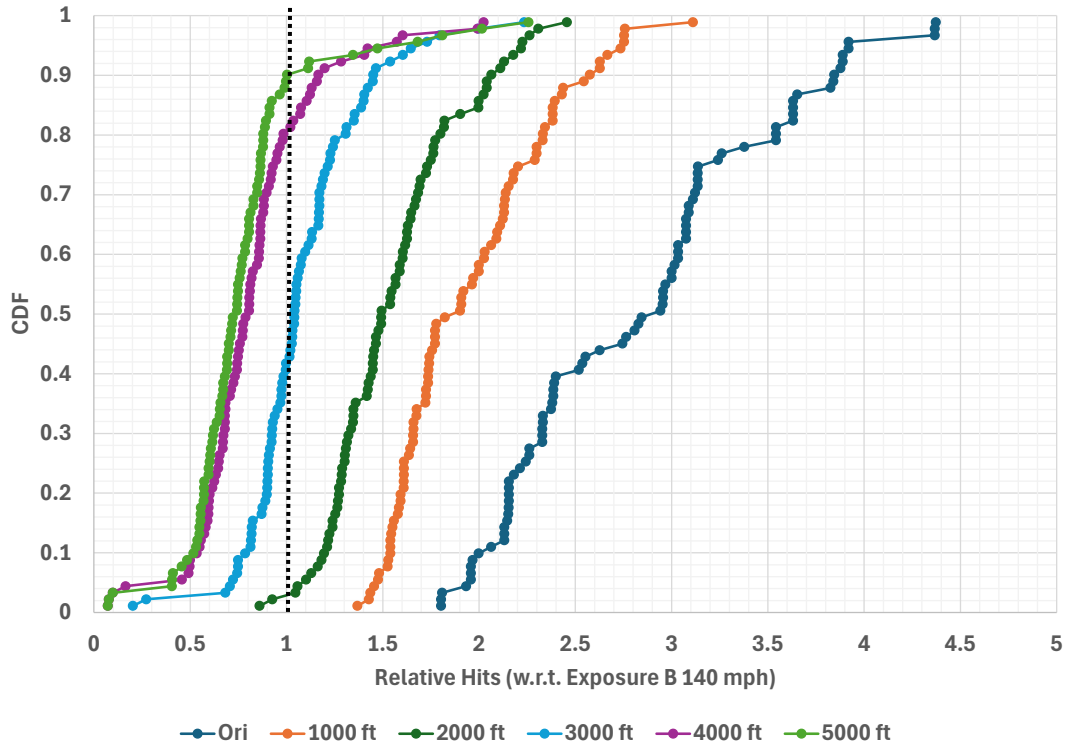


Figure 74. CDF of relative mean hits at origin and offset distances for 30 locations based on 139 mph reference wind speed.

### *6.3.3 Coastal Locations Vs. Inland Locations*

Figure 75 (a) and Figure 75 (b) present the CDFs of relative WBD risk for the seven coastal and twenty-three inland locations, respectively, under a 130-mph reference wind condition. The results show that, beyond an offset distance of 3,000 ft from the water body, more than 80% of the simulation cases yield relative risk values below 1.0 indicating a lower WBD risk than the baseline Exposure B condition at 140 mph for both coastal and inland sites.

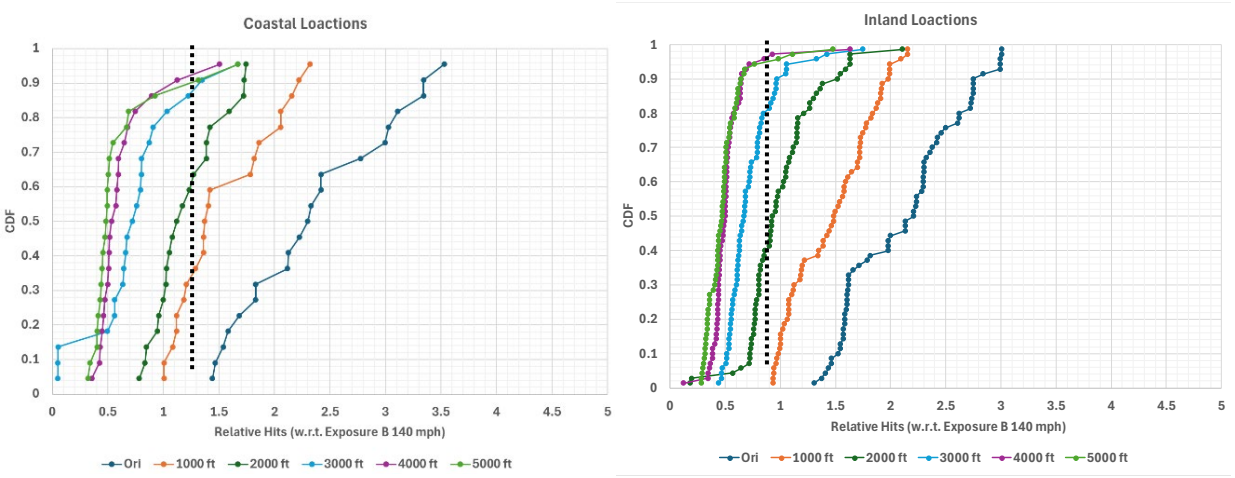


(a) (b)

Figure 75. CDF of relative mean hits at origin and offset distances based on 130-mph reference wind speed: (a) coastal locations (b) inland locations.

Figure 76 (a) and Figure 76 (b) present the corresponding CDFs for the same locations under a 139-mph reference wind condition. In this case, beyond an offset distance of 4,000 feet, over 60% of the simulation cases show relative risk values below 1.0 for both coastal and inland locations.

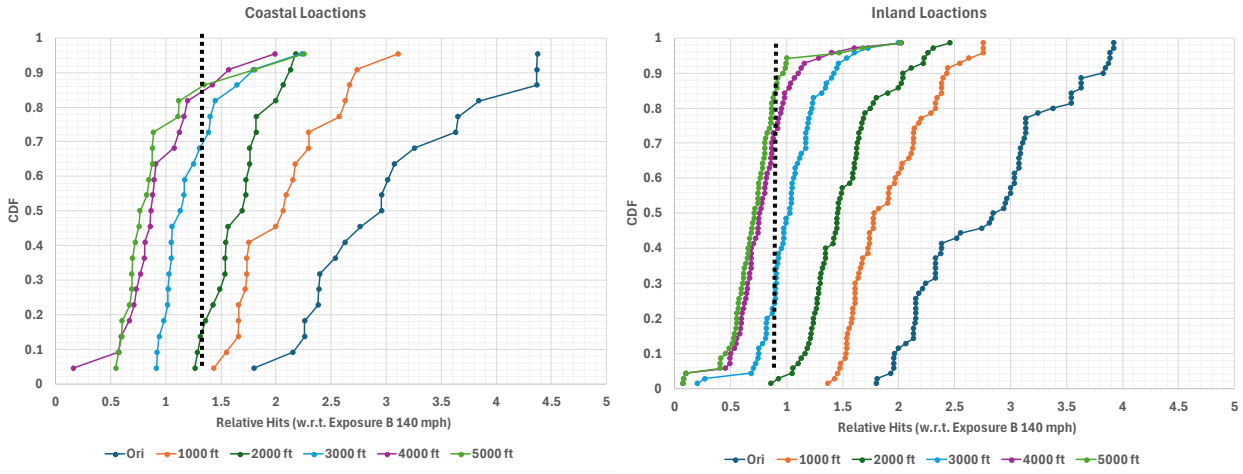


(a) (b)

Figure 76. CDF of relative mean hits at origin and offset distances based on 139 mph reference wind speed: (a) coastal locations (b) inland locations.

### *6.3.4 Changes in Risk with Distance from Open Water/Exposure D*

Simulation results demonstrate that, when conservatively assessing WBD risk based on the most critical directional exposure (i.e., the minimum directional $Z_0$) at each site and assuming the design wind originates from that direction, locations situated within 3,000 feet of an open water body show WBD risks comparable to those experienced under Exposure B conditions at a reference wind speed of 140 mph, despite being subjected to lower design wind speeds. This finding indicates a consistent pattern of elevated debris hazard in both coastal and inland settings where Exposure D conditions prevail.

## 7 Preliminary Benefit Cost Analysis

The objective of this benefit-cost (BC) analysis is to quantify the amount of benefit, measured in terms of reduction in tangible losses, that opening protections provide relative to their increased cost over standard windows. For new residences built within wind-borne debris regions (WBDR), the Florida Building Code requires that windows must either be impact resistant or covered with impact resistant coverings (e.g., shutters). Impact resistance must meet the requirements of ASTM E1996 and E1886; TAS 201, 202, 203; or AAMA 506.

### 7.1 Cost Analysis

To evaluate the cost difference between standard windows and doors and those with opening protection (e.g., impact resistant glass or shutters), the cost to construct two new prototype residences were determined using current (2025) RSMeans construction cost data applied to central Florida. These costs include material and installation labor.

The one-story house, shown in Figure 77 and Figure 78 has a hip roof, 21 windows, and three exterior doors. The standard windows and windows with impact resistant glass are a mix of fixed and single hung aluminum frame windows.

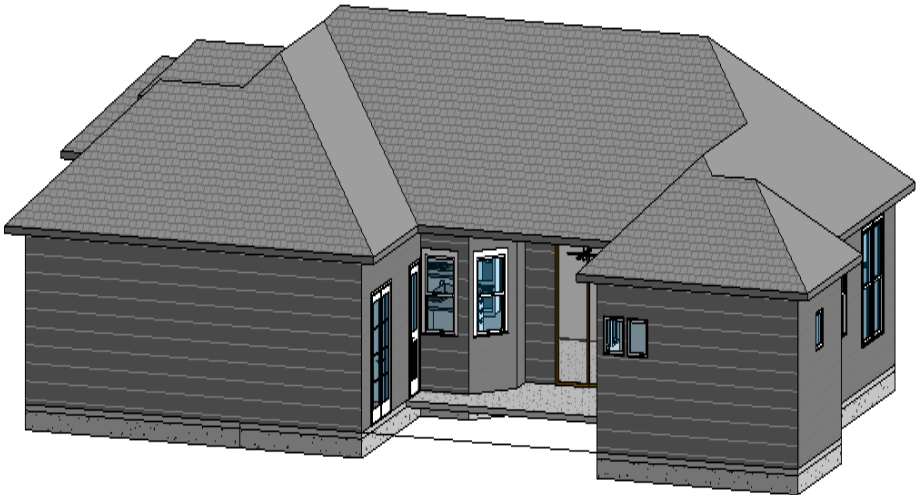

Figure 77. Northeast view of single-story house.

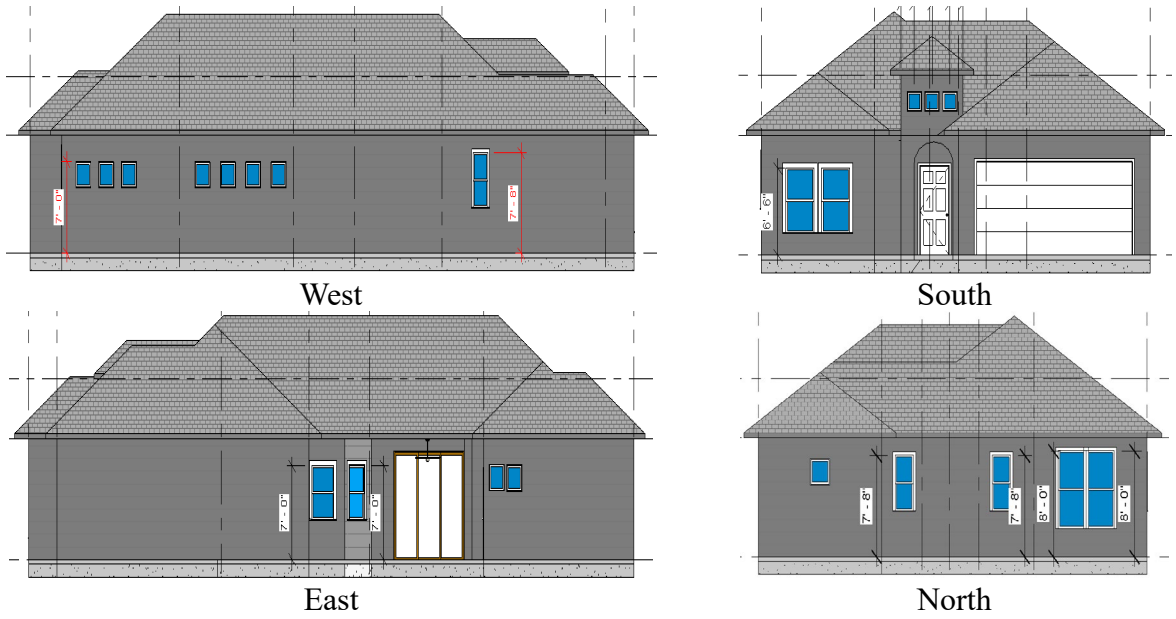


Figure 78. Elevation views of the single-story house.

The two-story house, shown in Figure 79 and Figure 80 has a combination of hip and gable rooflines with 33 windows on the lower level, eight windows on the upper level, and four exterior doors. The aluminum windows are a mix of fixed and single hung.

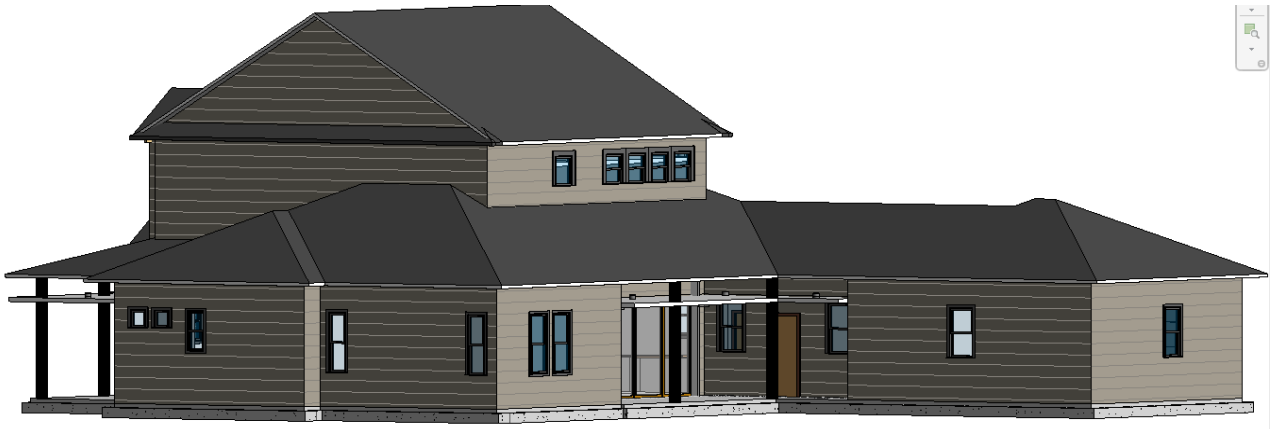

Figure 79. Northeast view of the two-story house.

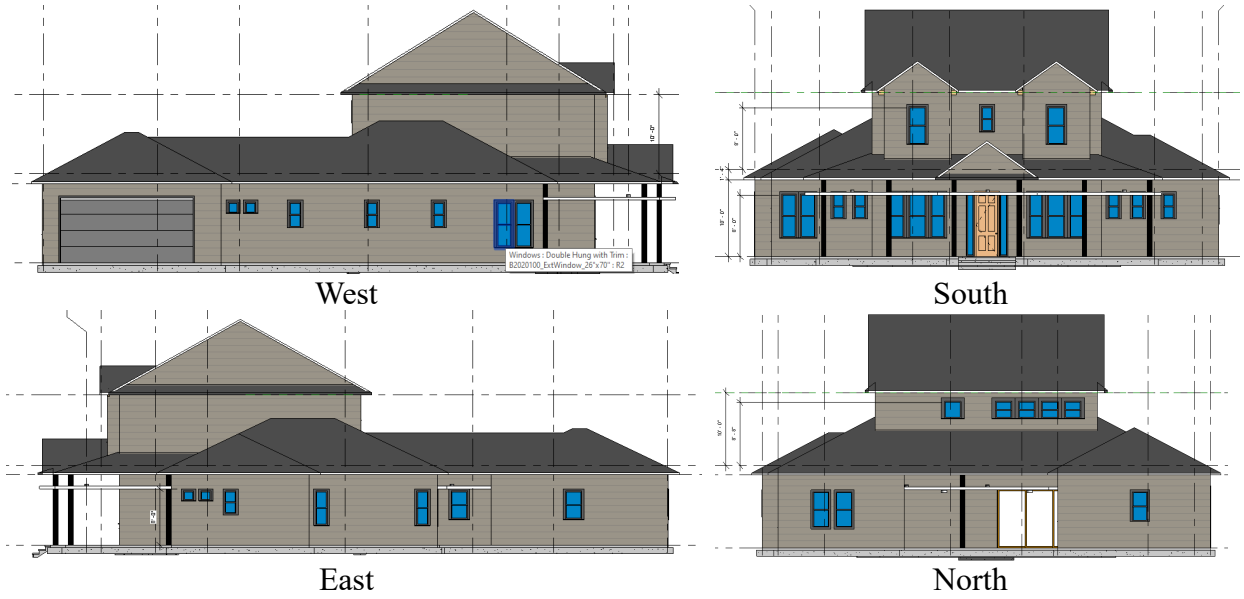

Figure 80. Elevation views of the two-story house.

In addition to comparing the cost difference between impact resistant windows and standard windows, the cost of adding shutters to standard windows on the lower level while keeping upper-level windows impact resistant, was also estimated.

Table 9 summarizes the total construction cost for each home, the cost of standard windows, the cost of impact resistant windows, and the cost for aluminum shutters on lower-level standard windows and upper-level windows with impact resistant glass. Note that the home cost does not include the cost of land.

Table 9. Cost summary for two prototype houses in central Florida with different opening protection options.

| | **One-Story House** | | | **Two-Story House** | | |
|---|---|---|---|---|---|---|
| **Home Cost** | $402,473 | | | $642,186 | | |
| **Opening Protection** | Standard Glass | Impact Resistant Glass | Shutters & Std. Glass on Lower Level | Standard Glass | Impact Resistant Glass | Shutters & Std. Glass on Lower Level |
| **Window & Door Total Cost** | $ 28,813 | $ 35,463 | $ 39,843 | $ 51,121 | $ 59,588 | $ 72,112 |
| **Cost Difference** | -- | $ 6,650 | $ 11,030 | -- | $ 8,466 | $ 20,991 |
| **Window & Door Cost Percent Difference** | -- | 23.1% | 38.3% | -- | 16.6% | 41.1% |
| **Total Home Cost Percent Difference** | -- | 1.7% | 2.7% | -- | 1.3% | 3.3% |

Impact resistant glass increases the cost of the residence by 1.7% and 1.3% for the one- and two-story houses, respectively. Shutters on the lower level with impact resistant glass on higher windows increases the cost of the residence by 2.7% and 3.3% for the one- and two-story houses, respectively. The additional cost of the shutters reflects the fact that labor and material costs of installing shutters in addition to standard windows exceeds the cost of windows with impact resistant glass.

## 7.2 Benefit Analysis

To evaluate the benefit of opening protections provided by impact resistant glass or shutters, this study used data generated by ARA for their 2024 Residential Wind-Loss Mitigation Study (Applied Research Associates, inc., 2024) for the Florida Office of Insurance Regulation (OIR). The results of ARA's simulations, documented in the report, are presented in the form of an average annual loss reduction realized by a wind resistant construction feature. In addition to the wind resistant construction features, the amount of loss reduction is dependent on exposure conditions, wind speeds, and house configurations. To align with the prototype homes for which costs were analyzed in this current study, the average annual loss reduction rates (per $1000 of total insured value including contents and additional living expenses) for a two story "other" roof and a one-story hip roof provided in the ARA OIR study report were used.

Several assumptions were made in the calculation of the benefit-cost ratios for the two houses in different wind speed and terrain conditions:

- The benefit-cost ratio was calculated ten years from the initial home construction
- A discount/interest rate for future payments was set to 5%
- The increased cost of opening protections retains some value over time. A conservative depreciation rate of 6% was used to calculate the depreciated value of the opening protection. This depreciation rate results in a residual value of opening protection of approximately 50% of the additional initial construction cost after ten years
- The insured value of the home, along with the cost of insurance for the home, increases by 3% annually

Table 10 presents the results of this analysis. For both houses, with either opening protection option, a greater BCR is realized at ten years when the residences are subject to lower wind speeds (130 mph) but with smoother terrain (Exposure C). The 130 mph, Exposure C condition is a proxy for houses built in proximity to open water (inland lakes or coastal creating Exposure D conditions)[3]. These results indicate that the requirement of opening protections for homes on the

[3] The relativity values from the OIR Loss Mitigation Study for 130 mph, exposure C conditions were considered to best represent areas upwind of Exposure D conditions created by both inland and coastal water bodies. This is due the fact that once the land area between the water line and the first row of buildings is considered, the actual directional surface roughness at the building fits the ASCE 7 definition of Exposure C. Specifically, Table C26.7-1 of the ASCE 7-22 commentary indicates that the expected range of z0 for Exposure C conditions ranges from 0.01 m to 0.15 m. This range encompasses the minimum direction z0 values calculated for the Big Harris Lake neighborhood as presented in Figures 59 and 61 for directions directly adjacent to open water.

coast or adjacent to large lakes provides greater benefit than for homes in currently accepted WBDRs (140 mph, Exposure B). Note that the highest BCR, at 109%, is for a two-story house with impact resistant glass in 130 mph, Exposure C conditions, indicating further benefit for two-story houses.

Table 10. Benefit-cost analysis over a ten-year period for opening protections under varying wind and terrain conditions for the two reference houses.

| | **Impact Resistant Glass** | | | | **Standard Window + Aluminum Shutters on Lower Level** | | | |
|---|---|---|---|---|---|---|---|---|
| | **Two-Story** | | **One-Story** | | **Two-Story** | | **One-Story** | |
| Opening Protection Cost Increase | $ 8,466 | | $ 6,647 | | $ 20,991 | | $ 11,030 | |
| Future Value of Opening Protection | $ 4,560 | | $ 3,580 | | $ 11,306 | | $ 5,941 | |
| Wind Speed | 130 mph | 140 mph | 130 mph | 140 mph | 130 mph | 140 mph | 130 mph | 140 mph |
| Exposure | C | B | C | B | C | B | C | B |
| Average Annual Loss Reduction Rate (per $1000 TIV) | 0.721 | 0.300 | 0.326 | 0.244 | 0.721 | 0.300 | 0.326 | 0.244 |
| Average Annual Loss Reduction | $ 741 | $ 308 | $ 210 | $157 | $ 741 | $ 308 | $ 210 | $ 157 |
| Present Value of Loss Reduction | $ 9,280 | $ 5,496 | $ 4,034 | $ 3,572 | $ 13,421 | $ 9,637 | $ 5,484 | $ 5,022 |
| Net Present Cost | -$ 814 | $ 2,970 | $ 2,613 | $ 3,075 | $ 7,570 | $ 11,354 | $ 5,546 | $ 6,008 |
| **Benefit-Cost Ratio (BCR)** | **1.096** | **0.649** | **0.607** | **0.537** | **0.639** | **0.459** | **0.497** | **0.455** |

## 7.3 Limitations of Benefit Analysis

The above analysis is limited and preliminary. Additional investigations are warranted to expand this preliminary benefit analysis to be more comprehensive in scope of code compliant product options, cost ranges, and structural configurations including price points from starter through luxury homes.

- The analysis uses a 10-year timespan based on the average time a homeowner owns the home in Florida. However, longer timespans should be considered, such as 15- and 30-years (typical mortgage terms) or the lifetime of shutters/impact resistant windows (20-30 years)
- Protection type, sourcing and pricing were not optimized to reduce the cost of mitigation for this study. The materials and cost of installation for the two systems considered were based on a standard source (RSMeans, 2025), yet spot-checking revealed wildly different material and installation pricing from one supply source to another, and from one region to another. Options were identified that projected lower costs than used in this analysis

- The analysis presents only two WBD risk mitigation options. Competing window protection options such as other panel shutter manufacturers and types and fabric protection systems exist, but their relative cost for materials and installation were not within the scope of this project nor feasible within the performance period. For example, fabric systems have been identified to be available as low as $5/sq ft, but were not included due to lack of confidence in quoted price for material and installation

## 7.4 Intangible Losses

While the BCR analysis provides a quantitative measure of loss reduction realized with the use of opening protections, it does not capture the often intangible losses experienced when homes are damaged during storm events. Water intrusion and structural damage can result in the loss of irreplaceable items, such as family heirlooms. Temporary or permanent displacement can cause distress from loss of work, lapses in schooling and an overall reduction in well-being that cannot be captured by insured loss metrics.

Beyond personal property loss, storm-induced displacement (whether temporary or permanent) can disrupt essential aspects of life, including employment, education, healthcare access, and community ties. Families forced to relocate may face a breakdown in social support systems and struggle to reestablish daily routines. Unoccupied damaged homes are more susceptible to invasion and theft, increasing risk of crime for all members of that community. Van de Lindt et al. (2020) showed how such consequences were especially pronounced in marginalized communities. Low-income households faced longer recovery timelines and greater displacement challenges, even when structural damage was similar to that of neighboring households.

Recent literature underscores that post-disaster well-being depends not only on the extent of physical damage but also on individuals' ability to access essential goods and services. Enderami et al. (2024) identified four critical dimensions that shape recovery experiences: proximity, availability, adequacy, and acceptability. Disasters routinely undermine all four, particularly for vulnerable populations. For instance, restored services may remain inaccessible due to affordability or cultural mismatches, thereby compounding hardship and delaying community recovery.

Despite their significance, intangible impacts are often underrepresented in damage assessments and recovery metrics. Tomiczek et al. (2023) point out that subjective survey methods, inconsistent definitions, and poor timing can obscure the true impact of disaster events on humans. When post-event evaluations rely only on economic or insurable data, they risk misrepresenting community needs and underestimating total losses.

In recognition of these limitations, tools like the *Economic Decision Guide Software (EDGeS)* developed by NIST (Helgeson & Zhang, 2020; NIST, 2020) offer an expanded approach to evaluating the benefits of mitigation. EDGeS support multi-criteria decision-making and encourages the inclusion of non-economic benefits, such as quality of life, psychological security, and social cohesion, that are typically excluded from conventional BCR calculations. This allows

for a more comprehensive and inclusive framework that better reflects the lived experiences of disaster-affected communities.

Intangible losses are not secondary; they are fundamental to how disasters are experienced and how recovery unfolds. Any serious attempt to assess mitigation effectiveness or inform resilience planning must incorporate these non-economic dimensions alongside the traditional ones.

## 8 Conclusions and Recommendations

The review of historical information, literature, and hurricane damage assessment reports confirmed the need for a rigorous scientific investigation to quantify the relative risk of wind-borne debris damage in hurricane-prone regions that are adjacent to Exposure D conditions, whether the conditions are due to proximity to the coast or a large inland body of water.

ASCE 7 introduced provisions for design against wind-borne debris in 1995 with a single trigger wind speed. Subsequent cycles of ASCE 7 increased the blanket-trigger wind speed but still included the lower wind speed trigger for buildings within one mile of the coast. The one-mile distance was based on anecdotal observations from post-hurricane damage assessments; however, this distance has not been validated through scientific methods within a risk consistent framework. In ASCE 7-22, the definition of a WBDR was simplified to remove reference to the coast and to replace it with an Exposure D condition (at least 5,000 ft of upwind fetch of water). This change was viewed by ASCE 7-22 Wind Loads Subcommittee members as a correction to a previous error and a path to simplifying the challenge of consistently defining the meaning of the coast. The result of this change in the standard, and subsequent adoption by the 8$^{th}$ Ed. of the Florida Building Code, Residential (2023) resulted in new WBDRs in Central Florida adjacent to large lakes and in the Florida Panhandle adjacent to bays. It should be noted that the 8$^{th}$ Ed. FBC was later amended to revert the definition of WBDRs to align with ASCE 7-16 and the 7$^{th}$ Ed. FBC.

Damage assessment reports from several major storms (Hurricane Charley, Hurricane Ike, Hurricane Michael, and Hurricane Harvey) demonstrated the potential for wind-borne debris damage at wind speeds between 125 and 140 mph at distances up to more than three miles from coastal Exposure D conditions. In both Hurricane Ike and Hurricane Harvey, extensive wind-borne debris damage was observed, despite Ike's winds being below design levels and Harvey's nearing design thresholds. Particularly, Hurricane Harvey caused inland damage that was intensified by local topographic effects. Despite these findings, we have not identified reports of wind-borne debris damage during design wind speed events in inland areas with Exposure D conditions from lakes with design wind speeds between 130 and 140 mph. Post-storm damage assessments are intended to provide a representative sampling rather comprehensive documentation and are typically prioritized to coastal regions due to relatively higher damage levels, so a dearth of observations does not preclude that such damage occurs.

Studies have demonstrated how building envelope breaches from wind-borne debris can increase wind loads, resulting in further damage to the structure in terms of both interior and content loss from water and wind ingress and cascading structural damage from changes in interior pressure. Studies have shown how protective measures, such as impact resistant glazing, can mitigate the

risk of wind-borne debris damage, and these results underpin the design code requirements for opening protection for buildings in designated WBDRs. Researchers have developed, and experimentally, validated debris transport models; however, there has been no specific study of how wind-borne debris regions should be designated relative to upwind terrain conditions and how the risk for wind-borne debris damage varies with distance from terrain condition transitions. While some limited research has demonstrated how transition regions between terrain conditions impact wind loads, this research has not yet been extended to the impact on debris generation, transport, and damage. Future studies should examine how changes in exposure conditions influence debris generation, flight trajectories, and impact probabilities. Such research would help address the existing knowledge gap, providing an assessment of the relative risk of wind-borne debris generation and damage between inland and coastal regions and how the risk decreases with distance from the smooth to rough exposure transition. Further investigation should also explore the interaction between wind-borne debris and evolving urbanization patterns. Understanding how surrounding structures and water bodies contribute to wind-borne debris dynamics can improve mitigation strategies.

In support of modeling activities to quantify the risk of wind-borne debris damage in coastal and inland WBDRs, a comprehensive summary of housing developments near Central Florida lakes and Panhandle bays was conducted. This includes the characterization of geometric metrics to inform a wind-borne debris generation, transport and impact computational simulation model that has been validated against post-event damage assessments.

Simulation results indicate that, when conservatively evaluating WBD risk by considering the highest directional exposure (i.e., minimum $Z_0$) at each location and assuming that the design wind speed will originate from that direction, regions located within 3,000 feet of an open water source experience WBD risks comparable to areas exposed to 140 mph winds under Exposure B conditions, even when subjected to lower wind speeds of in the range of 130–139 mph. This finding suggests a consistent debris hazard pattern across both coastal and inland environments when Exposure D conditions are present.

Reducing the boundary for WBDRs from the current ASCE 7-22 guideline of 5,280 feet to a proposed 3,000 feet would result in 43-56% decrease in the total land area classified under WBDR criteria in ASCE 7-22. Such a reduction has the potential to significantly impact construction requirements and associated costs. For coastal regions, the recommendation to reduce the distance to 3,000 ft would decrease the number of homes requiring impact protection under both ASCE 7-22 and the current 2023 FBC. For inland lake regions, this recommendation would decrease the number of homes requiring impact protection under ASCE 7-22 but would increase the number of homes requiring impact protection under 2023 FBC ($8^{th}$ Ed.).

The actual increase or reduction in costs for individual homeowners is dependent on the specific location, design, and overall cost of their home. A preliminary cost-benefit analysis was conducted to evaluate the practical implications and economic impacts of this proposed modification. The analysis demonstrates that the increase in the total cost of a home with impact protections can be made up for in the reduction in loss they provide for some homes, and that the benefit is higher for homes adjacent to open water in the 130 to 139 mph design wind speed region than for homes

designed for above 140 mph in currently accepted WBDRs. The footprint of this cost-benefit study should be greatly expanded, and significant and science-grounded intangible losses incorporated into the analysis and decision-making process.

Based on the outcomes of this study, the following recommendations should be considered:

- Homes built adjacent to open water creating an Exposure D condition (both coastal and inland) located in regions with design winds speeds between 130 and 139 mph should be designed for protection against WBD.
- In these regions, WBD protection should be required up to 3,000 feet inland from the shoreline where Exposure D conditions exist.
- Aerial imagery taken during previous damage assessments after storms with estimated wind speeds between 125 and 140 mph passing near large inland lakes and bays should be analyzed to identify the occurrence, source, and impact of WBD capable of damaging glazed fenestration.
- Post-storm damage assessments should be carried out when storms have estimated wind speeds above 125 mph in the vicinity of large inland lakes bays to evaluate the risk for the generation of WBD that has the potential to damage glazed fenestration and to document occurrences of associated damage.
- Simulation of WBD damage should be extended to account different neighborhood configurations representative of development in the panhandle and central Florida and should be validated with building damage assessments carried out after storms that impact inland lakes and bays
- The cost-benefit analysis provided in this study should be expanded to include additional price points for opening protections and home construction, consider different time horizons, and incorporate the impacts of intangible losses in the evaluation of benefits realized by opening protections.

# 9 References


Applied Research Associate, Inc. (ARA) (2024). *2024 Residential Wind-Loss Mitigation Study.* Report # 005480 to the Florida Office of Insurance Regulation. https://floir.com/docs-sf/default-source/property-and-casualty/other-property-casualty-reports/005480_fl_oir_report_final_240628.pdf?sfvrsn=bfaf26d9_3

American Society of Civil Engineers (1995). *Minimum Design Loads for Buildings and Other Structures*. ASCE Standard ASCE/SEI 7-95.

American Society of Civil Engineers (2017). *Minimum Design Loads and Associated Criteria for Buildings and Other Structures*. ASCE Standards ASCE/SEI 7-16.

American Society of Civil Engineers (2022). *Minimum Design Loads and Associated Criteria for Buildings and Other Structures*. ASCE Standards ASCE/SEI 7-22.

Abdelhady, A. U., Spence, S. M. J., & McCormick, J. (2022). *Exogenous windborne debris: Definition and required extent of surrounding buildings for modeling in hurricanes*. In Engineering Structures (Vol. 254, p. 113798). Elsevier BV. https://doi.org/10.1016/j.engstruct.2021.113798

Baker, C. J. (2007). *The debris flight equations*. In Journal of Wind Engineering and Industrial Aerodynamics (Vol. 95, Issue 5, pp. 329–353). Elsevier BV. https://doi.org/10.1016/j.jweia.2006.08.001

Bourriez, F., Sterling, M., & Baker, C. (2020). *Windborne debris trajectories in tornado-like flow field initiated from a low-rise building*. In Journal of Wind Engineering and Industrial Aerodynamics (Vol. 206, p. 104358). Elsevier BV. https://doi.org/10.1016/j.jweia.2020.104358

Crawford, K., 2012. *Experimental and Analytical Trajectories of Simplified Debris Models in Tornado Winds.* M.S. Thesis. Iowa State University.

Dowell, D. C., Alexander, C. R., Wurman, J. M., & Wicker, L. J. (2005). *Centrifuging of Hydrometeors and Debris in Tornadoes: Radar-Reflectivity Patterns and Wind-Measurement Errors.* In Monthly Weather Review (Vol. 133, Issue 6, pp. 1501–1524). American Meteorological Society. https://doi.org/10.1175/mwr2934.1

Enderami, S. A., Sutley, E., Helgeson, J., Dueñas-Osorio, L., Watson, M., & van de Lindt, J. W. (2024). *Measuring post-disaster accessibility to essential goods and services: proximity, availability, adequacy, and acceptability dimensions.* Journal of Infrastructure Preservation and Resilience, 5(1). https://doi.org/10.1186/s43065-024-00104-0

Federal Emergency Management Agency (FEMA) 2022. *Hazus Hurricane Model Technical Manual, Hazus 5.1.* FEMA, Washington, DC, July 2022.

Federal Emergency Management Agency. (2005). *Mitigation Assessment Team report: Hurricane Charley in Florida: Observations, recommendations, and technical guidance* (FEMA Report No. 488). U.S. Department of Homeland Security.

Federal Emergency Management Agency. (2005). *Mitigation Assessment Team report: Hurricane Ivan in Alabama and Florida: Observations, recommendations, and technical guidance* (FEMA Report No. 489). U.S. Department of Homeland Security.

Federal Emergency Management Agency. (2006). *Summary Report on Building Performances: Hurricane Katrina 2005* (FEMA Report No. 548). U.S. Department of Homeland Security.

Federal Emergency Management Agency. (2019). *Mitigation Assessment Team report: Hurricane Harvey in Texas: Building Performance Observations, Recommendations, and Technical Guidance* (FEMA P-2022). U.S. Department of Homeland Security.

Federal Emergency Management Agency. (2020). *Mitigation Assessment Team report: Hurricane Michael in Florida: Building Performance Observations, Recommendations, and Technical Guidance* (FEMA P-2077). U.S. Department of Homeland Security.

Florida Building Commission (2023). *Florida Building Code, Residential*, *8th Edition*.

Florida Building Commission (2020). *Florida Building Code, Residential*, *7th Edition*.

Giammanco, I. M., Newby, E., & Pogorzelski, W. H. (2023a). *Observations of building performance in Southwest Florida during Hurricane Ian (2022): Part I: Roof cover damage assessment on residential and light commercial structures* (IBHS Research Report). Insurance Institute for Business & Home Safety.

Giammanco, I. M., Newby, E., & Pogorzelski, W. H., Shabanian, M. (2023b). *Observations of building performance in Southwest Florida during Hurricane Ian (2022): Part II: Performance of the modern Florida Building Code* (IBHS Research Report). Insurance Institute for Business & Home Safety.

Grayson, J.M., 2011. *Development and Application of a Three-Dimensional Probabilistic Wind-Borne Debris Trajectory Model*. M.S. Thesis. Clemson University.

Gurley, K. and Masters, F. (2011), *Post 2004 Hurricane Field Survey of Residential Building Performance.* ASCE Natural Hazards Review, 12(4): 177-183.

Gurley, K., Pinelli, J.P., Subramanian, C., Cope, A., Zhang, L., Murphreee, J., Artiles, A., Misra, P., Culati, S. and Simiu, E. (2005), *Florida Public Hurricane Loss Projection Model engineering team final report*. Technical report. International Hurricane Research Center, Florida International University.

Helgeson, J. and Zhang, P. (2020). Economic Decision Guide Software (EDGe:Wildfire Urban Interface (WUI) case study, National Institute of Standards and Technology, Gaithersburg, MD, [online], https://doi.org/10.6028/NIST.SP.1260

Ho, T. C. E., Surry, D., & Davenport, A. G. (1991). *Variability of low building wind loads due to surroundings.* In Journal of Wind Engineering and Industrial Aerodynamics (Vol. 38, Issues 2–3, pp. 297–310). Elsevier BV. https://doi.org/10.1016/0167-6105(91)90049-3

Holmes, J. D. (2004). *Trajectories of spheres in strong winds with application to wind-borne debris.* In Journal of Wind Engineering and Industrial Aerodynamics (Vol. 92, Issue 1, pp. 9–22). Elsevier BV. https://doi.org/10.1016/j.jweia.2003.09.031

Holmes, J. D., Letchford, C. W., & Lin, N. (2006). *Investigations of plate-type windborne debris—Part II: Computed trajectories*. In Journal of Wind Engineering and Industrial Aerodynamics (Vol. 94, Issue 1, pp. 21–39). Elsevier BV. https://doi.org/10.1016/j.jweia.2005.10.002

Insurance Institute for Business & Home Safety. (2018, July). *Hurricane Harvey wind damage investigation*. Insurance Institute for Business & Home Safety.

Insurance Institute for Business & Home Safety. (2023, ). *Hurricane Harvey wind damage investigation*. Insurance Institute for Business & Home Safety.

Insurance Institute for Business & Home Safety. (2018, July). *Hurricane Harvey wind damage investigation*. Insurance Institute for Business & Home Safety.

Kakimpa, B., Hargreaves, D. M., Owen, J. S., Martinez-Vazquez, P., Baker, C. J., Sterling, M., & Quinn, A. D. (2010). *CFD modelling of free-flight and auto-rotation of plate type debris*. Wind and Structures, 13(2), 169–189. https://doi.org/10.12989/WAS.2010.13.2.169

Karimpour, A., & Kaye, N. B. (2012*). On the stochastic nature of compact debris flight*. In Journal of Wind Engineering and Industrial Aerodynamics (Vol. 100, Issue 1, pp. 77–90). Elsevier BV. https://doi.org/10.1016/j.jweia.2011.11.001

Kim, S., Alinejad, N., Jung, S., & Kim, H.-K. (2024). *The effect of open-to-suburban terrain transition on wind pressures on a low-rise building*. In Journal of Building Engineering (Vol. 85, p. 108651). Elsevier BV. https://doi.org/10.1016/j.jobe.2024.108651

Kordi, B., & Kopp, G. A. (2011). *Effects of initial conditions on the flight of windborne plate debris.* In Journal of Wind Engineering and Industrial Aerodynamics (Vol. 99, Issue 5, pp. 601–614). Elsevier BV. https://doi.org/10.1016/j.jweia.2011.02.009

Lin, N. (2005), *Simulation of windborne debris trajectories*, Doctoral Dissertation, Texas Tech University.

Lin, N., Letchford, C., & Holmes, J. (2006). *Investigation of plate-type windborne debris. Part I. Experiments in wind tunnel and full scale.* In Journal of Wind Engineering and Industrial Aerodynamics (Vol. 94, Issue 2, pp. 51–76). Elsevier BV. https://doi.org/10.1016/j.jweia.2005.12.005

Lin, N., Holmes, J. D., & Letchford, C. W. (2007). *Trajectories of Wind-Borne Debris in Horizontal Winds and Applications to Impact Testing*. In Journal of Structural Engineering (Vol. 133, Issue 2, pp. 274–282). American Society of Civil Engineers (ASCE). https://doi.org/10.1061/(asce)0733-9445(2007)133:2(274)

Lin, N., & Vanmarcke, E. (2008). *Windborne debris risk assessment*. In Probabilistic Engineering Mechanics (Vol. 23, Issue 4, pp. 523–530). Elsevier BV. https://doi.org/10.1016/j.probengmech.2008.01.010

Lin, N., & Vanmarcke, E. (2010). *Windborne debris risk analysis - Part I. Introduction and methodology.* Wind and Structures, 13(2), 191–206. https://doi.org/10.12989/WAS.2010.13.2.191

Lin, N., Vanmarcke, E., & Yau, S.-C. (2010). *Windborne debris risk analysis - Part II. Application to structural vulnerability modeling.* Wind and Structures, 13(2), 207–220. https://doi.org/10.12989/WAS.2010.13.2.207

Minor, J. E., Mehta, K. C., & McDonald, J. R. (1972). *Failures of Structures Due to Extreme Winds*. In Journal of the Structural Division (Vol. 98, Issue 11, pp. 2455–2471). American Society of Civil Engineers (ASCE). https://doi.org/10.1061/jsdeag.0003375

Minor, J. E., Beason, W. L., & Harris, P. L. (1978). *Designing for Windborne Missiles in Urban Areas*. In Journal of the Structural Division (Vol. 104, Issue 11, pp. 1749–1760). American Society of Civil Engineers (ASCE). https://doi.org/10.1061/jsdeag.0005032

Minor, J. E. (2005). *Lessons Learned from Failures of the Building Envelope in Windstorms*. In Journal of Architectural Engineering (Vol. 11, Issue 1, pp. 10–13). American Society of Civil Engineers (ASCE). https://doi.org/10.1061/(asce)1076-0431(2005)11:1(10)

Moghim, F., & Caracoglia, L. (2012). *A numerical model for wind-borne compact debris trajectory estimation: Part 1 – Probabilistic analysis of trajectory in the proximity of tall buildings*. In Engineering Structures (Vol. 38, pp. 153–162). Elsevier BV. https://doi.org/10.1016/j.engstruct.2011.11.020

NIST 2020. *EDGeS (Economic Decision Guide Software) Online Tool.* https://www.nist.gov/services-resources/software/edge-economic-decision-guide-software-online-tool. February 2020

Richards, P. J., Williams, N., Laing, B., McCarty, M., & Pond, M. (2008). *Numerical calculation of the three-dimensional motion of wind-borne debris*. In Journal of Wind Engineering and Industrial Aerodynamics (Vol. 96, Issues 10–11, pp. 2188–2202). Elsevier BV. https://doi.org/10.1016/j.jweia.2008.02.060

Roofing Industry Committee on Weather Issues, Inc. (2007). *Hurricane Katrina Wind Investigation Report*. U.S. Department of Energy.

Roofing Industry Committee on Weather Issues, Inc. (2009). *Hurricane Ike Wind Investigation Report*. U.S. Department of Energy.

Roofing Industry Committee on Weather Issues, Inc. (2022). *Hurricane Ian* Roofing Industry Committee on Weather Issues, Inc.

Structural Extreme Event Reconnaissance Network. (2018). *Hurricane Michael preliminary virtual assessment team (P-VAT) report*. (NHERI DesignSafe Project ID: PRJ-2112) Structural Extreme Event Reconnaissance Network.

Structural Extreme Event Reconnaissance Network. (2022). *Hurricane Ian Early Access Reconnaissance Report (EARR)*. (NHERI DesignSafe Project ID: PRJ-3709) Structural Extreme Event Reconnaissance Network.

Tachikawa, M. (1983). *Trajectories of flat plates in uniform flow with application to wind-generated missiles*. In Journal of Wind Engineering and Industrial Aerodynamics (Vol. 14, Issues 1–3, pp. 443–453). Elsevier BV. https://doi.org/10.1016/0167-6105(83)90045-4

Tachikawa, M. (1988). *A method for estimating the distribution range of trajectories of wind-borne missiles.* In Journal of Wind Engineering and Industrial Aerodynamics (Vol. 29, Issues 1–3, pp. 175–184). Elsevier BV. https://doi.org/10.1016/0167-6105(88)90156-0

Tomiczek, T., Helgeson, J., Sutley, E., Gu, D., Hamideh, S., & Crawford, P. S. (2023). *A Framework for Characterizing Uncertainty Factors in Postdisaster Structural Performance Assessment Data.* Natural Hazards Review, 24(1). https://doi.org/10.1061/(asce)nh.1527-6996.0000604

Twisdale, L. A., Dunn, W. L., and Davis, T.L. (1979). *Tornado Missile Transport Analysis*, Nuclear Engineering and Design, Vol. 51, 1979.

Twisdale, L.A., Vickery, P.J. and Steckley, A.C. (1996), *Analysis of hurricane windborne debris risk for residential structures,* Technical report, Raleigh (NC): Applied Research Associates, Inc.

Twisdale, L.A. et al., (2002). *Development of Loss Relativities for Wind Resistive Features of Residential Structures*, prepared for Florida Department of Community Affairs, Tallahassee, FL, March.

Van de Lindt, J. W., Peacock, W. G., Mitrani-Reiser, J., Rosenheim, N., Deniz, D., Dillard, M., Tomiczek, T., Koliou, M., Graettinger, A., Crawford, P. S., Harrison, K., Barbosa, A., Tobin, J., Helgeson, J., Peek, L., Memari, M., Sutley, E. J., Hamideh, S., Gu, D., … Fung, J. (2020). *Community Resilience-Focused Technical Investigation of the 2016 Lumberton, North Carolina, Flood: An Interdisciplinary Approach.* Natural Hazards Review, 21(3). https://doi.org/10.1061/(asce)nh.1527-6996.0000387

Vickery, P. J., Skerlj, P. F., Lin, J., Twisdale, L. A., Jr., Young, M. A., & Lavelle, F. M. (2006). *HAZUS-MH Hurricane Model Methodology. II: Damage and Loss Estimation.* In Natural Hazards Review (Vol. 7, Issue 2, pp. 94–103). American Society of Civil Engineers (ASCE). https://doi.org/10.1061/(asce)1527-6988(2006)7:2(94)

Visscher, B. T., & Kopp, G. A. (2007). *Trajectories of roof sheathing panels under high winds.* In Journal of Wind Engineering and Industrial Aerodynamics (Vol. 95, Issue 8, pp. 697–713). Elsevier BV. https://doi.org/10.1016/j.jweia.2007.01.003

Wang, F., Huang, P., Zhao, R., Wu, H., Sun, M., Zhou, Z., & Xing, Y. (2023). *Predicting Trajectories of Plate-Type Wind-Borne Debris in Turbulent Wind Flow with Uncertainties*. In Infrastructures (Vol. 8, Issue 12, p. 180). MDPI AG. https://doi.org/10.3390/infrastructures8120180

Wills, J. A. B., Lee, B. E., & Wyatt, T. A. (2002). *A model of wind-borne debris damage*. In Journal of Wind Engineering and Industrial Aerodynamics (Vol. 90, Issues 4–5, pp. 555–565). Elsevier BV. https://doi.org/10.1016/s0167-6105(01)00197-0

Yu, W., Zhang, Y., Ai, T., & Chen, Z. (2020). An integrated method for DEM simplification with terrain structural features and smooth morphology preserved. *International Journal of Geographical Information Science*, *35*(2), 273–295. https://doi.org/10.1080/13658816.2020.1772479

# 10 Appendix A. Inland WBDR Neighborhood Analysis Images

The following figures represent the neighborhoods selected for Central Florida (Figure 81- Figure 102 and the Florida Panhandle (Figure 103 - Figure 106) analysis. The neighborhoods are highlighted in magenta rectangles.

## 10.1 Central Florida neighborhoods around lakes/inland bays


Figure 81. Lake County – Lake Apopka neighborhood selection.

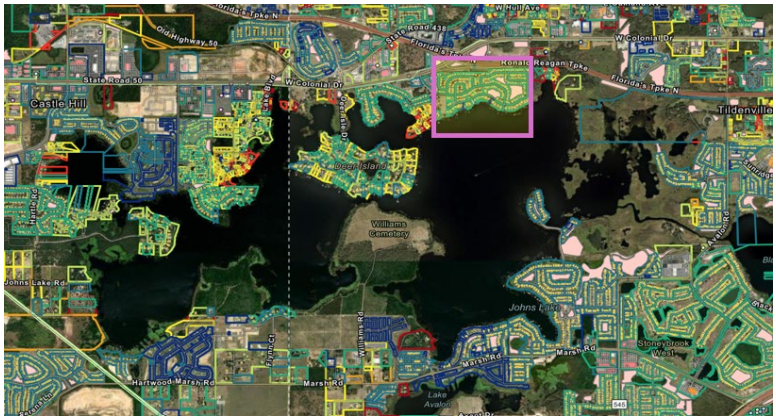


Figure 82. Lake County – John's Lake neighborhood selection


Figure 83. Lake County – Lake Louisa neighborhood selection


Figure 84. Lake County – Lake Minnehaha neighborhood selection

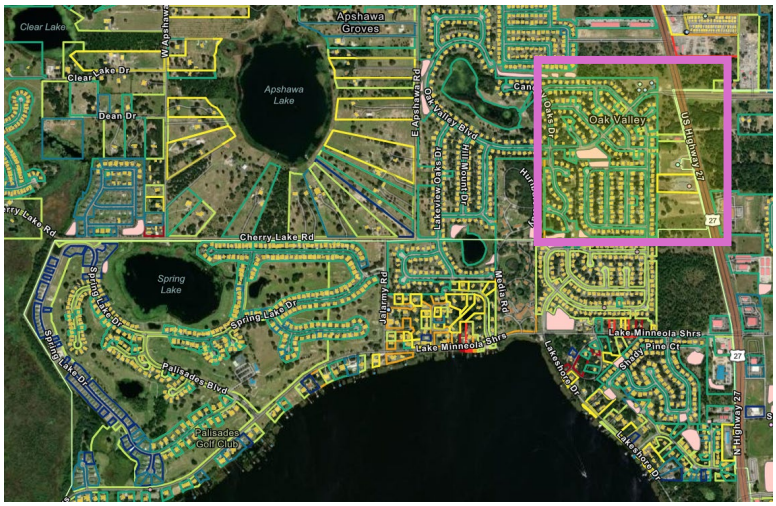


Figure 85. Lake County – Minneola neighborhood selection

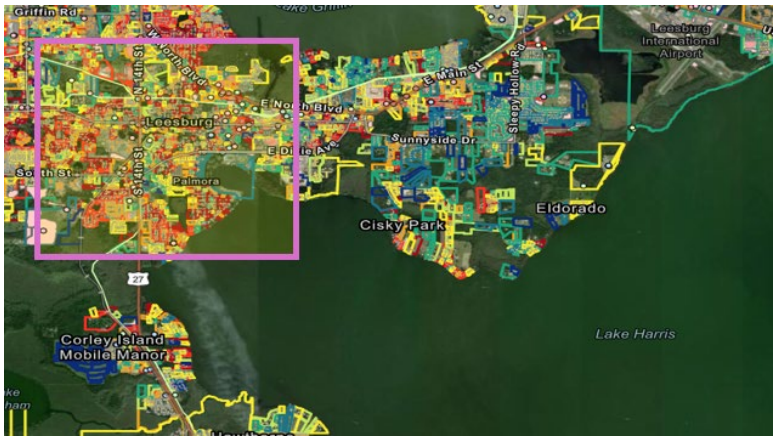

Figure 86. Lake County – Big Lake Harris neighborhood selection

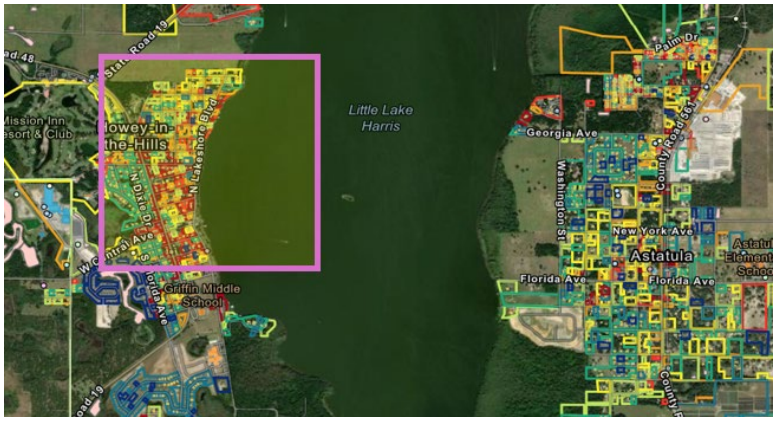

Figure 87. Lake County – Little Lake Harris neighborhood selection

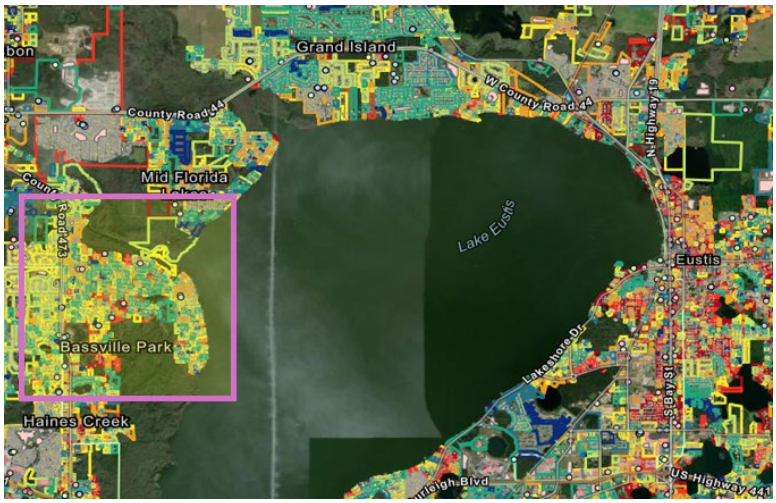

Figure 88. Lake County – Lake Eustis neighborhood selection

Figure 89. Lake County – Lake Dora neighborhood selection

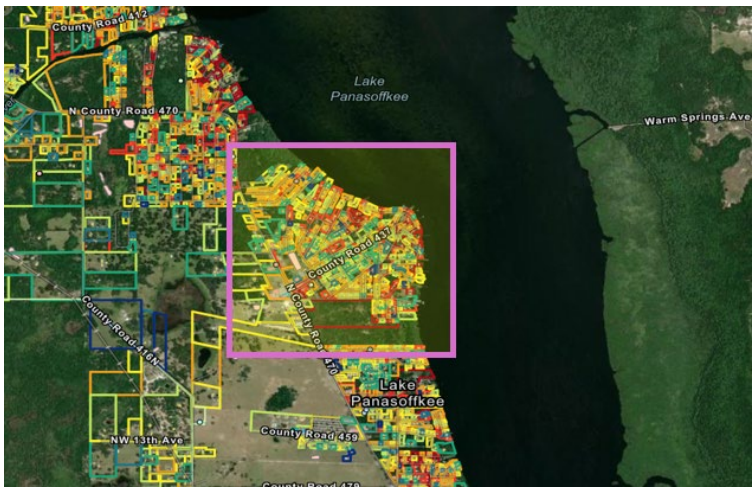

Figure 90. Sumter County – Lake Panasoffkee neighborhood selection

Figure 91. Marion County – Lake Weir neighborhood selection


Figure 92. Volusia County – Lake George neighborhood selection.


Figure 93. Polk County – Lake Alfred neighborhood selection.


Figure 94. Polk County – Lake Ariana neighborhood selection.

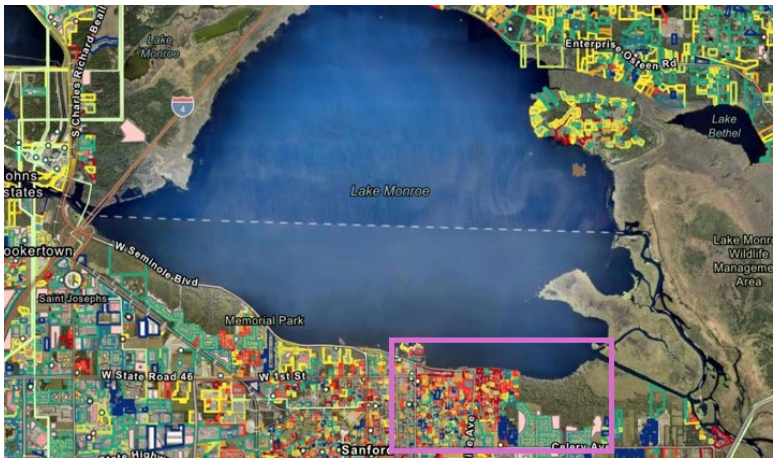

Figure 95. Seminole County – Lake Monroe neighborhood selection.

Figure 96. Seminole County – Lake Jessup/Lake Harney neighborhood selection.

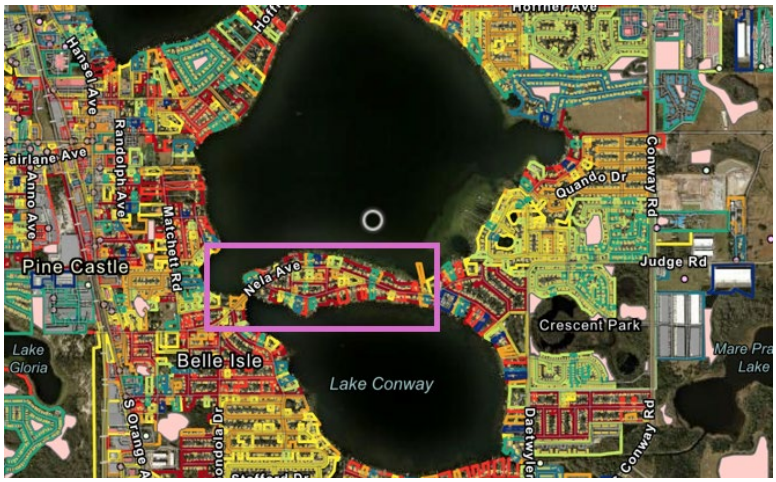

Figure 97. Orange County – Lake Conway neighborhood selection.

Figure 98. Orange County – Lake Butler neighborhood selection.

Figure 99. Orange County – Lake Down neighborhood selection.

Figure 100. Orange County – Lake Tibet neighborhood selection.

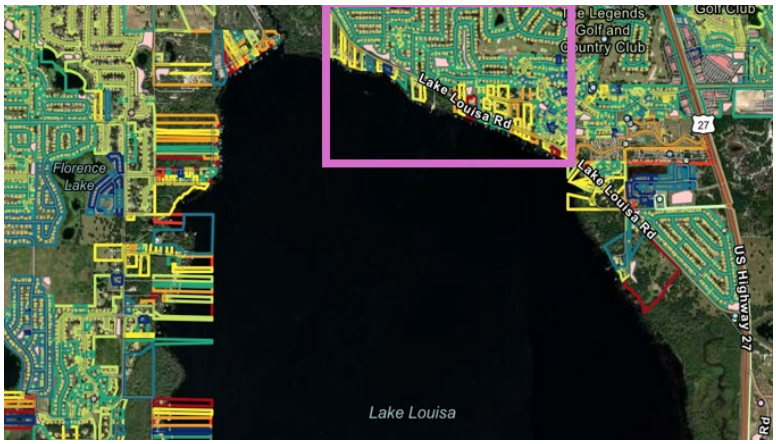

Figure 101. Orange County – Lake Louisa.

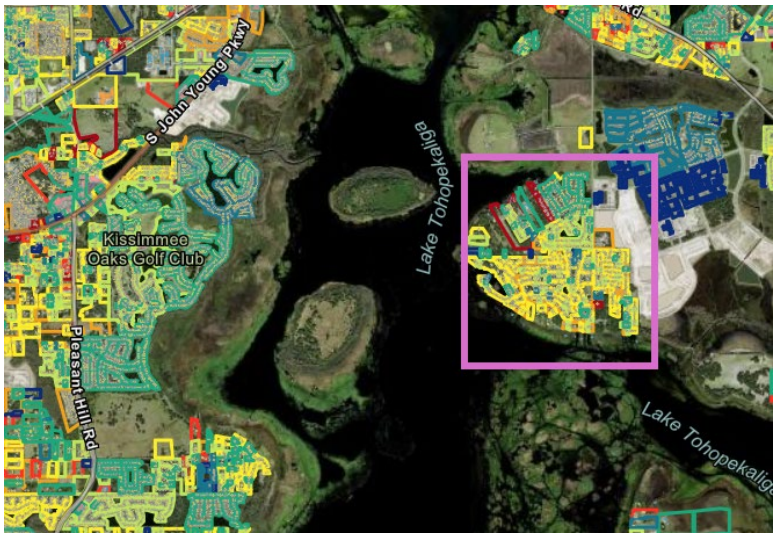

Figure 102. Orange County - Lake Tohopekaliga neighborhood selection.

## 10.2 Florida Panhandle neighborhoods around lakes/inland bays

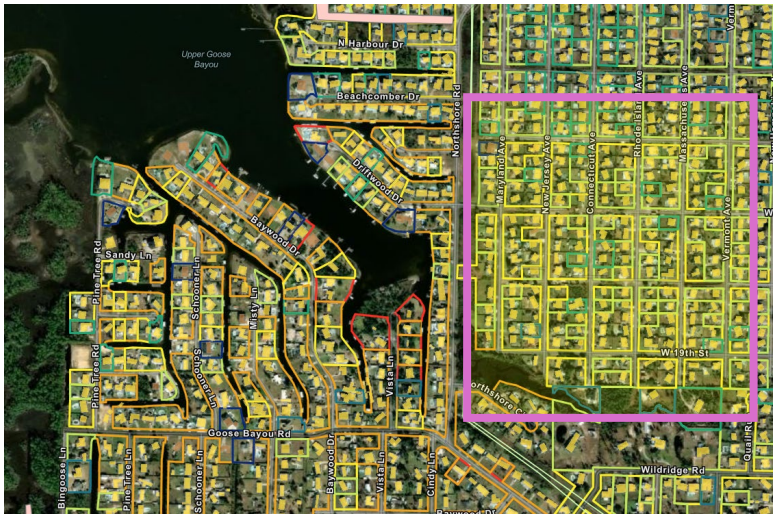


Figure 103. Bay County - Deer Point Lake neighborhood selection.


Figure 104. Bay County – St. Andrews Bay neighborhood selection.


Figure 105. Bay County – East Bay neighborhood selection.

Figure 106. Gulf County – St. Joseph Bay neighborhood selection.